

Applications of Aptamers in Flow Cytometry Assays

Von der Naturwissenschaftlichen Fakultät
der Gottfried Wilhelm Leibniz Universität Hannover

zur Erlangung des Grades
Doktor der Naturwissenschaften
Dr. rer. nat.

genehmigte Dissertation

von
M.Sc. Michael Meyer
geboren am 24. September 1985 in Hildesheim

2014

Referent: Prof. Dr. Thomas Scheper
Institut für Technische Chemie
Gottfried Wilhelm Leibniz Universität Hannover

Korreferent: Prof. Dr. Ursula Rinas
Institut für Technische Chemie
Gottfried Wilhelm Leibniz Universität Hannover

Prüfungsvorsitz: Prof. Dr. Jürgen Alves
Institut für Biophysikalische Chemie
Medizinische Hochschule Hannover

Tag der Promotion: 15. Mai 2014

“Stay hungry, stay foolish.”

Steve Jobs

Acknowledgements

I would like to express my sincere thanks to Prof. Dr. Thomas Scheper for giving me the opportunity to work on this interesting topic in the Institute of Technical Chemistry. I would also like to thank Prof. Dr. Ursula Rinas for her willingness to be co-supervisor of this work.

I express my thanks and appreciation to Dr. Johanna Walter for her constant support and the many fruitful discussions during my research. Thanks also to the other members from the aptamer group, especially Maren, Alex, Katha and Emilia for sharing ideas, solutions and also frustration.

I would also like to mention Martin Pähler and Martina Weiß and thank them for their commitment. Without you the day-to-day work at the institute would surely collapse. Furthermore I am also grateful to all students who were involved in parts of my research and hope that they have learned something useful and also enjoyed the team work as much as I did.

Thanks also to all members from the cell culture lab, especially to Tim, Alex and Christian for the many donated CHO cells that were sacrificed for a higher purpose in my experiments.

A lot of my other colleagues also contributed significantly to this work by keeping my spirit high and life inside and outside the institute so enjoyable. Some of them like Matthias, Christopher and Patrick, are old companions to whom others like Steffen, Bernd, Satish and Thore are comparatively new fellows, but I like to say thank you to all of them for the nice time. The same goes for my office girls, Emilia, Franzi and Mihri who assist me in running the "Headquarter". Thanks for everything, especially for all the laughter and happiness and all the tea. I will miss you a lot! This is also true for all other members of the TCI, whom I want to thank for their support and the nice atmosphere during the last three years.

I would also like to thank my family for their enduring support through all my life. Without you I would never have made it this far!

Finally I would like to thank my girlfriend Annette for everything she has done for me. Without her love, encouragement and support this thesis would not have been possible. Thank you.

Abstract

Keywords: Aptamers, flow cytometry, aptamer-quantum dot conjugates, diagnostics, cell line development, screening

The overageing population in countries of the western world presents huge challenges for the society. An enourmous pressure thereby lies on the health care system, which has to take care of a constantly increasing number of people in need for treatment due to the demographic change. In the future, the health care system will hence have to provide treatments for more patients with more complex and costly diseases. The resulting cost pressure is already affecting companies operating in the health care environment and will increase further. Suppliers of diagnostic tests and the pharmaceutical industry therefore have to try to produce new, innovative and above all cost-saving products to stay competitive in the market.

Through the use of certain innovative chemical reagents, called aptamers, it could be possible to develop cost-saving applications for diagnostics and more efficient processes for the manufacturing of drugs. This work points out two potential application areas for aptamers in these fields and explores the feasibility of the applications. In the first part of the work the use of aptamers as detection probes in flow cytometry is shown. Flow cytometry has a high clinical relevance and is used routinely for analysis of patient samples to screen for tumor cells. It could be demonstrated that aptamers can be used to specifically label certain cell surface molecules. In addition, the fabrication and characterisation of functional aptamer quantum dot conjugates is described. These probes are promising tools for future applications of aptamers in flow cytometry. The second part of the work investigates the use of aptamers for optimisation of biotechnological production processes. Many newly developed drugs are produced by processes that use cultured cells. A flow cytometry based screening could help to find the most productive cells in a population and thereby help to manufacture drugs more efficiently. The initial development of such an assay is described in this thesis.

Kurzzusammenfassung

Schlagwörter: Aptamere, Durchflusszytometrie, Aptamer-quantum dot Konjugate, Diagnostik, Zell-Linien Entwicklung, Screening

Die alternde Bevölkerung in den Ländern der westlichen Welt stellt die Gesellschaft vor große Herausforderungen. Sehr hoher Druck lastet dabei auf dem Gesundheitssystem, das durch den demografischen Wandel eine immer größere Anzahl kranker und behandlungsbedürftiger Menschen versorgen muss. Das Gesundheitssystem wird folglich in Zukunft mehr Menschen mit komplexeren und kostenintensiveren Krankheiten bei einem sinkenden Anteil an Beitragszahlern versorgen müssen. Der entstehende Kostendruck wirkt sich bereits jetzt auf die im Umfeld des Gesundheitssystems agierenden Unternehmen aus und wird weiter zunehmen. Hersteller diagnostischer Tests und die Pharmaindustrie müssen daher versuchen neue, innovative und vor allem kostengünstigere Produkte herzustellen, um weiter am Markt bestehen zu können.

Durch den Einsatz von innovativen chemischen Reagenzien, sogenannten Aptameren, könnten neue, kostengünstigere Anwendungen für die Diagnostik entwickelt werden und Produktionsprozesse für Medikamente effizienter gestaltet werden. Diese Arbeit zeigt zwei mögliche Einsatzbereiche für Aptamere und erforscht ihre Machbarkeit. Im ersten Teil der Arbeit wird der Einsatz von Aptameren als Detektionsmoleküle in der Durchflusszytometrie gezeigt. Die Durchflusszytometrie besitzt eine hohe klinische Relevanz und wird routinemäßig für die Analyse von Patientenproben auf Krebszellen verwendet. Die Arbeit zeigt den Einsatz von Aptameren zur spezifischen Färbung bestimmter Zelloberflächenmoleküle. Darüber hinaus wird die Herstellung und Charakterisierung funktioneller Aptamer Quantum Dot Konjugate beschrieben. Diese Reagenzien sind vielversprechende Werkzeuge für zukünftige Anwendungen von Aptameren in der Durchflusszytometrie. Im zweiten Teil der Arbeit wird der Einsatz von Aptameren für die Optimierung von biotechnologischen Produktionsprozessen erforscht. Viele der neu entwickelten Medikamente werden mit Hilfe von kultivierten Zellen hergestellt. Ein Durchflusszytometrie basiertes Screening könnte helfen die produktivsten Zellen hierfür zu finden und so Medikamente effizienter herzustellen. Die anfängliche Entwicklung eines solchen Verfahrens wird in dieser Arbeit dargelegt.

Table of contents

1	Introduction	1
2	Aim and scope	2
3	Theoretical background	4
3.1	Flow cytometry	4
3.2	Aptamers in flow cytometry	5
3.2.1	Cell-SELEX	7
3.2.2	Current applications of aptamers in flow cytometry	10
3.2.3	Aptamer-quantum dot conjugates as probes for flow cytometry	13
3.3	Immobilisation of aptamers on the cell surface	15
3.3.1	High-producer screening for cell line development	16
4	Experimental investigations	21
4.1	Aptamers as stains for cell surface proteins in flow cytometry	21
4.1.1	Basic investigations of aptamer target binding for the model system TD05 and IgM using microarrays	21
4.1.2	Detection of TD05 binding to IgM beads by flow cytometry	25
4.1.3	Microscopic investigations on TD05 binding to Ramos cells	26
4.1.4	Detection of TD05 binding to IgM on Ramos cells by flow cytometry	27
4.1.5	Aptamer-quantum dot conjugates targeting Ramos cells	32
4.2	Immobilisation of aptamers on the cell surface and their characterisation by flow cytometry	36
4.2.1	Indirect immobilisation of aptamers using a biotin streptavidin bridge	37
4.2.1.1	Indirect immobilisation – proof of principle using streptavidin modified beads	38
4.2.1.2	Immobilisation of aptamers against IgG on the cell surface	41
4.2.1.3	Indirect immobilisation of VEGF aptamers on the cell surface	48
4.2.1.4	Indirect immobilisation of aptamers on the yeast <i>Pichia Pastoris</i>	49
4.2.2	Direct immobilisation of aptamers	52
4.2.2.1	Direct immobilisation – proof of principle using beads as immobilisation substrates	52
4.2.2.2	Direct immobilisation of aptamers on liposomes	59
4.2.2.3	Direct immobilisation of aptamers on cells	62
4.2.2.4	Cultivation of modified cells – effects on cell viability and growth	65
4.2.2.5	Investigation on a cell based aptamer-sandwich assay for VEGF detection	67
5	Conclusions and outlook	72
6	Appendices	76

6.1	Methods	76
6.1.1	Preparation and analysis of reverse phase protein microarrays for analysis of fluorescently labelled aptamers and aptamer-quantum dot conjugates.....	76
6.1.2	Microscopic analysis of aptamer-stained Ramos cells.....	78
6.1.3	Protein coupling to tosyl-activated beads.....	78
6.1.4	Staining of cells with fluorescently labelled aptamers for flow cytometry analysis	79
6.1.5	Proteinase K treatment of Ramos cells	79
6.1.6	Fabrication of aptamer-QD conjugates	80
6.1.7	Staining of cells with aptamers and aptamer-QD conjugates for flow cytometry.....	80
6.1.8	Micro BCA assay.....	80
6.1.9	Cell cultivations	81
6.1.10	Production of VEGF using a recombinant <i>E.coli</i> strain.....	82
6.1.11	Labeling of aptamers with R-phycoerythrin (R-PE)	85
6.1.12	Labeling of proteins with fluorescein isothiocyanate (FITC)	85
6.1.13	Immobilisation of aptamers on streptavidin-modified beads	85
6.1.14	Immobilisation of aptamers on carboxyl-modified magnetic beads	86
6.1.15	Activation of aptamers via cyanuric chloride	86
6.1.16	Immobilisation of cyanuric chloride-activated aptamers on living cells.....	87
6.1.17	Immobilisation of aptamers on living cells using a biotin-streptavidin bridge	87
6.1.18	Flow cytometry analysis of protein binding to modified beads and CHO K1 cells.....	88
6.1.19	Preparation of liposomes / GUVs (giant unilamellar vesicles) by lipid film rehydration ...	88
6.1.20	Modification of beads for analysis via Biorad Bioplex 200 and MagPix	90
6.1.21	Measurement of binding affinity by microscale thermophoresis	92
6.2	Materials.....	93
6.2.1	Chemicals.....	93
6.2.2	Disposables	94
6.2.3	Equipment.....	94
6.2.4	Buffer compositions.....	95
6.2.5	Aptamers and oligonucleotides	96
7	References	98

List of abbreviations

BSA	Bovine serum albumin
ca.	<i>lat. circa</i>
CD	Cluster of differentiation
CHO	Chinese hamster ovary
Cyt	Cytochrome c
DMSO	Dimethylsulfoxid
DNA	Deoxyribonucleic acid
D/P ratio	Dye to protein ratio
<i>et al.</i>	<i>lat. et alii</i>
EDC	1-Ethyl-3-(3-dimethylamino-propyl)carbodiimide hydrochloride
Em.	Emission
Exc.	Excitation
FACS	Fluorescence-activated cell sorting
Fc-fragment	Fragment crystallizable (part of an antibody)
FCS	Fetal calf serum
FDA	US Food and Drug Administration
FITC	Fluorescein isothiocyanate
FSC	Forward scatter
GMP	Good manufacturing practise
GUV	Giant unilammilar vesicle
h.i.	Heat inactivated
IPTG	Isopropyl- β -D-thiogalactopyranosid
Lys	Lysozyme
Lys-Apt	Aptamer against lysozyme
mAb	Monoclonal antibody
MeOH	Methanol
MES	2-(N-morpholino)ethanesulfonic acid
MST	Microscale thermophoresis
MWCO	Molecular weight cut-off
NHS	N-Hydroxysuccinimide
OD₆₀₀	Optical density, $\lambda = 600$ nm
PBS	Phosphate-buffered saline
pH	<i>lat. Potentia Hydrogenii</i>
pI	Isoelectric point
PFEI	Pseudomonas fluorescence esterase I
QD	Quantum dot
R-PE	R-Phycoerythrin

rel. AU	Relative absorption units
RNA	Ribonucleic acid
RPM	Rounds per minute
RT	Room temperature (~23 C)
SELEX	Systematic evolution of ligands by exponential enrichment
SSC	Side scatter
VEGF	Vascular endothelial growth factor

1 Introduction

Constant improvement of medical diagnostics and therapeutic treatments over the last decades have lead to a great increase of life expectancy in the developed world. A man born in Germany in the year 1960 has an average life expectancy of 67 years, whereas a boy born 50 years later in 2010 can now expect to live over 10 years longer to the age of 78 (1). Although this trend is a huge success of the civilisation and a benefit for people who are fortunate to grow old in good health, it also has to be managed properly to keep the social and health care systems intact and effective. The demographical development imposes a series of challenges on the society as a whole but especially on organisations and companies that act in the environment of the health care system.

More patients will have to be treated while fewer people will be paying contributions to the healthcare system. The resulting cost pressure onto the manufacturers of diagnostic test systems and the pharmaceutical industry is likely to increase in the future. These companies are forced to adapt to the changing environment and will have to innovate massively to keep their businesses growing and stay profitable. The innovations needed in this context are e.g. new products that can be produced more cost-efficiently or improvements of production processes that help to lower the cost of goods.

Aptamers, a certain class of molecules, could help to meet these challenges by replacing more expensive substances and opening up new applications that deliver benefits for patients and companies in the health care market.

In the area of diagnostic tests this could be possible by substituting antibodies in molecular detection assays. Flow cytometry, a widely used diagnostic method that is used to detect and identify different types of cells, like e.g. cancer cells, nowadays routinely works with antibodies. There are many references which indicate that aptamers are equally suited for this purpose while exhibiting longer shelf lives at lower costs (2).

In the pharmaceutical industry aptamers could be used in screening assays to find highly productive cells at the very start of the process development for drug manufacturing. Many of the newly developed drugs, especially in the area of cancer treatment are so called “biologics” which means that they are produced by genetically modified cells. Of these biologics the monoclonal antibodies (mAbs) are the most important class with some of them having the “blockbuster” status by reaching an annual sales of more than

1 billion US \$. Biologics are expected to stay a huge trend for years to come and their efficient production is hence an important issue for keeping the drugs affordable.

The first step in the development of the production process is the selection of a suitable cell clone that can be used in the final large scale cultivation process. The task is termed “cell line development” and involves the cultivation and screening of typically hundreds or even thousands of individual cell clones. An important trait of a suitable clone is its ability to secrete the product in high amounts. A screening assay, based on cell immobilised aptamers that capture the secreted product and allow its quantification by flow cytometry is conceivable. Cells that show a good secreting performance could be isolated by using fluorescence activated cell sorting (FACS) and used for further characterisation.

Another issue underlining the importance of cell-based drug production and its increase in the future is the emergence of so called “biosimilars”. Biosimilars are essentially generics of already approved biologics, but because of proprietary rights for the original cell line, biosimilar producing companies will have to select their own production cell lines. This fuels the need for innovative approaches to facilitate the cell line development. New screening assays will help to improve the efficiency of cell based drug production. This is crucial to ensure that new and innovative drugs will still be affordable for the health care system and given to patients in need.

2 Aim and scope

The overall goal of this thesis was the proof of principle for the application of aptamers in flow cytometry assays. The thesis is therefore structured in two parts that deal with different assay systems used to demonstrate the applications.

One aim was to show the specific binding of aptamers to cell surface markers by flow cytometry and investigate potential future directions, such as the use of novel fluorescence labels, for this application. This study should be done with a representative aptamer-target system. Suitable model systems should be developed and employed to investigate the binding of the model aptamer and validate the system for further use. Later investigations should then increase in complexity until finally analysing the

aptamer binding to cells via flow cytometry. The same approach should then be used for aptamers conjugated to novel quantum dot fluorophores to assess their applicability as probes for flow cytometry.

The aim of the second part of this thesis was to investigate the feasibility of an aptamer-based screening for high secreting cells by flow cytometry. The task was to show the functional immobilisation of aptamers on the cell surface and the detection of bound target molecules. On this way, simple model systems should be studied for the immobilisation of aptamers and their functional evaluation by flow cytometry. Another aim was the development of a suitable method for the immobilisation of aptamers on the surface of living cells without compromising their viability. Therefore a new direct immobilisation approach for aptamers on the cell surface should be developed and compared to an already existing and rather complicated indirect approach. Finally, a detection method for the captured protein on the cell surface should be developed that could be used for a later high producer screening.

3 Theoretical background

3.1 Flow cytometry

Flow cytometry is a bioanalytical method that measures the interaction of particles, such as cells, with light. Cells from a sample are suspended in a fluid stream and hydrodynamically focused by a second stream, called sheath fluid. By this approach the cells are singularized so that they pass a laser beam one after another. The method thereby allows collection of data on the single cell level at high throughput of up to thousands of cells per second. The parameters that are analysed are the light scatter caused by the cell and the fluorescence emitted from probes used to label the cell. The forward scatter correlates to the size of the cell, whereas the side scatter is a measure of the inner complexity and compartmentalisation of the cell. Fluorescence labelled reagents can be used to label intracellular structures or molecules exposed on the cell surface. The basic principle of a flow cytometer is shown in **Figure 1**. Through innovations in the laser, instrument and reagent technology, the amount of simultaneously measurable parameters has increased from 5 in the year 1995 (3) to 18 today (4).

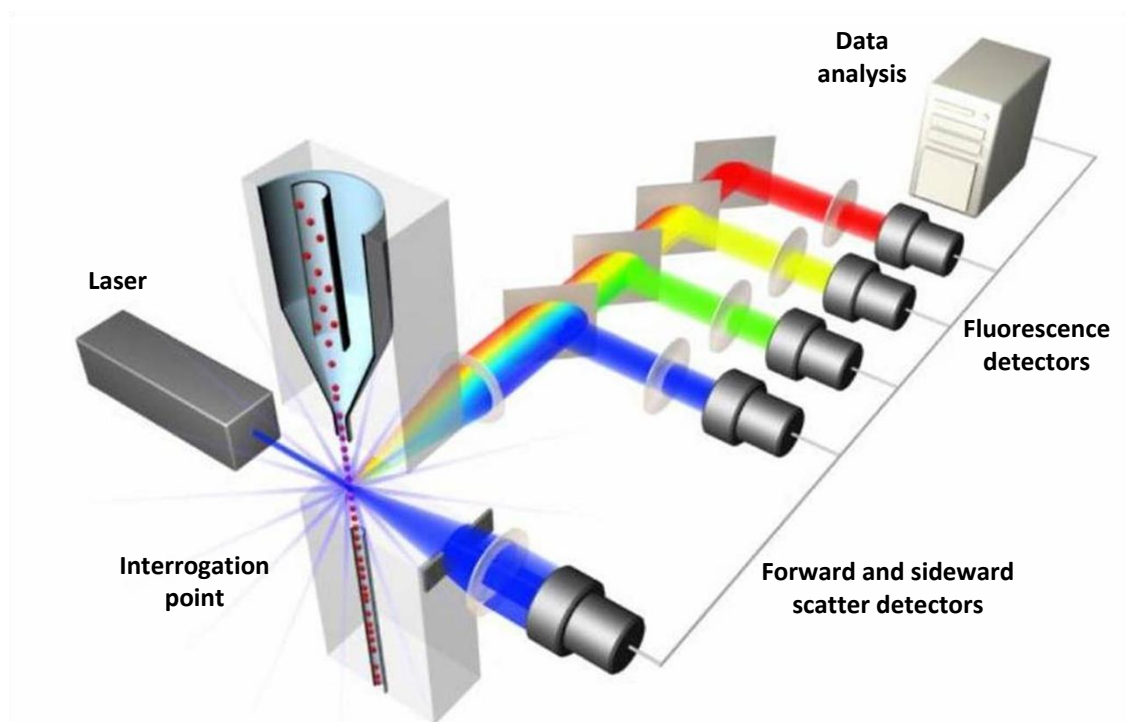


Figure 1: Basic principle and setup of a flow cytometer. Cells are hydrodynamically focused so that they pass a laser one by one. The resulting scatter and fluorescence light is split into separate signals by an optical system and finally analysed using a computer. (Image modified from (5))

Flow Cytometry is used for various applications in the detection and analysis of cell populations in clinical (6), environmental (7,8) and research applications (9). A widespread application is immunophenotyping, an analysis in which certain cellular surface molecules, known as clusters of differentiation (CD), are fluorescently stained with labelled antibodies to identify the cell type. The capability to rapidly analyse huge quantities of cells and increasing automation of the process make it a promising technology for the era of systems biology (10).

Fluorescence-activated cell sorting (FACS) presents a special type of flow cytometry where the instruments analytical strength is combined with the capability to isolate certain cells from the analysed population. This is done by sorting the cells of interest according to their fluorescence labelling. Different technical implementations exist that use for example cells in liquid drops to extract them from the sample stream and collect them in a different tube for further cultivation or analysis (11,12).

3.2 Aptamers in flow cytometry

Aptamers are single stranded oligonucleotides that fold into distinct three-dimensional shapes that render them capable of binding targets with high affinity and specificity. Aptamers are selected against a certain target by a process called *systematic evolution of ligands by exponential enrichment* (SELEX), in which a library of $\sim 10^{15}$ random sequences is incubated with the target and screened for binding species (13). Various targets have been used successfully to select aptamers, such as amino acids (14), proteins (15), viruses (16) and even whole cells (17). Since the discovery of aptamers by Ellington, Szostak, Tuerk and Gold in 1990 (18,19) the applications have spread into many bioanalytical areas covering capillary electrophoresis, chromatography, microarrays (20–22) and many more (23).

The potential of aptamers as molecular probes for flow cytometry has been evaluated first in the late 1990ies with promising results (24,25). Despite the dominance of antibodies, that still present the standard labelling probes in flow cytometry, aptamers show some advantages that might attract interest for this application. Aptamers, for example, are accessible by chemical synthesis and can be easily modified with fluorophores and other functional groups. In addition they show a higher stability to degradation by heat or pH shifts and usually refold into their native structure after

thermal denaturation. These issues would alleviate handling and storage of fluorescence probes for customers and manufacturers. Another benefit might be their small size of ~15 kDa which is much smaller than an antibody ~150 kDa. This might be advantageous for staining intracellular structures in flow cytometry assays.

Besides the mentioned advantages another factor might favour aptamers entering the stage as commercially available probes: economics. The costs for oligonucleotide synthesis have decreased substantially over the past decade. **Figure 2** shows the development of the costs per base of synthetic DNA for genes and short oligonucleotides like aptamers. It is expected that this trend proceeds or will even be enhanced by hundreds of siRNA projects that are currently in clinical trials, which will lead to expansion of the existing synthesis capacities and drive technological improvements in the field (26).

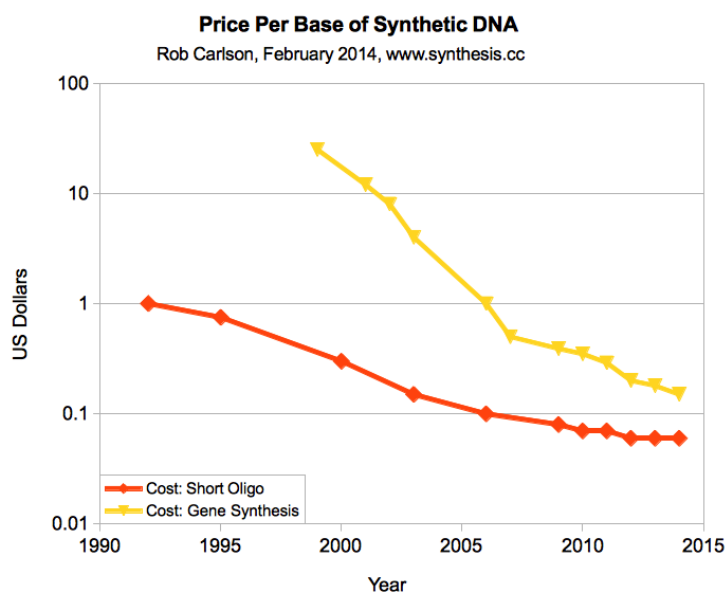


Figure 2: Development of the costs per base of synthetic DNA oligonucleotides. Aptamers fall under the classification of “short oligo” shown in the graph (27).

A comparison of assay costs between a custom synthesized RNA aptamer and the corresponding commercial antibody conjugate done by Zhang and his group revealed the small price of US\$ 0.002 for the aptamer and US\$ 2 for the antibody probe per analysis (28). This indicates that aptamers might already be cheaper today for many applications that use antibodies. The case why aptamers have not found a wider dispersion in commercial available technologies has been discussed in an interesting contribution by G. S. Baird (29), with the conclusion that the prevailing antibody technology is very well rooted and serves most needs. With regard to future

developments in the field of recognition molecules this will likely change. The antibody technology is still advancing but at a much slower pace, indicating that it might have reached the status of maturation shown in a typical S-curve that can be used to describe technology development (see **Figure 3**) (30). Another important aspect is that the original patents on the aptamer technology from the 1990s are expiring soon, granting freedom to operate and encouraging innovators to develop new commercial applications.

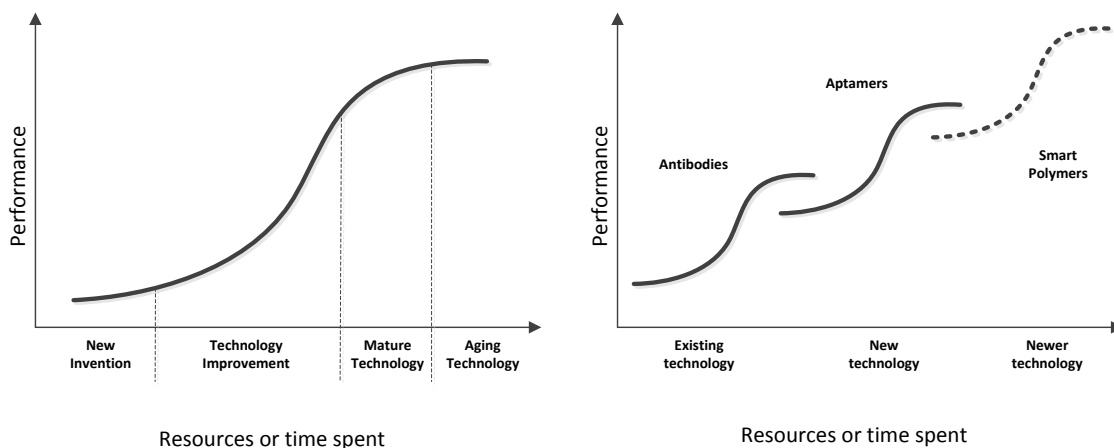


Figure 3: The technology S-curve concept. Left: New inventions at some point enter a phase of rapid performance improvement that later slows down as the technology matures. Right: A hypothetical succession of technology S-curves that could occur in the field of recognition and targeting molecules.

Many of the above mentioned aspects and the dynamic and diverse research environment in the field of aptamers support the hypothesis that aptamer technology has not reached this saturation yet. The future will show in which part of the “technology improvement” section aptamer technology is today. It is quite possible that there is still a huge increase of aptamer applications ahead.

3.2.1 Cell-SELEX

Cell-SELEX describes the process of generating cell specific aptamers by using whole cells as targets in the selection. A schematic of the approach is depicted in **Figure 4**. A pool of random oligonucleotides is incubated with live cells followed by the separation of bound from unbound sequences and the amplification of the bound species. The whole process is then repeated in successive cycles (31,32). A counterselection using non-target cells can be employed to eliminate sequences that bind common and ubiquitous structures which are cell type unspecific. At the end of the Cell SELEX

process the selected oligonucleotide population with the enriched aptamers is cloned and sequenced to identify the cell binding oligonucleotides. The enrichment of aptamers is typically analysed by flow cytometry. Fluorescence-labelled sequences derived from the selected pools are incubated with their target cells and then subjected to flow cytometry to measure the amount of binders. With proceeding rounds of selection the fluorescence signals should increase because more aptamers are enriched. Alternatively the enrichment of sequences can be monitored by next generation sequencing, which also makes the final cloning step unnecessary (33).

The selection with whole cells is more efficient than using isolated targets because the molecule is present in its native environment presenting its “real” fold. If it is known that the target molecule requires the cell membrane or other co-receptors for proper folding, a Cell-SELEX is mandatory. Another option is the use of membrane fractions of cells, which has also been shown to yield functional aptamers (34).

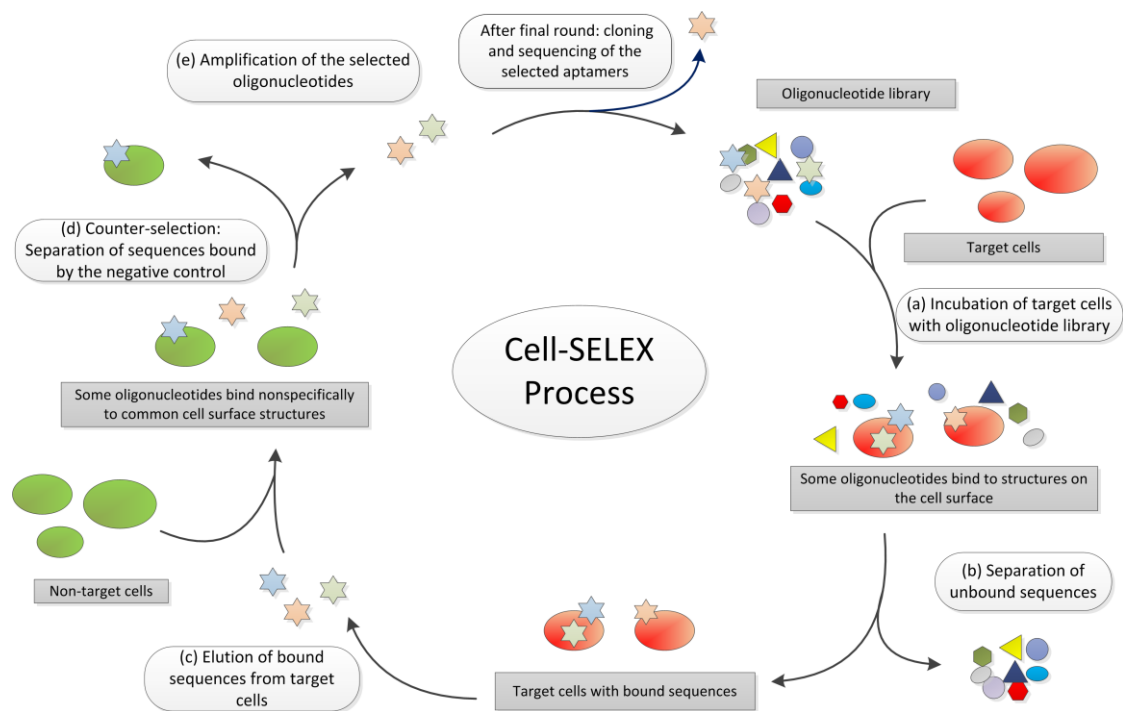


Figure 4: Schematic presentation of the Cell-SELEX process (2).

In theory, any types of cells can be distinguished by employing non target cells in a counterselection step. This makes the Cell-SELEX approach a promising tool for the development of new reagents in cancer diagnostics, therapy and research applications. An interesting fact is that there is no need for prior knowledge of the target molecule, as the aptamer evolves to the target on the cell surface during the selection process. This is very promising for the discovery of new biomarkers that are correlated to certain

diseases (35). A proof of concept has been shown for a case, where the aptamers target was separated and subsequently identified by mass spectrometry after a successful Cell-SELEX (36,37). The vast majority of the aptamer targets resulting from Cell-SELEX are proteins, although there are indications that it is also possible to select aptamers against other cell surface structures like carbohydrates and lipids (38).

Different protocols for the implementation of the Cell-SELEX process have been published (39–41). A critical task is the separation of cell bound sequences from unbound sequences. This issue is complicated by the presence of dead cells during the selection. These cells are often fragmented or exhibit no intact membrane so that oligonucleotides can bind to intracellular or released DNA or RNA impairing the enrichment of aptamers (42). One option is to separate the cell-bound species by a simple centrifugation step that yields a pellet with the cells and the bound aptamers (43). Another approach is the use of fluorescence-activated cell sorting, which also helps to exclude dead cells with unspecifically bound sequences from the enrichment process (**Figure 5**).

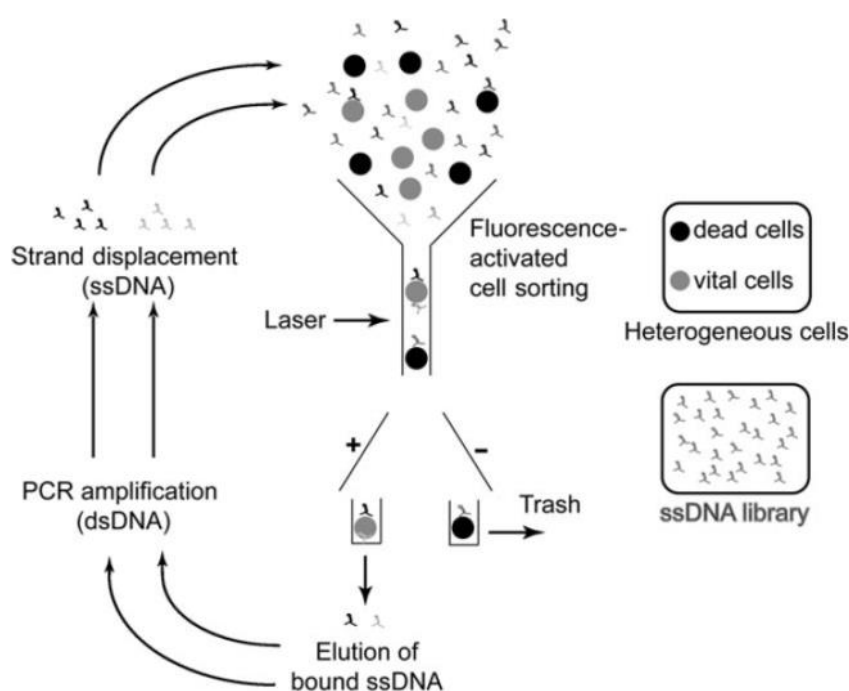


Figure 5: CELL-SELEX using a fluorescence-activated cell sorter (FACS) (41).

Aptamers have been successfully selected by the Cell-SELEX process against a variety of cells including eukarya (44), bacteria (45), and also virus-infected cells (46).

3.2.2 Current applications of aptamers in flow cytometry

Aptamers as cost-effective labelling probes meet an increasing demand for bioanalytical assays. The ageing populations in western societies will lead to an even higher need for technologies to detect abnormal and degenerated cells. The WHO “World Cancer Report 2014” estimates that until 2025 the number of people diagnosed with cancer will rise to about 20 million, an increase of 40 % from today's figures (47). For the successful outcome of the treatment, early detection is a crucial factor. The development of cost effective sample analysis with aptamers could help to improve the early screening of patients worldwide. A large part of this screening could be done using flow cytometry assays.

Aptamers have been applied in various applications as probes for flow cytometry, including cell-phenotyping, detection of cancer cell lines, virus-infected cells and pathogens. This topic has recently been summarized in a comprehensive review (2).

Table 1: Applications of aptamers in flow cytometry (2):

Application	Example	Reference
Labelling of cell surface markers	Labelling of CD4 positive cells	Zhang <i>et al.</i> 2010 (28)
Cancer cell detection	Detection of small-cell lung cancer	Chen <i>et al.</i> 2008 (56)
Bacterial pathogen detection	Detection of <i>Staphylococcus aureus</i>	Cao <i>et al.</i> 2009 (65)
Food-contamination analysis	Detection of <i>Campylobacter jejuni</i>	Dwivedi <i>et al.</i> 2010 (67)
Environmental water analysis	Detection of <i>Vibrio parahaemolyticus</i>	Duan <i>et al.</i> 2012 (66)
Detection of virus infected cells	Vaccinia virus infected cells	Tang <i>et al.</i> 2009 (68)

Aptamers have already been selected against various cancer cell lines including lymphomas (44), brain (48), lung (49,50), breast (51), prostate (52) and liver (53,54).

Especially in small-cell lung cancer (SCLC), early detection is very important, because the cancer cells are quickly disseminating and building metastases (55). Aptamers against SCLC cells have been generated using Cell-SELEX and used in various assay formats (56). The specificity has been enhanced by using non-small cell lung cancer (NSCLC) for counter selection. The selected aptamers were able to distinguish between the two cell types, something that is hard to achieve with common antibody assays (57).

Subtyping lung cancer patients with this aptamers could help to save NSCLC patients from disproportionately harsh treatments. Another reported case for aptamers targeting lung cancer cells showed the successful discrimination between lung adenocarcinoma cells and normal lung epithelial cells (58).

A critical point is the adaption of the selected aptamers to analysis of real clinical samples derived from patients. These samples often have a complex composition and contain substances that can interfere with the aptamer. Shangguan *et al.* achieved promising results with aptamers evolved with cultured cancer cell lines that were also able to detect differences in real patient samples (53). This fuels hope that a transfer of aptamers developed with cell lines in the lab to routine clinical diagnostics could be feasible.

Table 2: Aptamers for cancer cell detection by flow cytometry (modified from (2)):

Aptamer	Target cell line	Cancer type	Target molecule	DNA/RNA	References
HCA12, HCC03, HCH07, HCH01	NCI-H69	small cell lung cancer	unknown	DNA	Chen <i>et al.</i> 2008 (56)
EJ2, EJ4, EJ5, EJ7, etc.	H23	lung adenocarcinoma	unknown	DNA	Jiménez <i>et al.</i> 2012 (58)
apt1	Karpas 299	Hodgkin's lymphoma	CD30	RNA	Zhang <i>et al.</i> 2009 (61)
CD4 aptamer	Jurkat	T cell leukemia	CD4	RNA	Zhang <i>et al.</i> 2010 (28)
sgc3, sgd2, sgd3, sgc4, sgc8	CCRF-CEM	T cell leukemia	unknown	DNA	Shangguan <i>et al.</i> 2006 (44)
A9, A10	LnCaP	prostate adenocarcinoma	PSMA	RNA	Lupold <i>et al.</i> 2002 (52)
E9P2-2	U251	brain cancer	Tenascin-C	RNA	Hicke <i>et al.</i> 2001 (48)
A30	MCF7	breast cancer	HER3	RNA	Chen <i>et al.</i> 2003 (51)
SYL1, SYL2, SYL3, SYL4	HT-29 (e.g.)	colorectal adenocarcinoma (e.g.)	EpCAM	DNA	Song <i>et al.</i> 2013 (60)

Another example for an application aimed at cancer cells can be found in the work published by Shigdar *et al.* (59). They developed an RNA aptamer against the cancer stem cell marker EpCAM (CD326) and demonstrated that it was able to bind certain cancer cell lines that are known to express the stem cell marker. Other cancer cell lines that did not express the marker were not bound by the RNA aptamer. Another group

recently reported a DNA aptamer against EpCAM, which is preferred because DNA has a higher stability than RNA (60). Further molecules of the cluster of differentiation (CD) class were used as targets in the SELEX process and yielded functional aptamers that bound corresponding cell types, including CD30 (61) and CD4 (25).

All of the promising results described above have to be considered critically before becoming over-optimistic and expecting the fast emerging application of aptamers in routine clinical diagnostic. The Ellington group revealed that some aptamers, which were reported to be specific targeting agents, showed considerable binding to a variety of non-target cell lines (62).

Besides cancer cells, aptamers have been used for the detection of pathogens by flow cytometry. Whole bacteria cells and also viruses were employed as targets for aptamer selection in Cell-SELEX processes (63). This strategy provides new approaches for the detection of pathogen contaminated samples from environmental or food samples.

A standard protocol for bacterial Cell-SELEX has been published with the organism *Lactobacillus acidophilus* as target (45). A modified approach using cell sorting by flow cytometry was recently reported by Dwivedi *et al.* (64) for a Cell-SELEX with the *Salmonella* serovar Typhimurium. An example with huge potential application is the selection of aptamers targeting the gram positive bacterium *Staphylococcus aureus* (65). Other aptamers with a potential application are described for the analysis of environmental samples for the presence of the pathogen *Vibrio parahaemolyticus* (66) or the analysis of food samples to detect *Campylobacter jejuni* (67).

Table 3: Aptamers against pathogens for detection by flow cytometry (2):

Aptamer	Target pathogen	Target molecule	DNA/RNA	References
hemag1P	<i>Lactobacillus acidophilus</i>	S-layer protein (putative)	DNA	Hamula <i>et al.</i> 2008 (45)
SA20, SA23, SA31, SA34, SA43	<i>Staphylococcus aureus</i>	unknown	DNA	Cao <i>et al.</i> 2009 (65)
20A9P, 20A9, 20A24P, 20A12P, 20A14P, 15A3P	<i>Streptococcus pyogenes</i>	unknown	DNA	Hamula <i>et al.</i> 2011 (63)
ONS-23	<i>Campylobacter jejuni</i>	unknown	DNA	Dwivedi <i>et al.</i> 2010 (67)
A1P, A1, A3P, A3	<i>Vibrio parahaemolyticus</i>	unknown	DNA	Duan <i>et al.</i> 2012 (66)

ST2P, ST2, ST9P, ST9, S8-46, S8-7	<i>Salmonella</i> Typhimurium	unknown	DNA	Duan <i>et al.</i> 2013 (84); Dwivedi <i>et al.</i> 2013 (64)
TV01, TV02, TV07, TV08	Vaccinia virus	unknown	DNA	Tang <i>et al.</i> 2009 (68)

Aptamers derived from Cell-SELEX have also shown to be capable of distinguishing between virus infected and uninfected cells. Tang *et al.* demonstrated this for vaccinia virus-infected lung cancer and Hela cells (68,46).

Aptamer detection probes like the ones listed above could be useful for improved detection of various diseases caused by infectious agents which are on the rise again according to WHO reports (69).

The application of aptamers for staining cell surface molecules is investigated in the experimental part of this thesis.

3.2.3 Aptamer-quantum dot conjugates as probes for flow cytometry

For the use of aptamers as recognition tools in flow cytometry, they have to be modified with fluorophores that can be excited and detected. A certain class of nanoparticles, so called quantum dots (QDs), have recently attracted huge interest by researchers working with fluorescence assays (70). QDs are inorganic semiconductors with a size between 4 and 8 nm and show unique optical properties leading to narrow emission and broad absorption spectra, enhanced photostability and high quantum yield (71). **Figure 6** shows examples for the absorption and emission spectra of CdSe QDs.

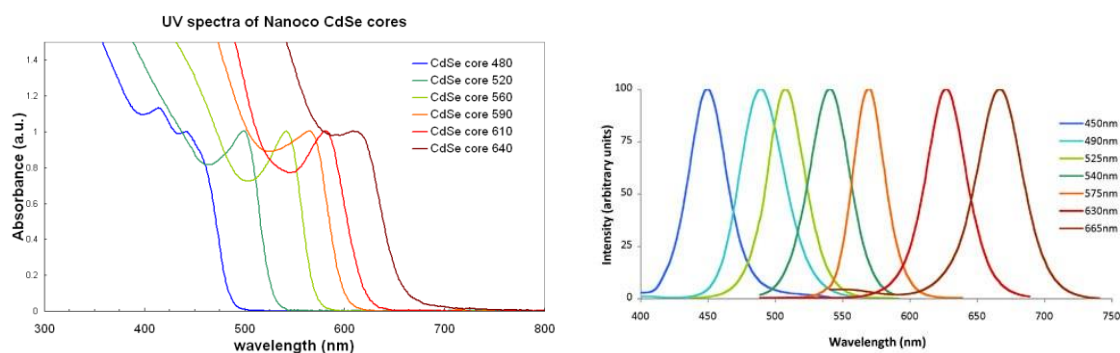


Figure 6: Absorption and emission spectra of CdSe quantum dots (72,73).

The emitted colours are depending on the size of the QDs and are red-shifted for increasing sizes **Figure 7**. Especially the possibility to excite various different QDs with the same excitation wavelength presents an advantage for the application in multicolour flow cytometry analysis using a single laser source (74,75).

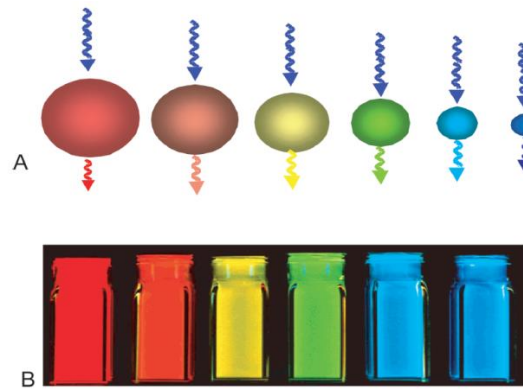


Figure 7: The emitted fluorescence of quantum dots is dependent on their size (76).

Another interesting feature of QDs is that they can be modified with certain functional molecular groups and easily coupled to other molecules like antibodies or aptamers (77–79). Several aptamer-quantum dot conjugates have been tested for purposes like imaging and targeting prostate cancer cells (80,81), mouse liver cancer cells (82), human leukemia cells (83) and bacteria (84,85). Some of the applications used other bioanalytical assays than flow cytometry but in principle the detection should be transferable to this assay format.

3.3 Immobilisation of aptamers on the cell surface

The cell surface has been recognized as a fertile ground for modifications to manipulate cell functions and phenotypes. Different approaches have used this strategy for basic research but also for development of targeting mechanisms for cell therapy applications (86–93). For example Dennis *et al.* engineered the surface of mesenchymal stem cells by immobilising an antibody to target the cells to activated endothelial cells (94). The immobilisation of molecules on the surface is not restricted to antibodies and has also been shown for DNA (95).

There are two described approaches for immobilisation of molecules on the cell surface, that have both proved to work for aptamers as well as antibodies. Schematic drawings of the methods are shown in **Figure 8**. The first involves the chemical modification of amine groups exposed by molecules on the surface. The amine groups are treated with sulfonated biotinyl-N-hydroxy-succinimide (NHS) to couple biotin groups onto the cell. This step is followed by addition of the tetrameric protein streptavidin, which binds to the biotin and subsequently offers unoccupied binding sites. These binding sites are then used to attach biotinylated recognition molecules like aptamers (96). The second approach uses aptamers (or antibodies) that are modified with a lipid anchor (e.g. cholesterol or fatty acids) that is incorporated into the lipid bilayer of the cell membrane via hydrophobic interactions (97).

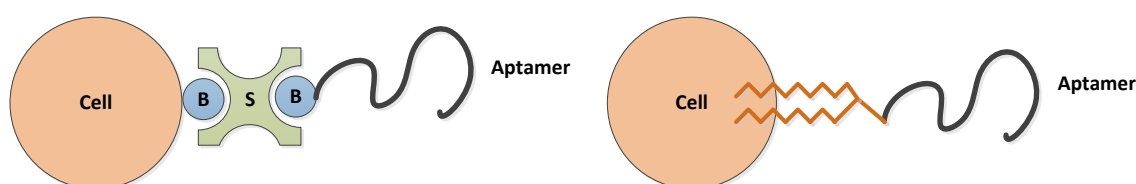


Figure 8: Reported approaches for immobilising aptamers on the cell surface. Left: Immobilisation via a streptavidin/avidin bridge. Right: Immobilisation using a hydrophobic anchor.

The current applications of cell-immobilized aptamers are confined to the field of cell-surface sensors, where they are used for real time probing of cellular environments (98) and imaging of chemical transmitter dynamics (99). The approach used by Zhao *et al.* to detect the concentration increase of PDGF in the environment of mesenchymal stem cells is shown in **Figure 9**. The cells are modified with a PDGF aptamer, that carries a fluorophore and a quencher molecule. In the presence of PDGF the aptamer undergoes a

structural change and emits fluorescence which can be detected by fluorescence microscopy. The system has been used to study mesenchymal stem cells in mouse bone marrow.

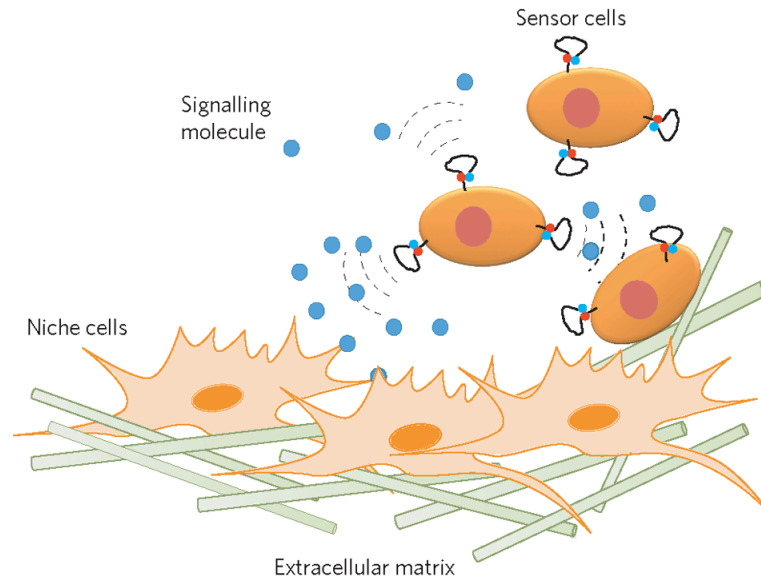


Figure 9: Basic principle of the cell-surface sensor developed by Zhao *et al.* (98). The sensor cells are modified with an aptamer and detect signalling molecules which are released by the surrounding cells. The detection works via a fluorophore-quencher system that emits fluorescence after binding of the signalling molecule.

3.3.1 High-producer screening for cell line development

Therapeutic proteins produced by cell culture processes have advanced medical treatments tremendously over the past two decades. The number of approved drugs of this class increases steadily. During the years 2006-2011 the US Food and Drug Administration (FDA) approved 15 novel recombinant protein therapeutics per year. The most successful therapeutics of this class by sales are monoclonal antibodies (mAbs) which account for an annual revenue of about 100 billion US\$ and have been called “magical bullets” because of their directed and effective mechanism of action (100). This development, together with the advent of biosimilars and the large number of new biologics in the pipeline of pharmaceutical companies raises the demand for production cell lines with high productivity (101).

Although many efforts are currently under way to increase the productivity of protein manufacturing by improving process technology and media composition of the cell culture production process (102), the key component of the biotechnological process

will always be the cell. Although alternatives like improved transient transfections with high product titers have been reported and are further explored (103), the method of choice for the production of antibodies will be based on stable transfected cell clones for a foreseeable future. The initial transfection with the product gene is usually done with 10^8 cells of which ~60% get the plasmid. The resulting cell population is highly heterogeneous, because the product gene can be integrated at various sites of the host genome leading to a high variability of production characteristics (104). A huge interest has therefore been focused on strategies to screen cell populations and isolate individual clones with high productivity characteristics (105). The whole process from the initial transfection of the cells to the generation of stable clones for large scale pharmaceutical production is termed cell line development. In order to obtain correct post translational modifications of the therapeutic protein, mammalian cell lines are used for production of the majority of recombinant therapeutics (106). Chinese hamster ovary cells (CHO) present the most important cell line which is used in many processes because of their human-like glycosylation and have been engineered for improved production characteristics (107). Although CHO cells are used in various production processes, they exhibit some disadvantages compared to other production cell lines. Unlike mouse myeloma cells (NS0), CHO cells originate from ovary cells, which are no professional secretors and hence do not possess a highly evolved protein secretion machinery. Another disadvantage of CHO cells is their genetic instability which can result in the loss of production capability or product quality (108). The factors contributing to enhanced productivity have been investigated in various studies aimed at understanding the cellular physiology (109). **Figure 10** shows an overview of the combination of attributes that are needed to yield a hyperproducer. Besides energy metabolism, redox balance and growth/death control, the cells capability of protein secretion is a key characteristic that needs to be highly developed to render it a high producer.

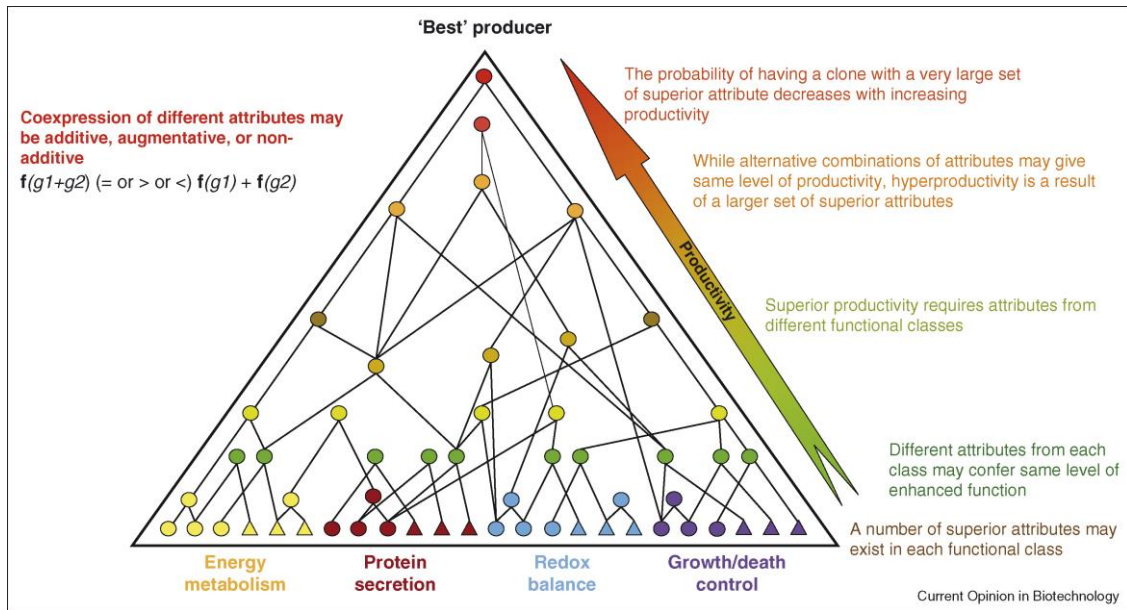


Figure 10: A high producing cell clone exhibits a combination of multiple highly developed traits that render it capable of synthesising and secreting large quantities of protein while still showing good growth characteristics (109).

The analysis of the cells secretory performance is a good starting point for evaluating the suitability for production processes. Different approaches for the analysis of single cell protein secretion have been developed to screen transfected cell populations for this trait (110). Many of these approaches use flow cytometry with cell sorting to identify and isolate single cells of interest for further characterisation. The assays that are used to assess the specific secretion of cells by flow cytometry use capturing of the product secreted by individual cells in its vicinity. Subsequently the relative product concentration can be determined by labelling it with antibodies and finally correlating its concentration with the cells secretory performance. Methods reported so far include gel microdrops with encapsulated cells, cold capture and affinity capture.

The screening based on gel microdrops is based on the isolation of single cells by encapsulating them in a gel matrix that retains the product secreted by the cell. The gel used for this purpose is typically made of biotinylated agarose, which is then modified with streptavidin and, in a next step, with biotinylated antibodies that capture the product (111). An advantage of the approach is the restricted diffusion of the product, which is partially held back by the porous gel matrix and prevented from attaching to other cells, causing false positive signals. A drawback is the necessity to recover the cells from the gel microdroplets, mostly by enzymatic treatment (112). The screening has been successfully applied to select secreting hybridoma cells out of a mixed population with low and non secreting cells (113).

The cold capture screening method has been used successfully for some hybridoma and CHO cell lines and showed fairly good results (114,115). The basic principle behind the correlation was deciphered by Pichler *et al.* who demonstrated that the anti-product antibodies precipitate with the product because of high local concentrations at the sites of product release from vesicles at the cell surface (116).

Another screening approach is based on the modification of the cell surface with an affinity matrix that captures the secreted product and allows the detection of the captured proteins by labelled antibodies. The affinity matrix was originally developed to sort lymphocytes according to secreted cytokines but soon discovered to work as well for production cell lines (117,118,11). The method requires the immobilisation of anti-product antibodies on the cell surface, which is achieved by biotinylation of the surface followed by incubation with streptavidin which serves as a bridge or connector to immobilize the biotinylated antibody (see section 3.3). A schematic of the assay structure is shown in **Figure 11**.

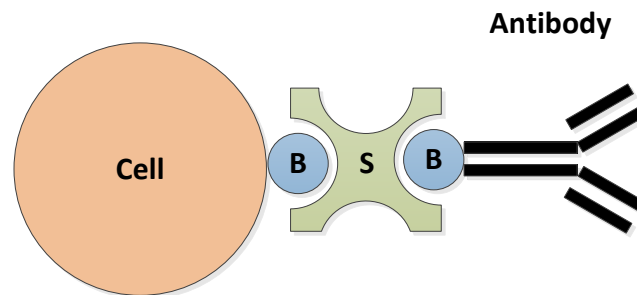


Figure 11: Schematic drawing of the antibody affinity matrix. The biotinylated antibody is immobilised via a streptavidin/avidin (S) bridge that binds biotin (B) molecules on the modified cell surface. For illustrative purposes only one bound antibody is shown and sizes are disproportional.

The use of avidin as a connector molecule multiplies the binding capacity because the tetrameric protein offers three docking sites for antibodies after immobilisation on the biotinylated cell surface. After modification the cells are transferred to a medium of high viscosity to restrict the diffusion of secreted proteins and reduce cross contamination of neighboring cells. The cells are then incubated to give them time to secrete their product. After a certain time the cell-bound product is detected by a second labelled antibody and the cells are sorted according to their fluorescence signal. The highest signals should be caused by cells with a strong secretory machinery. The time used for incubation of the modified cells is crucial, as the binding sites on the cells are

limited and will get saturated with product after a certain time, eventually prohibiting a differentiation of high and low producers (119).

Although screening of transfected cells in order to select clones suited for production of pharmaceutical proteins is tedious and time consuming, it is still required to establish economically viable processes for large scale production. The use of an antibody affinity matrix, which is a preferred method for screening, is hampered by several issues. Firstly the procedure of applying the matrix involves several steps that are potential stress to the cells and lowering the viability. Secondly the matrix consists of proteins (avidin, antibodies) from recombinant or animal sources that have to comply with strict regulations or are even prohibited by authorities for use in pharmaceutical production. A screening method based on immobilised aptamers would present an attractive alternative to the above described approaches and circumvent the mentioned problems. This topic is investigated in the experimental part of this thesis in section 4.2.

4 Experimental investigations

The aim of this work is to demonstrate the application of aptamers in flow cytometry assays. The experimental investigations shown below address this aim and show the use of aptamers in two different types of assays. The investigations are therefore divided into two sections. The first shows the use of aptamers for staining cell surface proteins and the fabrication and testing of aptamer quantum dot conjugates for this purpose. The second part describes the initial development of an assay for screening high secreting cells based on cell-immobilised aptamers and flow cytometry analysis.

4.1 Aptamers as stains for cell surface proteins in flow cytometry

The experimental investigations on the use of aptamers as stains for flow cytometry were performed with a model system consisting of the DNA aptamer TD05. The aptamer was selected in a Cell-SELEX process by Mallikaratchy *et al.* by using Ramos (Burkitt's lymphoma) cells as targets (17). The group subsequently published their efforts to decipher the target molecule on the cell surface and suggested membrane bound IgM as target (137). Because of problems reported with the specificity of Cell-SELEX derived aptamers (62), basic investigations were performed initially to verify the binding of TD05 to the supposed target. The experiments were done using simple protein microarray binding assays with IgM and other non-target proteins. Afterwards the binding of TD05 to Ramos cells and non-target cells was analysed by fluorescence microscopy before transferring the analysis to the flow cytometry format. Finally the aptamer was used for the fabrication of aptamer-quantum dot conjugates, which were then characterised and tested as labelling agents for flow cytometry.

4.1.1 Basic investigations of aptamer target binding for the model system TD05 and IgM using microarrays

Investigations were performed to verify the postulated target of the TD05 aptamer. Protein microarrays were chosen as simple test systems to check the binding of TD05 to isolated IgM. The assay was performed in the "reverse phase" format, in which the target protein is spotted onto a microarray support and then incubated with the

fluorescently labelled aptamer. A schematic of the assay is shown in **Figure 12**. Aldehyde functionalised glass surfaces were chosen as immobilisation substrates for the target protein. The aptamers were labelled with the fluorescence dye Cy3, a standard organic fluorophore, which is detectable with the used microarray scanner. Details concerning the preparation and analysis of the microarrays can be found in the appendix (6.1.1).

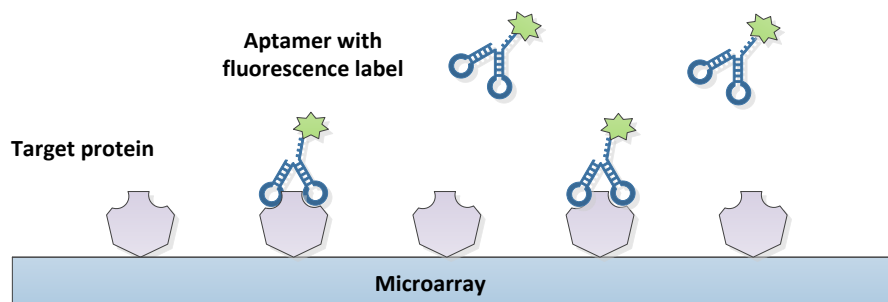


Figure 12: Schematic presentation of the used “reverse phase” microarray approach to investigate aptamer binding to the target protein.

The microarrays consisted of several blocks of spotted protein dots that comprised different IgM concentrations and also three negative controls. Bovine serum albumin (BSA), *Pseudomonas* fluorescence esterase I (PFEI) and fetal calf serum (FCS), a protein mixture, were used as negative controls. **Figure 13** shows the predicted structure of the TD05 aptamer and a typical scan from a used microarray. The coloured dots are spotted target proteins that are detected by the fluorescence labelled aptamer. Target concentrations decrease to the right and the negative controls on the far right do not yield any visible signal. After acquisition the images were analysed with the software GenePixPro 6.0 (Molecular Devices LLC, USA) to quantify the measured fluorescence intensities.

A comprehensive analysis was set up which involved two differently labelled versions of the aptamer TD05, which were modified with Cy3 either at the 3'-terminus or at the 5'-terminus. Although the predicted two dimensional structure of TD05 appears to be more or less symmetrically, in reality there can be influences caused by the position of the fluorescence label.

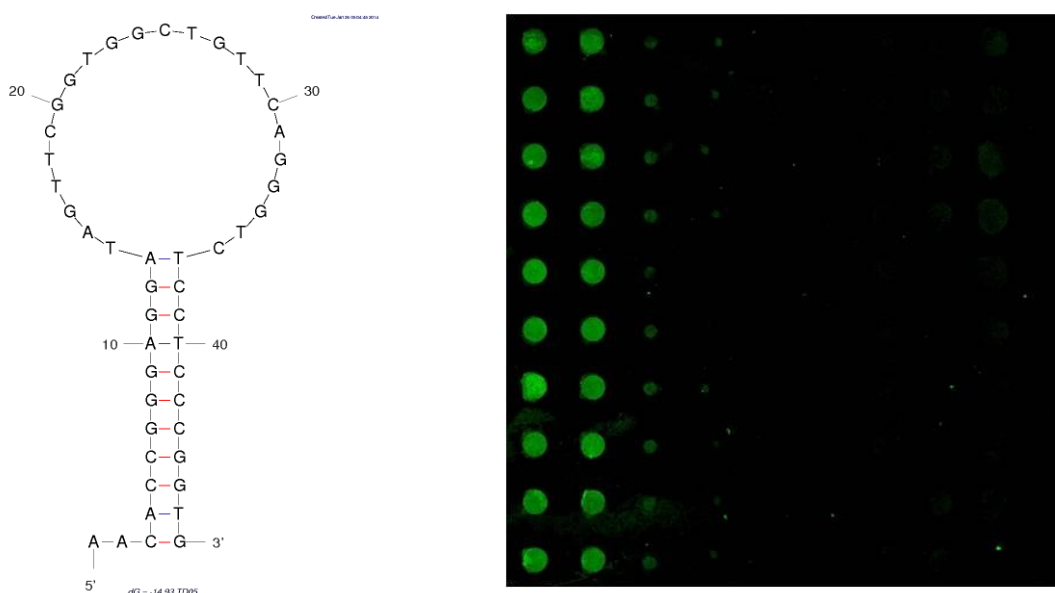


Figure 13: Left: Structure of the aptamer TD05 calculated using the tool Mfold (120). Right: Image of a microarray block with TD05 3'-Cy3 stained IgM spots. Aptamer concentration 400 nM; laser power 100 %; gain 300. Further details can be found in section 6.1.1.

In addition to the negative controls on the target site, further negative controls were introduced on the site of the aptamer. A defined random oligonucleotide sequence of the same length as TD05 was generated using the online tool “Random DNA Generator” provided by the Maduro lab at the University of California in Riverside. The sequence was also used with a Cy3 modification at the 3'-terminus. The sequences of all used oligonucleotides are listed in section 6.2.5. A second negative control was conceived of a pool of random sequences of 47 nucleotides in length. This control is termed “sequence pool” or “pool” in the following sections. The pool, as all other probes, were obtained with a Cy3 modification from a DNA synthesis company (Biospring GmbH) and estimated to contain 10^{14} different sequences in 60 nmol (information from the supplier).

Figure 14 shows the signal intensities resulting from the microarray analysis for both aptamer variants and the negative controls. It can be seen that the TD05 3'-Cy3 shows the highest signal intensities and hence binding of the aptamer to the spotted target protein IgM. The signals from the protein negative controls are substantially lower. These negative controls were all used with the same concentration as the highest target protein concentration (1 mg/ml). The 5'-Cy3 labelled TD05 shows much weaker binding to the target protein, with signal intensities just slightly above that of the random or pool negative control.

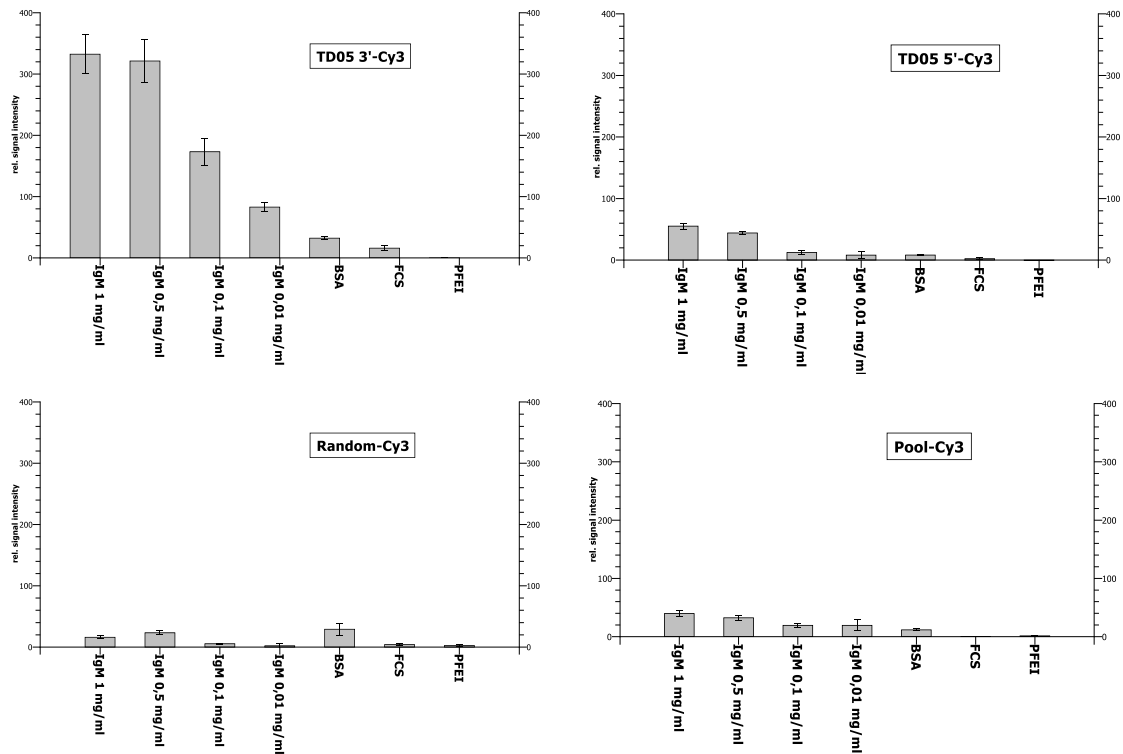


Figure 14: Comparison of the 3'- and 5'-labelled TD05 and the random and pool negative controls. All aptamers and oligonucleotides were used with a concentration of 800 nM. Concentrations of protein negative controls BSA, FCS and PFEI were 1 mg/ml. Scanner settings: Power 100 %; gain 300.

The data reveals a clear influence of the label position for the used aptamer TD05. The 3'-terminus labelled variant is clearly superior with regard to target affinity. **Figure 15** shows a direct comparison and underlines this predominance. It can be concluded that the 5'-terminus labelled aptamer seems to be dysfunctional, which is probably caused by an impaired structural fold through the Cy3-fluorophore.

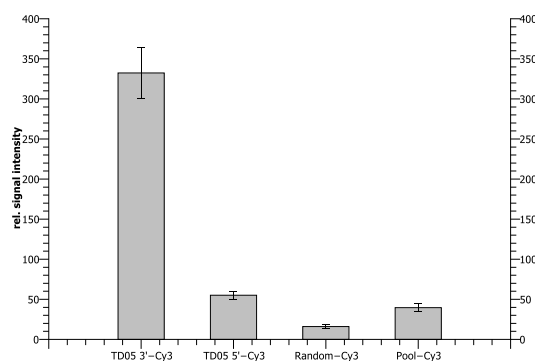


Figure 15: Direct comparison of the signal intensities for the 3'- and 5'-labelled aptamer and the negative controls. The values are derived from the 1 mg/ml IgM spots incubated with 800 nM aptamer or negative control. Scanner settings: Power 100 %; gain 300.

The microarray experiments confirmed the affinity and specificity of the TD05 aptamer for the postulated target IgM. They also revealed a probable susceptibility to misfolding of the aptamer depending on the labelling position.

4.1.2 Detection of TD05 binding to IgM beads by flow cytometry

After confirming the binding of the aptamer model system by microarray analysis, the target protein IgM was immobilized on small microbeads (Dynabeads-280-tosyl) to transfer the analysis of TD05 binding into the flow cytometry format. The aptamers were now used with the fluorescence label FITC, which is an optimal fluorophore for the flow cytometers excitation with a blue (488 nm) laser.

The target protein IgM and the negative control BSA were immobilised on microbeads and subsequently incubated with 10 μM of TD05 3'-FITC as described in 6.1.3. After incubation the beads were analysed by flow cytometry. 10,000 events were recorded and analysed for their fluorescence in the FL1 detector, which collects green light as emitted by FITC. **Figure 16** left shows an overlay of the histograms for the BSA-modified beads (without filling) and the IgM-modified beads (red filling). The fluorescence intensities of the IgM beads are higher which can be seen by the shift to higher FL1 values (towards right). This was also confirmed after analysis of the fluorescence mean values for both samples in **Figure 16** (right).

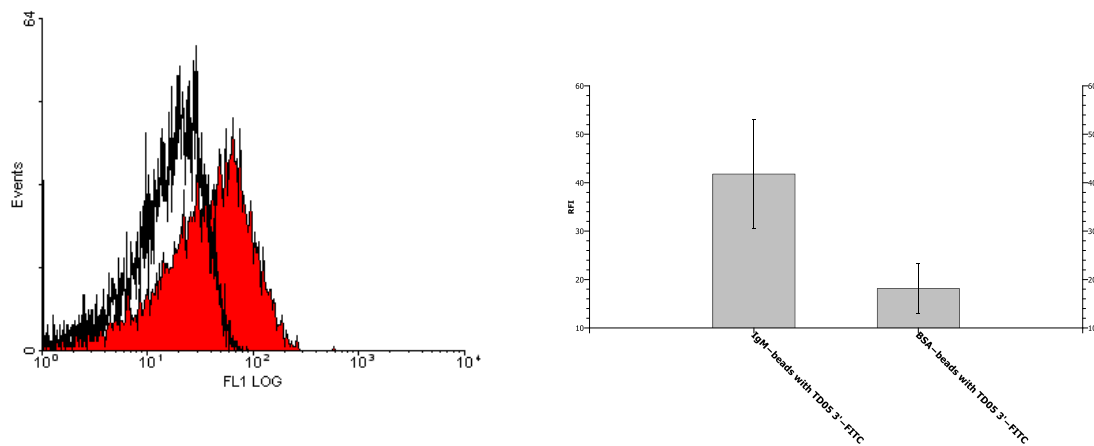


Figure 16: Left: Overlay of the histograms for the IgM beads (red filling) and the negative control BSA beads (no filling). Right: Fluorescence mean values obtained from the histograms. The TD05 aptamer shows a higher binding to the beads carrying its target protein IgM.

It can be concluded that the binding of TD05 to its target protein can also be detected in a flow cytometric format, where the protein is immobilised on beads.

4.1.3 Microscopic investigations on TD05 binding to Ramos cells

Before starting the analysis of aptamer labelled Ramos cells by flow cytometry, the cells were stained and subjected to fluorescence microscopy analysis to confirm the specificity and binding to Ramos cells. CHO K1 cells were used as negative control.

Cells were cultured, prepared and incubated with 500 nM of the 3'Cy3 labelled TD05 aptamer as described in 6.1.2 and 6.1.9. **Figure 17** and **Figure 18** show pictures of unstained and stained cells that were taken in brightfield mode and with the microscopes filter suitable for Cy3 detection. None of the cells show any autofluorescence that would result in false positive signals after the staining process.

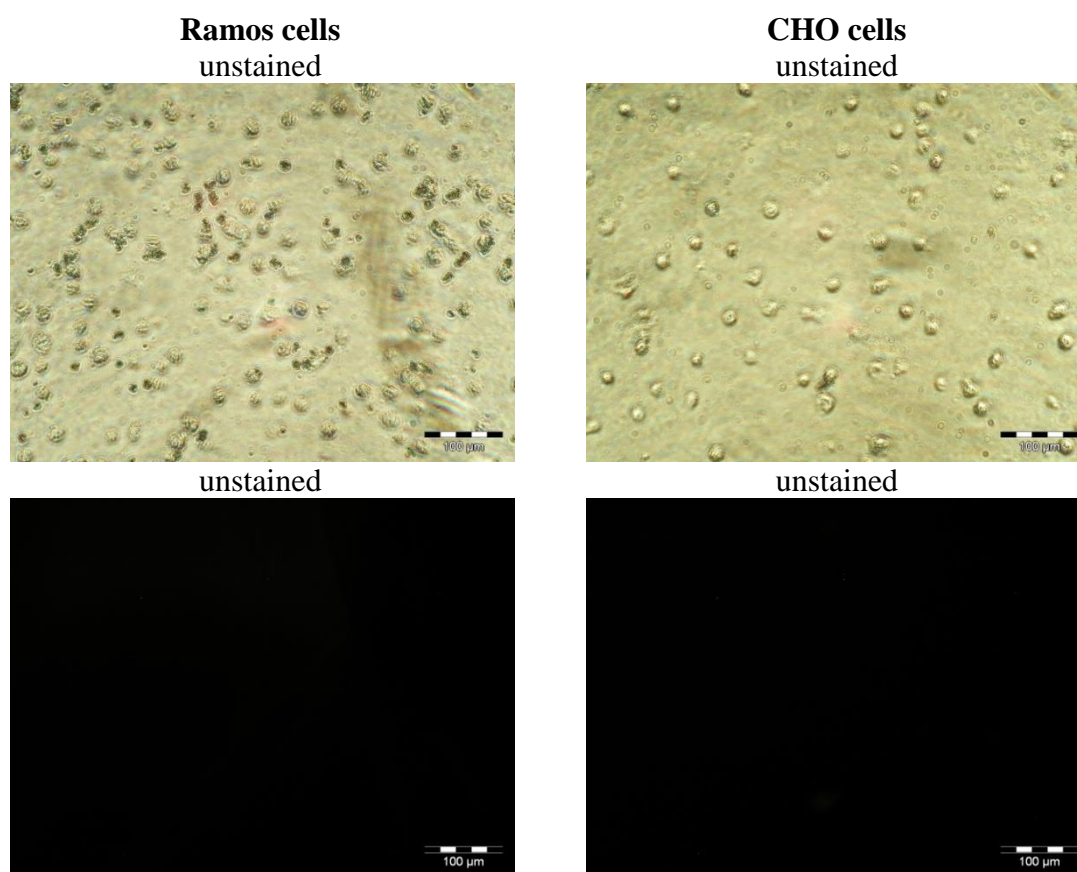


Figure 17: Microscopic analysis of unlabelled Ramos and CHO cells in brightfield mode (top) and with the NG filter (Exc. 530-550; Em. BA 590) which is later used for Cy3 detection (bottom). Both cell lines show no autofluorescence.

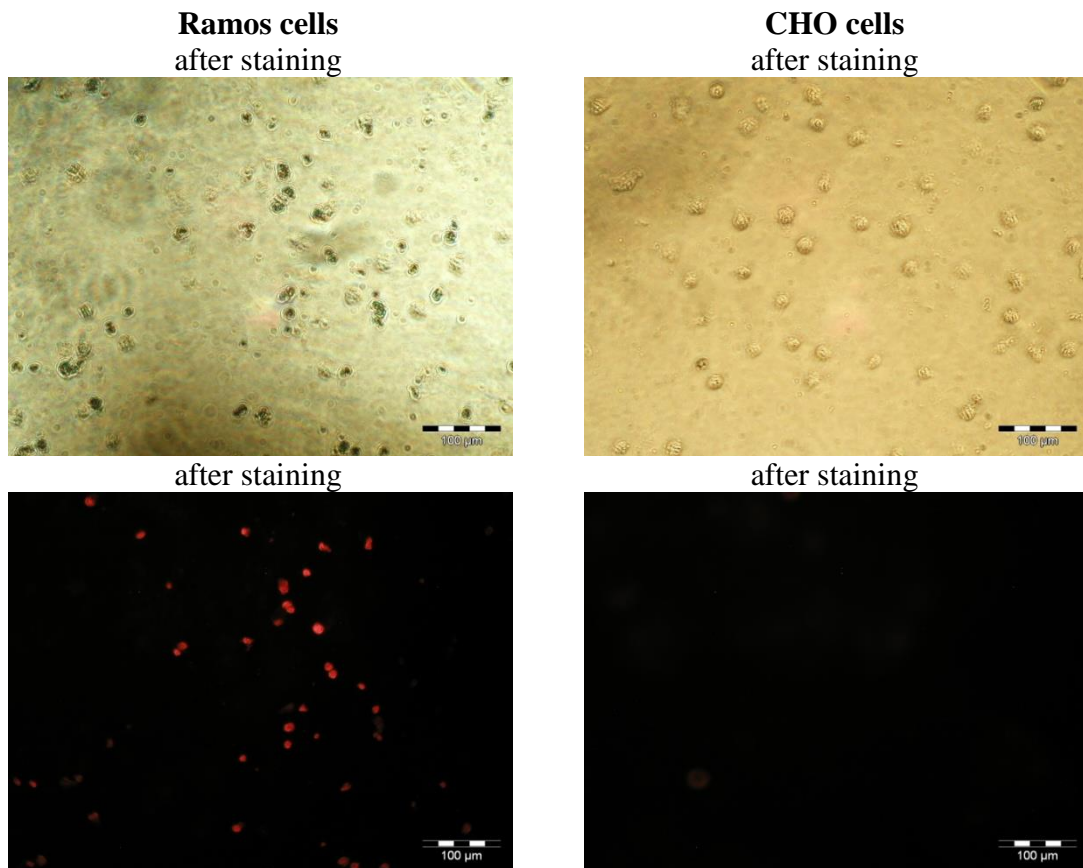


Figure 18: Microscopic analysis of TDO5-Cy3 labelled Ramos and CHO cells. Pictures were taken in brightfield mode (top) and with the NG filter (Exc. 530-550; Em. BA 590) to detect the Cy3 label. There is no observable binding to the negative control cells (CHO) whereas Ramos cells are stained by the aptamer.

Pictures of the aptamer stained cells are shown in the lower section **Figure 17**. The results confirm the binding of the TD05 aptamer to the Ramos cells, which are clearly stained. Only one or two faint signals are found on the picture showing the negative control cells resulting from unspecific binding.

4.1.4 Detection of TD05 binding to IgM on Ramos cells by flow cytometry

After demonstrating the ability to detect the binding of the aptamer to cells via fluorescence microscopy, it was finally tested with living cells in a flow cytometer. The original target cells which were used in the cell SELEX procedure were cultured and taken for the analysis.

The cells were prepared and incubated with 1 µM of FITC-labelled aptamers as described in 6.1.4. After incubation the cells were analysed by flow cytometry. The histograms resulting from the FL1 detector (FITC fluorescence) were subjected to a

marker analysis. The marker was set so that less than 1 % of the unlabelled cells were found in the marker region. The other samples were analysed and the percentage of cells falling into the set marker region served as an indication how many aptamers bound to the cell. **Figure 19** shows the principle of the marker analysis.

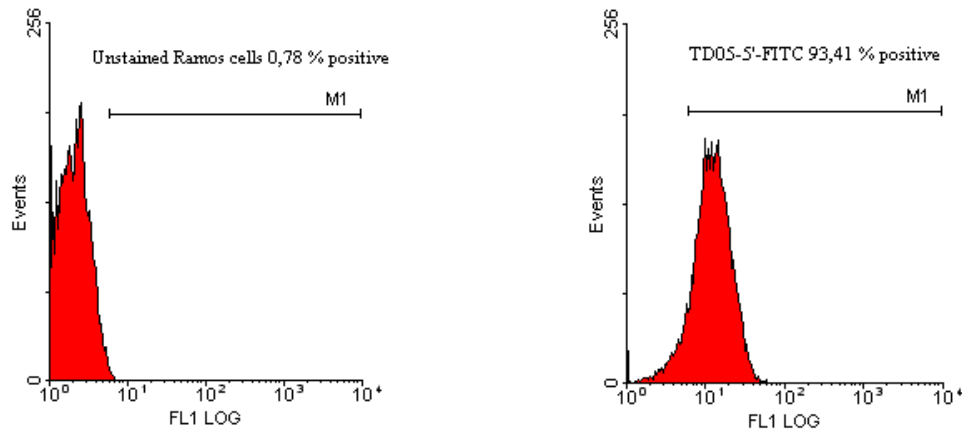


Figure 19: Principle of the marker analysis used to detect aptamer stained cells. Left: Unstained Ramos cells. Right: Ramos cells stained with the FITC labelled aptamer. The percentage of cells found in the marker region (M1) are denominated as positive.

The results are depicted in **Figure 20** were the percentage of cells stained with the aptamer can be seen. Again several negative controls were included in the experiment to assure the results. The random oligonucleotide and the sequence pool were incubated with the Ramos cells to test if the binding to the cell surface is unspecific and sequence independent. CHO K1 cells served as simple negative controls on the cell site to test the specificity and eliminate the possibility that the aptamer recognizes common structures generally found on the cell surface.

The data presents a clear specificity of the TD05 aptamer to the Ramos cells. The aptamer neither binds the non-target CHO cells nor does a comparison with the random and pool sequences reveal a general affinity of oligonucleotides to Ramos cells. In contrast to the microarray experiments there is no difference between the two differently labelled variants.

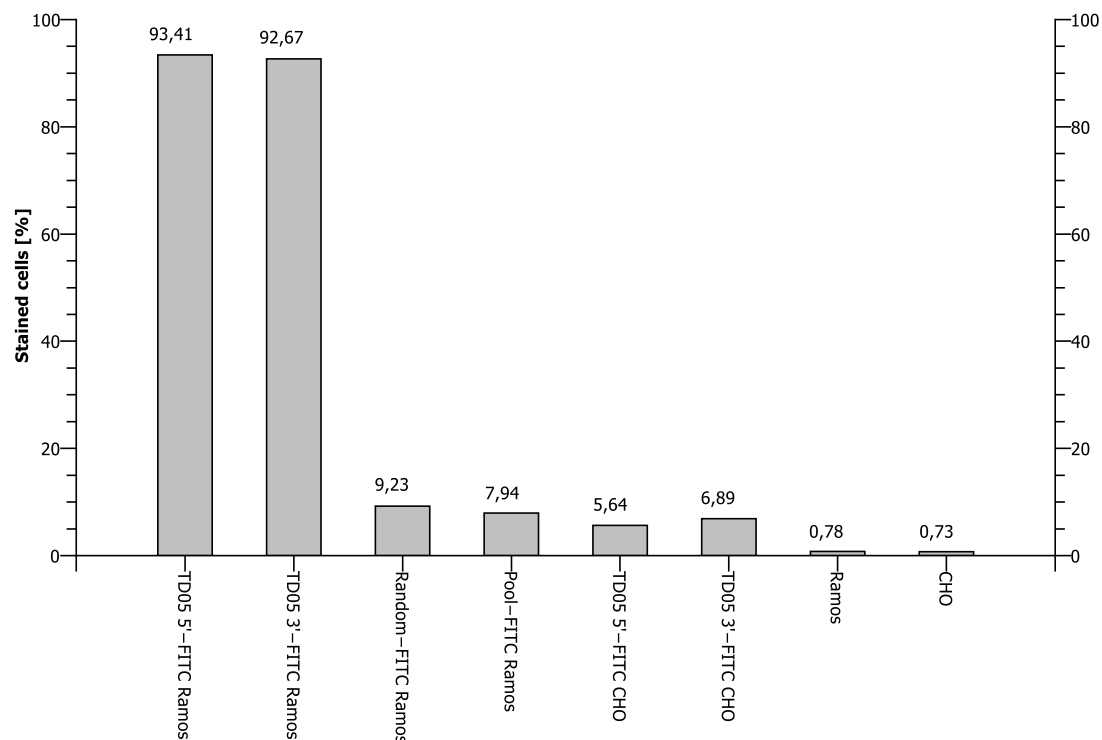


Figure 20: Comparison of Ramos and CHO cells labelled with the two aptamer variants TD05 5'-FITC and TD05 3'-FITC and the negative controls random and pool. The marker analysis shows that over 90 % of the Ramos cells are stained by the aptamers, whereas the unspecific binding to CHO cells stains less than 10 % of the cells. The percentage of Ramos cells stained by unspecific binding from random and pool are also below 10 %.

The reason for this is not obvious but it can be speculated that it is caused by the orientation and accessibility of the target protein for the 5'-labelled aptamer. For the microarray analysis the protein is spotted onto the microarray surface, resulting in a random orientation of the target molecule. On the cell surface, the IgM will have a more defined orientation that can be bound by the 5'-labelled aptamer. In the microarray assay this aptamer probably fails to bind most of the deposited IgM on the surface.

After confirming the specificity of the aptamer TD05 to Ramos cells, a concentration series of the two differently labelled aptamers was incubated with the target cells to estimate a binding constant for the interaction with the cell bound IgM (17).

The samples were prepared and incubated as described (6.1.1) and afterwards analysed by flow cytometry to measure the fluorescence of the cell bound aptamers. **Figure 21** shows the resulting fluorescence intensities for the different aptamer concentrations. The fluorescence reaches a saturation for concentrations over 100-200 nM. The comparison to the negative control consisting of the pool of labelled sequences confirms again the specificity of the binding.

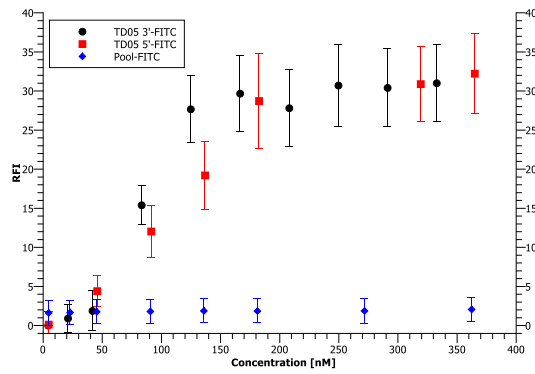


Figure 21: Analysis of Ramos cells incubated with concentration series of the two differently labelled TD05 variants and the negative control pool. The fluorescence reaches saturation for concentrations above 100-200 nM.

The data was used to fit a logistic function to the fluorescence values with the software QtiPlot (Figure 22). The estimated binding constant (K_D) can afterwards be extracted as the value of the inflection point (x_0) of the fitted curve. The analysis yields an estimated K_D of 82.89 nM for TD05 3'-FITC and an estimated K_D of 115.5 nM for TD05 5'-FITC. The obtained results are similar to the published values of ~75 nM for the aptamer TD05 (17).

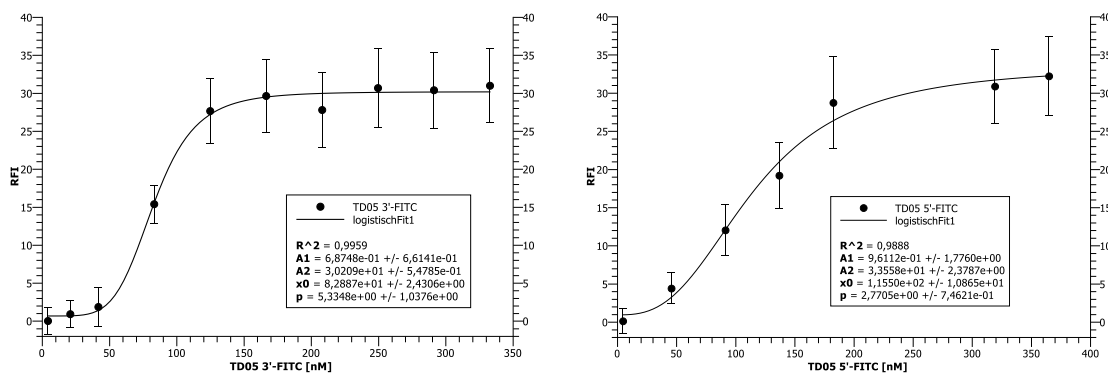


Figure 22: Plots show the curve fitting used to estimate the aptamers binding constants for the aptamer cell interaction. Left: TD05 3'-FITC with a K_D of 82.89 nM. Right: TD05 5'-FITC with a K_D of 115.5 nM.

Further experiments focused on the validation of the postulated target IgM, which is expected to be the cell bound target of the aptamer. Although the microarray analysis and cell binding studies support this assumption, an additional test was carried out to assure that the aptamers target is indeed a protein. This was done by incubating the Ramos cells with a solution containing proteinase K and comparing it to untreated cells in an aptamer binding assay. The proteinase K treatment should lead to a digest of protein structures on the cell surface, thereby destroying the target of the aptamer. The

sample preparation was done as described (6.1.5) and the cells finally subjected to the standard flow cytometry measurement.

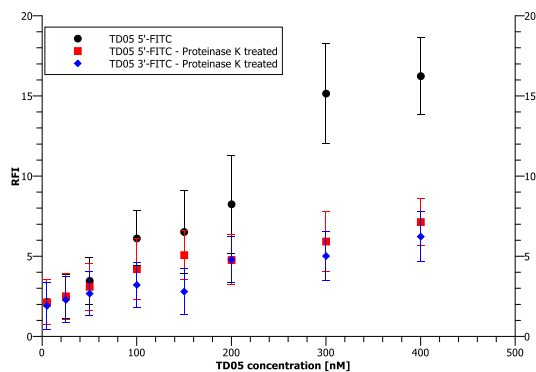


Figure 23: Comparison of aptamer binding to proteinase K treated cells and untreated cells. The treated cells exhibit less target molecules and show lower aptamer binding.

The results are illustrated in **Figure 23** and show considerably lower amounts of cell bound aptamers on the proteinase K-treated cells compared to the untreated cells. This data further supports the identity of IgM as the target molecule on the surface of Ramos cells.

Another negative control was tested to ascertain the specificity of the aptamers cell targeting. The cell line CCRF-CEM was chosen as it is closely related to the Ramos cell line because both originate from human lymphocytes. The cells should hence have a higher similarity of the cell surface structure than the previously used CHO cells and present a higher challenge to the aptamers specificity.

The CCRF-CEM cells were cultured as described (6.1.9) and then incubated with aptamers by the same procedure used for Ramos cells (6.1.4). **Figure 24** presents the results of flow cytometry analysis with concentration series of the TD05 aptamer and the sequence pool. There is no detectable binding of any of the used probes to the CCRF-CEM cells. The aptamer is hence also able to differentiate between closely related cell lines.

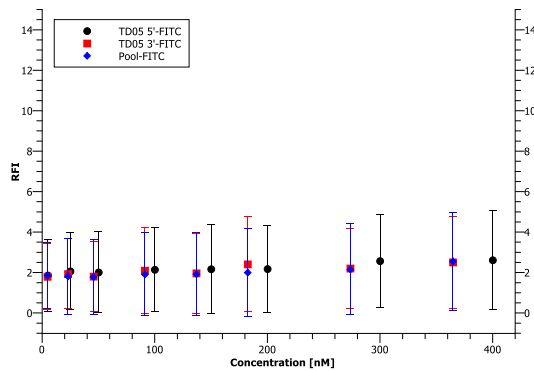


Figure 24: Analysis of the non-target cell line CCRF-CEM with the two differently labelled aptamer variants and the negative control sequence pool. The aptamer TD05 shows no affinity to the CCRF-CEM cells.

4.1.5 Aptamer-quantum dot conjugates targeting Ramos cells

After confirming the affinity and specificity of the DNA aptamer TD05 to Ramos cells in the previous experiments, it was now used for fabrication of aptamer-quantum dot (QD) conjugates. Quantum dots are semiconductor nanoparticles that possess unique optical properties that make them interesting labels for bioanalytical applications like flow cytometry (3.2.3). For the use in cell-specific staining they have to be coupled to a recognition molecule like an antibody or an aptamer. Due to the great potential of cell SELEX derived aptamers, the conjugation of aptamers to QDs is particularly promising. The aptamer TD05 was chosen to construct such conjugates and characterize their binding properties.

The conjugation procedure used for fabrication of the TD05-QD655 conjugates is described in detail in section (6.1.6). In a nutshell, amino-modified aptamers were activated with EDC and coupled to carboxyl-modified quantum dots, resulting in a covalent binding of the aptamers to the QDs surface. After conjugation, the constructs were characterized by microarray binding studies. It was tested if the aptamer was still able to bind the target molecule IgM after conjugation to QDs. The same experimental layout as in section 4.1.1 was used to study the interaction.

Different IgM concentrations and protein negative controls were spotted onto a microarray support and subsequently incubated with the aptamer-QD conjugates.

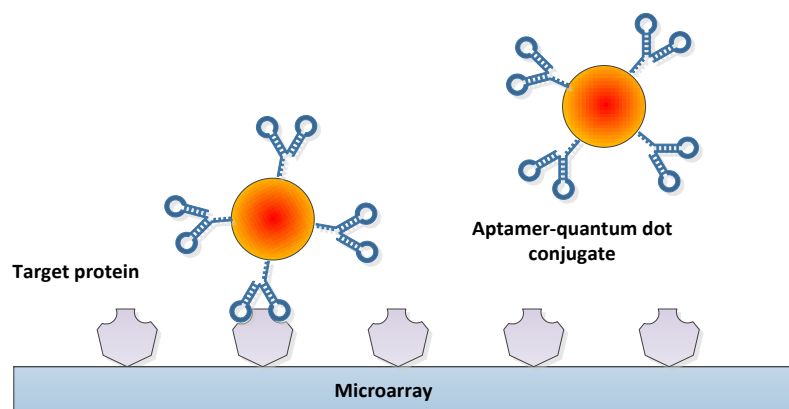


Figure 25: Schematic presentation of the used “reverse phase” microarray approach to investigate aptamer-QD conjugate binding to the target protein.

The experimental procedure for the microarray preparation and analysis is described in (6.1.1). The microarrays were scanned with the laser setup suitable for the detection of QD655, which present red QDs with 655 nm emission wavelength. **Figure 26** shows an image of a typical microarray block on the left. The red stained dots are immobilised IgM, the negative controls are further on the right and give weak or no signals. The right part of the figure presents the data obtained from the image analysis by using the software GenPixPro 6.0.

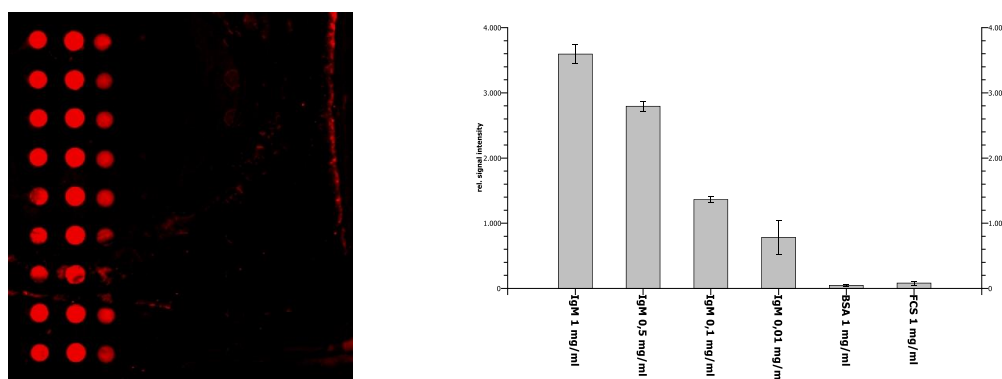


Figure 26: Characterisation of aptamer-QD conjugates by microarray binding studies. Left: Typical image of a scanned protein microarray block incubated with the conjugates. The block consists of four columns of the target molecule IgM (1, 0.5, 0.1, 0.01 mg/ml, from left) and two negative controls further right (BSA and FCS with 1 mg/ml). Each column consists of 9 replicates. Right: Results of the image analysis for the shown block. The conjugate concentration was 40 nM.

The data shows that the TD05-QD655 conjugates are able to specifically bind the target molecule IgM on microarrays. Very weak signals are obtained for the two negative controls BSA and FCS, indicating a high specificity of the aptamer-QD conjugates for their target.

Afterwards a concentration series of the conjugates was used to incubate microarrays with deposited IgM. **Figure 27** shows the signal intensities for conjugate concentrations from 10 nM to 60 nM. As expected there is a signal increase with higher concentrations.

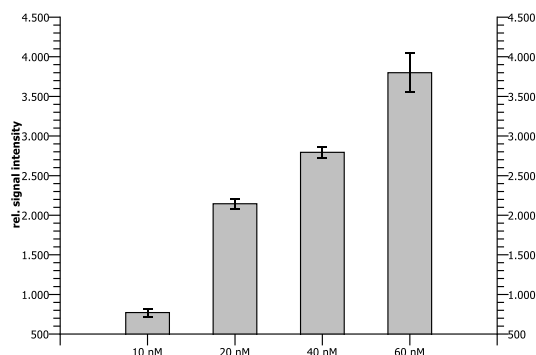


Figure 27: Concentration series of the aptamer-QD conjugates incubated with the target protein IgM (0.5 mg/ml) on microarrays. Increasing concentrations yield higher fluorescence signal caused by binding of more conjugates to the protein spots.

The conjugates were subsequently used for cell staining experiments. Ramos and CHO cells were incubated with the conjugates at concentrations of 3 nM and 30 nM. The detailed sample preparation procedure can be found in section (6.1.7). The cells were finally analysed by flow cytometry to measure the fluorescence of the cell bound TD05-QD655 conjugates in the FL3 (red) detector of the cytometer.

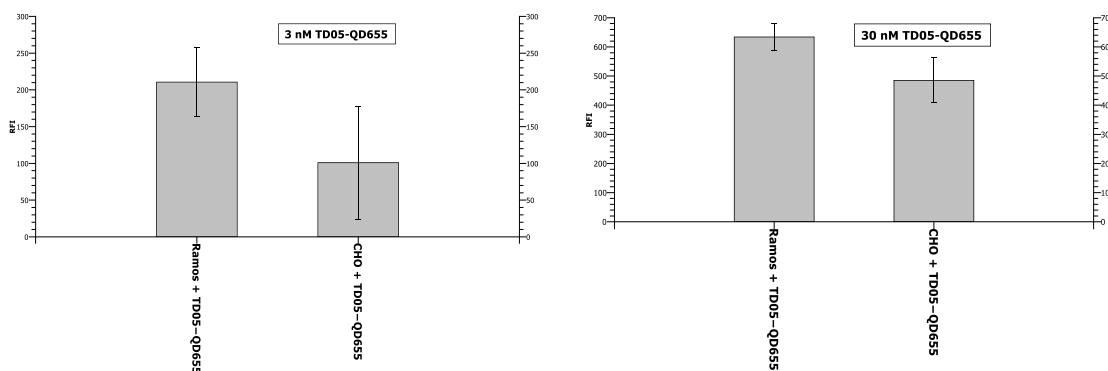


Figure 28: Analysis of Ramos and CHO cells stained with the aptamer-QD conjugates. Left: Cells incubated with 3 nM of the TD05-QD655 conjugate. Right: Cells incubated with 30 nM of the TD05-QD655 conjugate.

It can be seen that the Ramos cells incubated with the conjugates show a higher fluorescence mean value than the non-target CHO cells. But the difference is not significant because the binding of the aptamer-QD conjugates to CHO cells exhibits large error bars. A reason for the unspecific binding could be the non-specific cellular uptake of the conjugates which has been reported to occur frequently for coated nanoparticles (121).

The fabrication of functional aptamer-QDs with specificity to the target protein could be shown in microarray binding experiments. However, the conjugates failed to exhibit this specificity when analysed with the target Ramos cells. Unspecific binding to non-target cells presents a challenge for the routine application of these stains for flow cytometry. By further improving the labelling procedures and washing steps it could be possible to decrease the unspecific binding and establish aptamer-QDs as stains for flow cytometry.

4.2 Immobilisation of aptamers on the cell surface and their characterisation by flow cytometry

While many examples of applying aptamers in cell staining for flow cytometry exist, the literature on cell-immobilised aptamers is relatively scarce. The applications of cell-immobilised aptamers until now are found in the field of biosensors as described by Zhao *et al.* (98). The goal of this work is to demonstrate the use of a cell-immobilised aptamer affinity matrix for screening protein producing cells in order to identify the cells that secrete the most product. These cells are assumed to be the best producers and it would be beneficial to select them early in cell line development to speed up further process development and identification of cell lines for efficient production.

Aptamers are chemically synthesized molecules that can be easily produced under GMP regulations that apply for pharmaceutical production. Furthermore they can be specifically functionalised which should allow a directed immobilisation on cells. Ideally an aptamer based molecular beacon (consisting of a fluorophore-quencher system) is conceivable that would allow the detection of secreted molecules without the use of a second detector molecule. **Figure 29** shows schematic drawings of potential high producer assays based on immobilised aptamers.

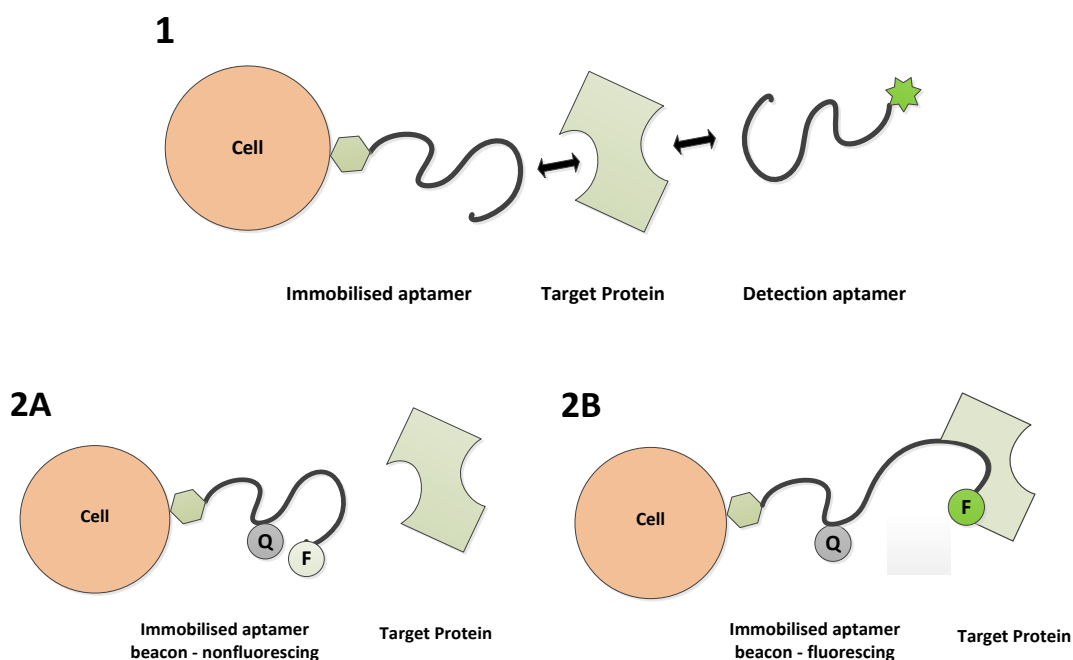


Figure 29: Principle of high producer assays based on immobilised aptamers. Top: Capturing of secreted proteins by cell surface-immobilised aptamers followed by detection of bound protein by a second fluorescently labelled aptamer. Bottom: Principle of a high producer assay based on an immobilised aptamer beacon. Bottom 1: If the aptamer is not interacting with the target protein, a quencher (Q) silences the attached fluorophore (F). Bottom 2: During binding of the target protein the aptamer

undergoes a structural change to fit to the target, thereby separating fluorophore and quencher which leads to an increase of the fluorescence signal.

An antibody based affinity matrix has been evaluated for screening in the cell line development process but has, however, failed to establish itself as a common standard (11). This might be because of the complicated modification of the cells that is needed to build up the antibody affinity matrix, which might not justify the procedure when reasonable results can be achieved by using easier methods for identifying high producers (115). Using aptamers as recognition tools prevents the problems associated with introducing additional proteins like antibodies into the cell line development process, which is subject to strict regulations under GMP. The ability to specifically modify aptamers within their sequence also opens up the possibility to immobilise aptamers in a directed and uncomplicated way on the cell surface. These features, paired with the option of selecting aptamers against virtually all kinds of molecules which are currently produced in cell based biotechnological processes, make it worth to explore the potential and feasibility of immobilising intact aptamers on living cells. Initial experiments were carried out with beads, which served as simple cell models to test the immobilisation and the possibility to detect the aptamer target interaction in a flow cytometer. **Figure 30** shows a schematic of the general experimental approach.

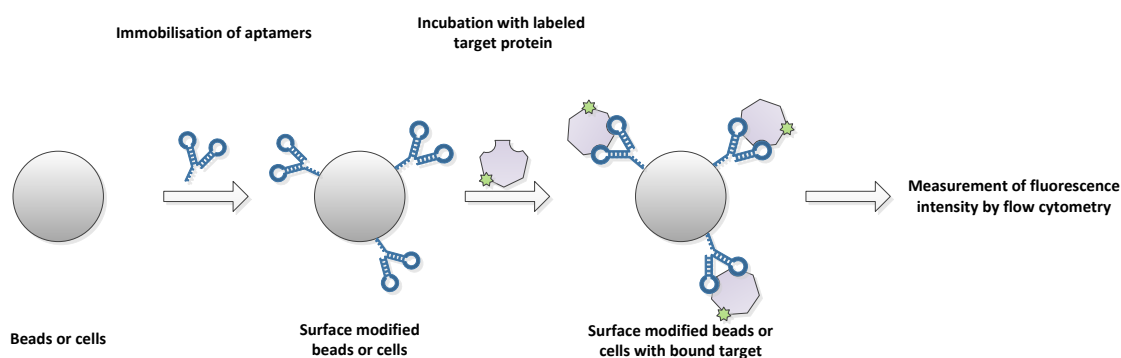


Figure 30: Schematic of the experimental investigations. Aptamers were immobilised on beads or cells using different immobilisation strategies and afterwards incubated with fluorescently labelled target protein. The amount of bound target was then analysed by flow cytometry.

4.2.1 Indirect immobilisation of aptamers using a biotin streptavidin bridge

As a first approach to immobilise aptamers on cells the modification of the cell surface with biotin and streptavidin followed by immobilisation of biotinylated aptamers is

investigated. The streptavidin molecule thereby serves as a bridge between the biotinylated cell surface and the biotin modified aptamer. The immobilisation concept is shown in **Figure 31**. The approach seems complicated but has successfully been used to immobilise antibodies on the cell surface, indicating that this might work with aptamers, too. The immobilisation was first done on streptavidin coated beads which served as simple model system to test the approach.

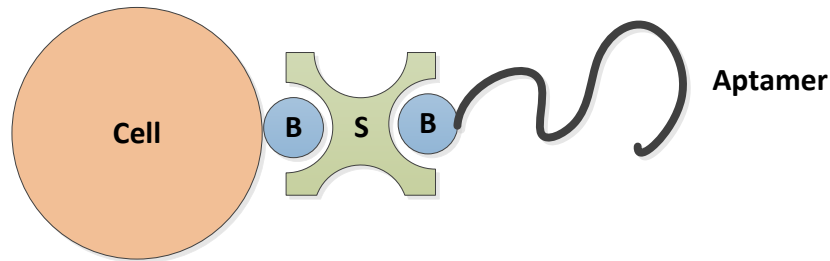


Figure 31: Scheme of the aptamer immobilisation approach using a biotin-streptavidin “bridge”. Biotinylated cells are incubated with streptavidin and afterwards with biotin modified aptamers.

4.2.1.1 Indirect immobilisation – proof of principle using streptavidin modified beads

Streptavidin coated beads with a diameter of 2.8 μm were incubated with a lysozyme aptamer that was biotin-modified at the 5'-terminus and fluorescently labelled at the 3'-terminus (122). The incubation was done according to the suppliers protocol (6.1.13). After incubation and washing, the beads were analysed by flow cytometry to measure the fluorescence of the labelled aptamer. **Figure 32** shows that the binding of the biotinylated aptamers to the streptavidin coated beads is successful and that a saturation of the beads with aptamers can be observed for aptamer concentrations above 50 nM.

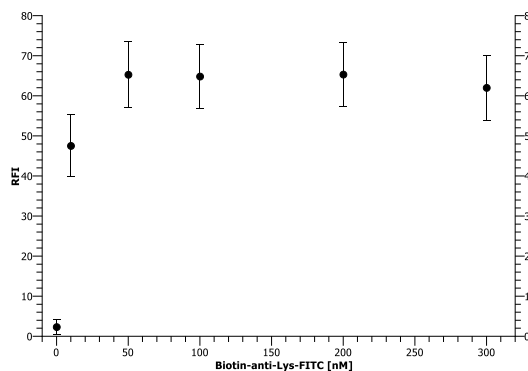


Figure 32: Proof of immobilisation of biotin and FITC-modified aptamers on streptavidin beads.

After showing the successful immobilisation of biotin-modified aptamers on the streptavidin-coated beads, aptamer-modified beads were incubated with the fluorescently labelled target protein. A lysozyme binding aptamer was chosen as a test system for this study (122). Aptamer beads were freshly prepared according to the manufacturers protocol (6.1.13). 2 μl of the resulting bead solution were incubated with 500 μl lysozyme-FITC for 30 min in the dark at room temperature in a rotator. Afterwards the beads were washed with 300 μl aptamer binding buffer with additional 50 mM NaCl for further 30 min. Finally the samples were analysed by flow cytometry to measure the fluorescence of the bead bound target. The negative control consisted of beads modified with the aptamer 264 which is not supposed to bind lysozyme. The results in **Figure 33** show stronger binding of the lysozyme to the negative control beads. This might be a result of high unspecific binding of lysozyme to the streptavidin beads or due to problems with the aptamers fold which might be impaired after the immobilisation on the beads.

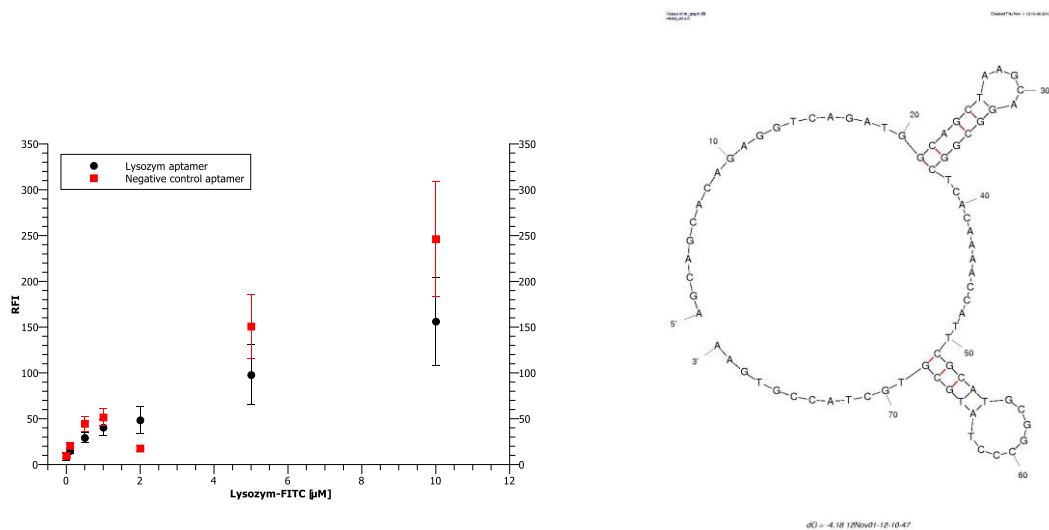


Figure 33: Left: Incubation of lysozyme aptamer-modified streptavidin beads with the target protein. The results show a higher binding of the target to the negative control which was modified with an aptamer that was not selected against lysozyme. Right: Structure of the lysozyme aptamer calculated with Mfold (120).

To investigate if the incapability of the aptamer beads to specifically bind their target is generic or only a result of the chosen lysozyme aptamer, another aptamer-target system was chosen. The aptamers Del5-1 and V7t1 which target the vascular endothelial growth factor (VEGF) were chosen for this purpose (123,124). The predicted aptamer structures can be seen in **Figure 34**.

The target protein VEGF was produced using a recombinant *E.coli* strain and purified as described in (6.1.10). After purification the protein was labelled with the

fluorescence dye FITC by standard procedures (6.1.11) and its concentration determined using a micro-BCA assay.

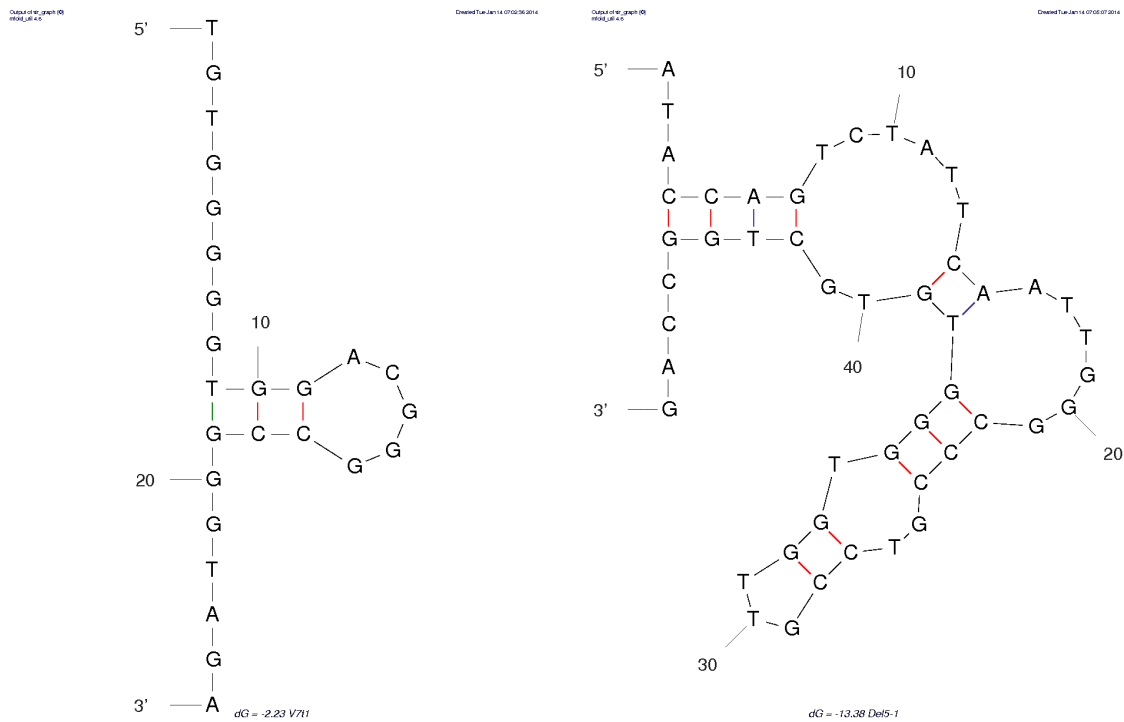


Figure 34: Calculated structures for the two VEGF binding aptamers V7t1 (left) and Del5-1 (right) using the tool Mfold (120).

After immobilisation of the two biotin modified aptamers on the streptavidin beads, the modified beads were incubated with fluorescently labelled VEGF for 30 min in the dark at RT in a rotator. Afterwards the samples were analysed by flow cytometry. The negative control was the same as used above for the lysozyme aptamer. **Figure 35** shows that one of the aptamers (V7t1) binds the target while the second (Del5-1) only yields fluorescence signals on the same level as the negative control. It can be concluded that the binding of targets by aptamers immobilised on streptavidin coated beads is possible but depends on the used aptamer.

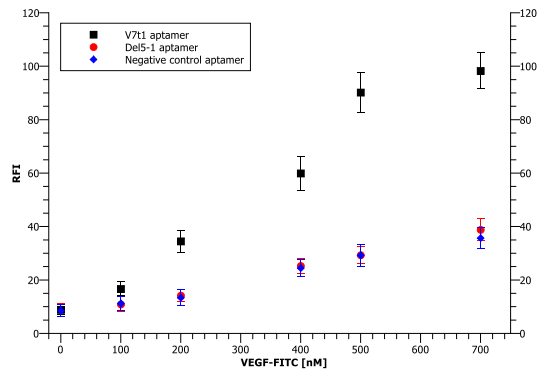


Figure 35: Incubation of VEGF aptamer-modified streptavidin beads with VEGF-FITC. The aptamer V7t1 shows higher signal intensities than the aptamer Del5-1 which exhibits the same binding as the negative control.

4.2.1.2 Immobilisation of aptamers against IgG on the cell surface

As a model system for investigating whether aptamers stay functional after immobilisation on the cell surface the aptamer 264 and its target the Fc-fragment of human IgG antibodies were chosen. CHO K1 cells were used as immobilisation substrates because of their widespread application in biotechnological production (102). **Figure 36** is an illustration of the predicted structure for the aptamer, consisting of a stem-loop motif.

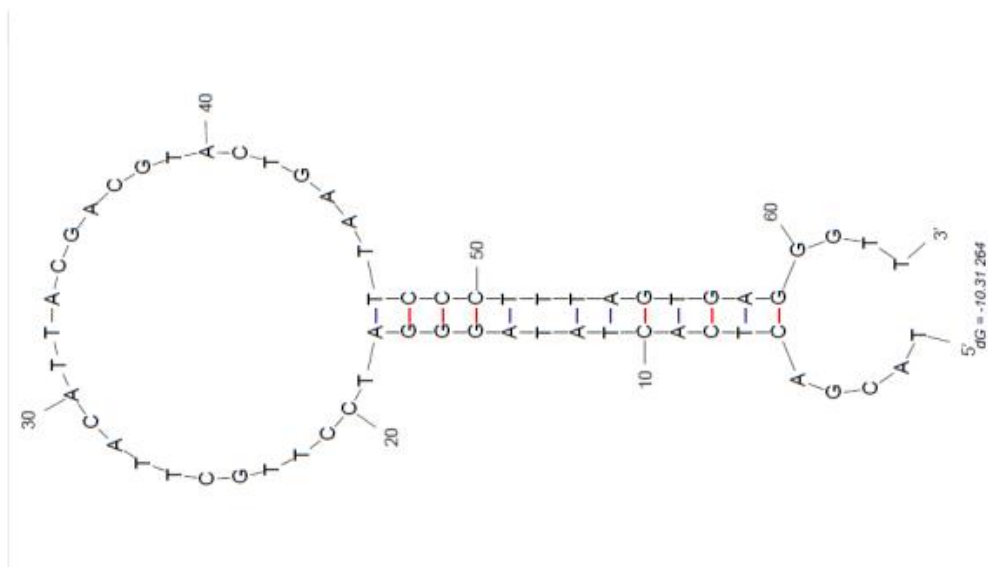


Figure 36: Structure of the aptamer 264 calculated using the tool Mfold (120).

The model system also presents a starting point for a potential application of an aptamer based affinity matrix on cells. A similar approach, based on immobilized antibodies, has

been used in cell line development for screening and sorting monoclonal antibody (mAb) secreting cells by FACS (117). An aptamer-based version of this assay could help to improve efficiency of cell line development by screening for high producers early in the process.

To demonstrate the immobilisation approach step by step, all modifications involved in building up the aptamer affinity matrix were investigated. A schematic of the immobilisation is shown in **Figure 31**. Each step was performed with a fluorescence label at the respective component (cell-surface biotinylation agent, streptavidin and biotinylated aptamer) to prove that the modification of the cells works as intended.

Firstly the reactive N-Hydroxysuccinimide (NHS) ester which is used to biotinylate the cell surface was used as a NHS-FITC derivative. Cells were incubated for different times with increasing concentrations of the component and analysed via flow cytometry. The NHS binds to primary amino groups that should be present on the cell surface, e.g. in the lysine site chains of proteins.

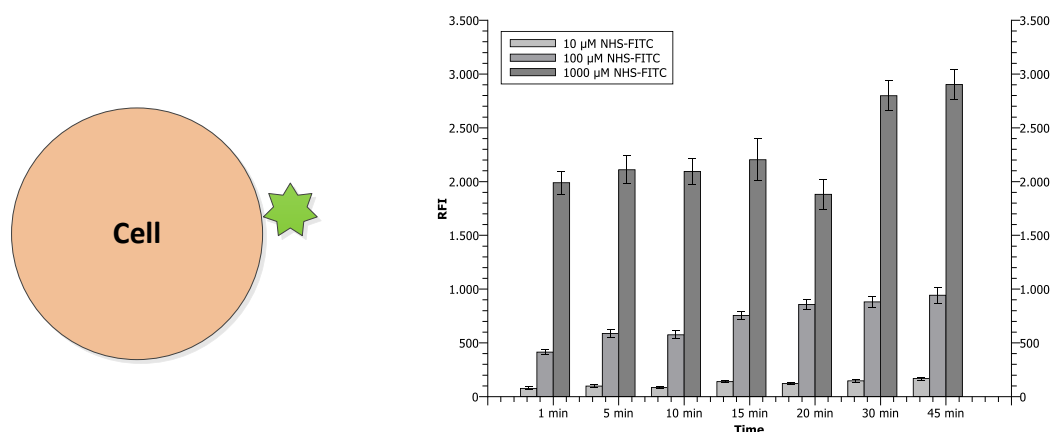


Figure 37: Binding of different NHS-FITC concentrations to the cell surface. The highest concentration (1000 μM) yields the highest signal.

The data in **Figure 37** proves that the NHS-ester is capable of binding to amino groups of structures on the cell surface. It further shows that the amount of bound NHS-FITC depends on the concentration used to incubate the cells. The highest concentration yields the strongest fluorescence signal. The reaction appears to be very fast as only slight increases in fluorescence can be seen when comparing the samples analysed after one and five minutes. For all further experiments a concentration of 1000 μM NHS-biotin and an incubation time of five minutes were used.

As a next step the binding of streptavidin to the biotinylated cell surface was investigated by incubating biotin modified cells with FITC labelled streptavidin. The cells were subsequently analysed by flow cytometry and showed increasing fluorescence at higher concentrations (Figure 38). For concentrations higher than 25 $\mu\text{g/ml}$ the fluorescence reaches saturation. To assure that this saturation is reached 50 $\mu\text{g/ml}$ are used in all further experiments with this immobilisation approach.

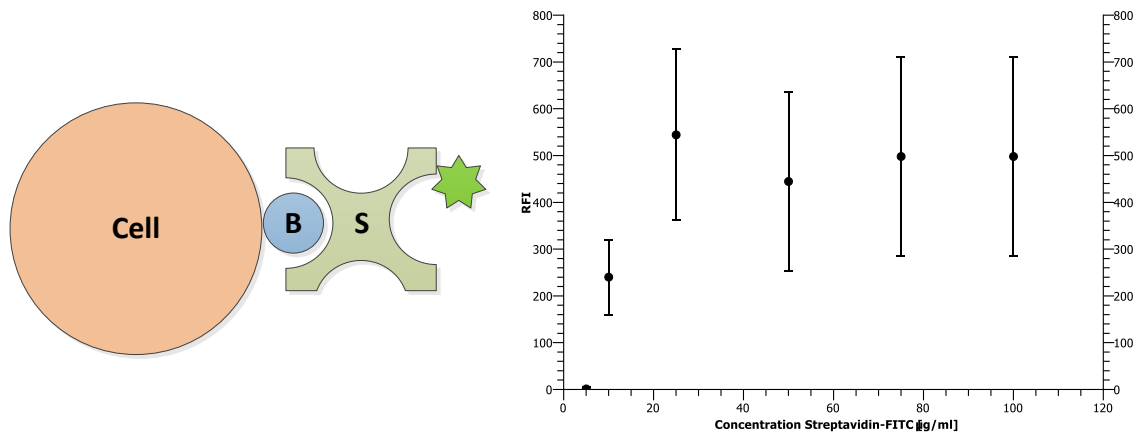


Figure 38: Binding of streptavidin-FITC to biotinylated cells.

To show that the last step, the immobilisation of biotinylated aptamers takes place, 264 aptamers with biotin at the 5'-terminus and FITC at the 3'-terminus were incubated with the prepared cells (Figure 39). Figure 40 illustrates that increasing concentrations of the aptamer used for immobilisation yield higher fluorescence signals. For the later experiments with the complete assay, 6 μM biotinylated aptamer were used. Negative controls were analysed to demonstrate that the immobilisation of the aptamer is specific for the biotin-streptavidin treated cells and does not result from unspecific binding of the aptamer to the cells. The data proves that the immobilisation approach works and that it requires the complete prior modification protocol with biotin and streptavidin. Figure 40 also shows that no aptamer can be immobilised if one of the components (biotin/streptavidin) is left out.

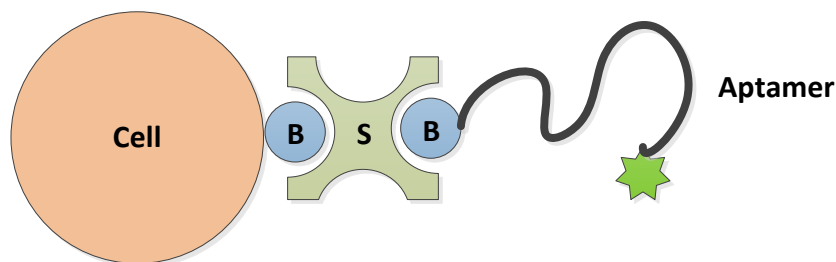


Figure 39: Proof of aptamer immobilisation via biotin-streptavidin: A fluorescence labelled aptamer is immobilised and detected by flow cytometry.

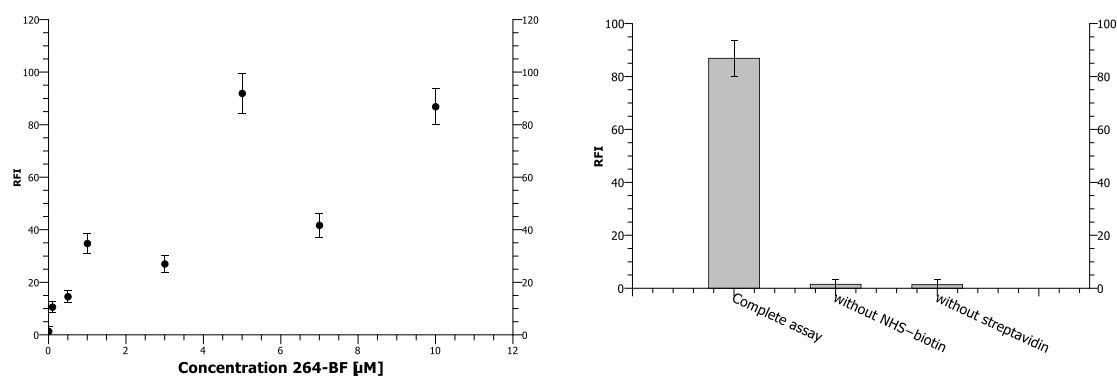


Figure 40: Immobilisation of biotin-modified and fluorescently labelled aptamers in the last step of the matrix build up. Left: Fluorescence intensities for increasing concentrations used for incubation of the cells. Right: The immobilisation only takes place on cells modified with biotin and streptavidin.

After proving that the intended immobilisation procedure can successfully be applied, it was investigated whether the aptamer stays functional. Aptamer modified cells were incubated with fluorescently labelled target (Fc-fragment-FITC). Although the affinity of the aptamer had not been determined an estimation based on microarray experiments expected it to be in the nanomolar range (125). Therefore target concentrations for initial experiments were set to 2-6000 nM. As negative controls and to investigate unspecific binding by the Fc-fragment, samples lacking NHS-biotin, streptavidin and the aptamer were incorporated in the analysis. The results show that although the binding to the cells increases with higher target concentrations, the interaction is unspecific and binding is also found for all negative controls (**Figure 41**). It can be concluded that there is unspecific binding of the Fc-fragment to the cell surface. In addition the actual specific binding of the target by the aptamer could be impaired by steric effects.

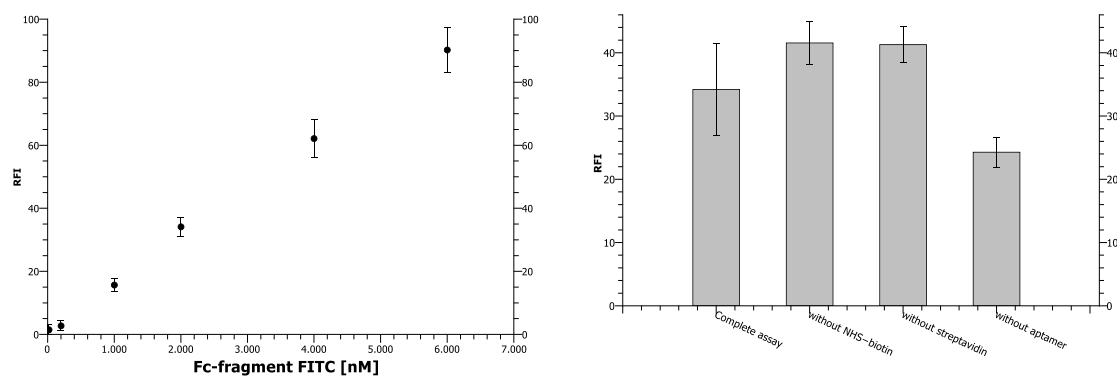


Figure 41: Fluorescence of the aptamer modified cells after incubation with the target molecule Fc-FITC. Left: Concentration series of the target and resulting fluorescence intensities. Right: Comparison of fluorescence intensities for the modified cells and negative controls for 2000 nM target.

To exclude possible interference of the aptamers which could occur by too dense immobilisation, samples with different concentrations of immobilised aptamers were analysed. The modified cells were all incubated with 10 μM of the fluorescently labelled Fc-fragment. **Figure 42** shows that the concentration of aptamer which is used to incubate the cells during immobilisation has no effect on the binding of the Fc-fragment. The fluorescence of modified and unmodified cells does not differ when measured directly after incubation or after centrifugation and resuspension of the cells in binding buffer. After resuspension of the cells the fluorescence decreases strongly which indicates a weak binding of the target to the modified cells.

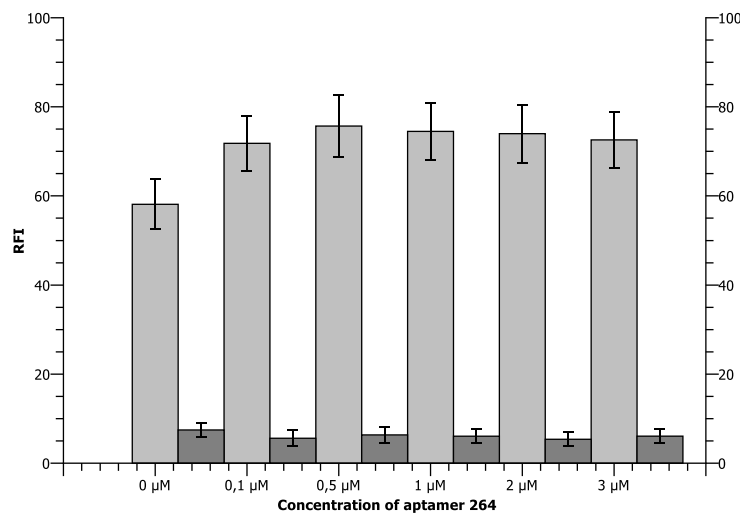


Figure 42: Binding of the target to cells modified with different aptamer concentrations. Directly after incubation (left bars, light grey) and after centrifugation and resuspension of cells in binding buffer (right bars, dark grey).

To investigate if the aptamer is not functional because of steric hindrance from the relatively large streptavidin molecule, a spacer system was used to increase the distance between the aptamer and the streptavidin bridge. The spacer consists of a double stranded DNA section which is formed between a biotin modified oligo and its complementary sequence which is used as direct elongation of the aptamer sequence (98). The oligonucleotide sequences are listed in appendix 6.2.5. An illustration of the approach can be seen in **Figure 43**.

The structure of the aptamer with the elongated sequence was again used to calculate its predicted structure. The structures with spacer and without are shown in **Figure 44**. The predicted structures do not differ significantly and show no indication that the spacer might interfere with the aptamers fold.

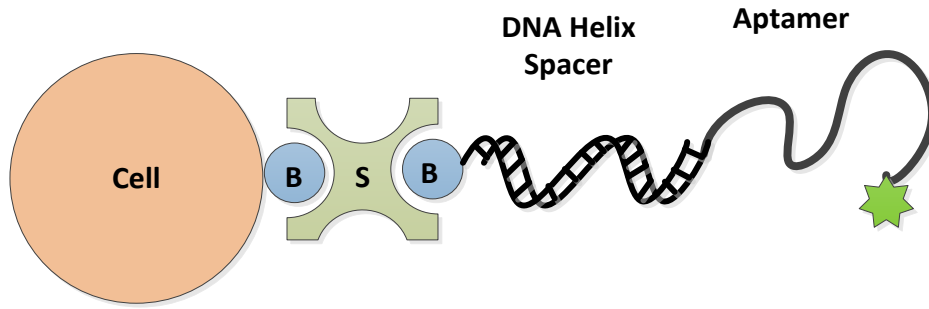


Figure 43: Proof of aptamer immobilisation using a DNA helix spacer. After hybridisation and immobilisation the aptamer can be detected by its fluorescence label.

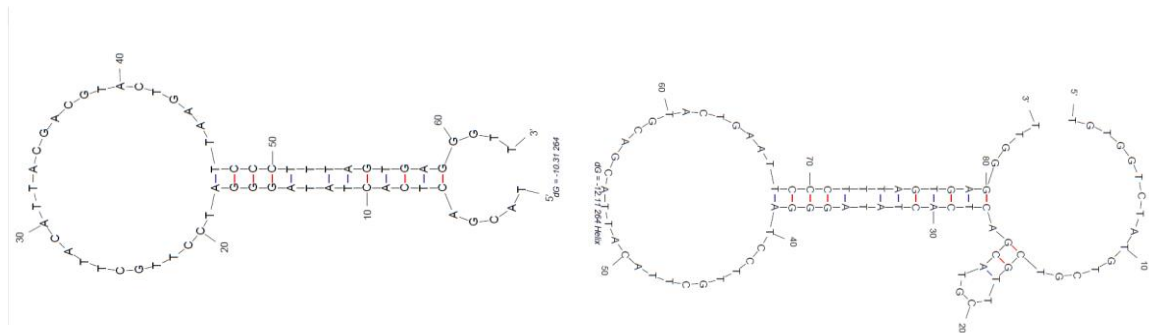


Figure 44: Comparison of the aptamer fold for 264 without (left) and with the described spacer elongation (right). The stem-loop structure of the aptamer is not effected. Structures were calculated using Mfold (120).

Cells were modified with biotin (1 mM NHS-biotin) and streptavidin (50 $\mu\text{g/ml}$) as described in section 6.1.17 and subsequently incubated with different concentrations of the 264 aptamer containing the DNA helix spacer. The aptamer also contained a FITC label at the 3'-terminus of its sequence. The fluorescence values of the modified cells increase with higher concentrations of the aptamer, indicating a successful immobilisation of the aptamer with the spacer. A saturation of the streptavidin on the cell surface can be observed for concentration of 5 μM aptamer or higher. However, also with consideration of the different labelling ratios of the aptamers, the fluorescence values are slightly lower than for the aptamer without spacer (**Figure 45**). The immobilisation may be compromised by unhybridised biotin oligos or steric effects.

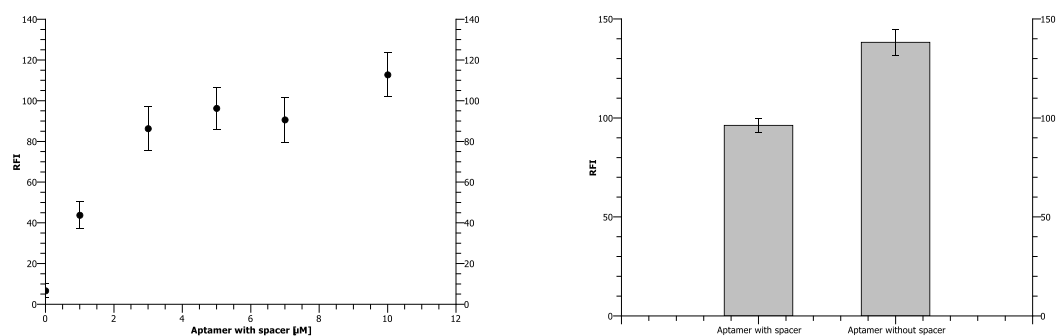


Figure 45: Left: Immobilisation of increasing concentrations of aptamer. Right: Comparison of resulting fluorescence intensities for cells modified with fluorescently labelled aptamers with the above described spacer and without (different labelling ratios of the oligos were taken into account).

The effect of the spacer on target binding was investigated by comparing it to unmodified cells and the aptamer without spacer. The aptamers were immobilised as described above and incubated with high concentrations of the Fc-fragment (20 μM and 40 μM). The cells were subsequently analysed by flow cytometry. The results in **Figure 46** show no difference between the aptamer with spacer and without. The spacer could not help to achieve a successful binding of the immobilised aptamer to the Fc-fragment.

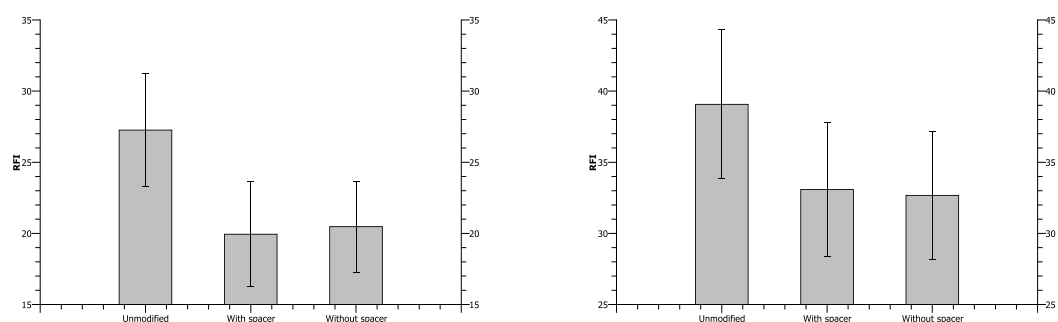


Figure 46: Binding of fluorescence labelled Fc-fragment to aptamer modified cells using aptamers with a DNA double helix spacer compared to unmodified cells and an aptamer without spacer. Left: 20 μM target concentration. Right: 40 μM target concentration.

Determination of aptamer-affinity against IgG by MST

After several failed attempts to detect binding of the cell-immobilised aptamer 264 with the Fc-fragment, the affinity of the aptamer was determined by microscale thermophoresis. Microscale thermophoresis (MST) is a method to measure binding constants of two partners. It presents an alternative to methods such as isothermal titration calorimetry (ITC) or surface plasmon resonance (SPR). The MST principle is described in section 6.1.20.

The aptamer 264 was analysed with the Fc-fragment and also with an intact polyclonal human IgG antibody. The experiments reveal very low affinities for both interactions. The analysis of the aptamer binding to the Fc-fragment yields a dissociation constant (K_D) of 28 μM or higher. But according to the data, the affinity is probably lower because there is no data point supporting the saturation of the binding curve in figure **Figure 47**. For the analysis of the aptamer 264 binding to the IgG antibody there is no detectable binding at all, which might be due to problems with the buffer conditions that cause considerable noise in the data (**Figure 47**). A reason for this could be the agglomeration of IgG or the adherence to capillary walls in the MST device which could prohibit the correct measurement of the aptamer-target interaction.

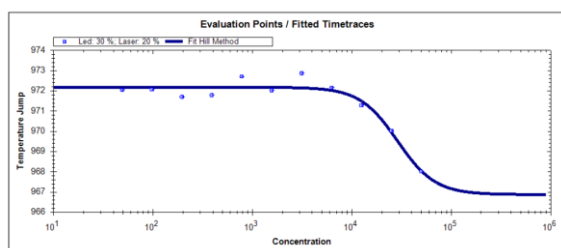
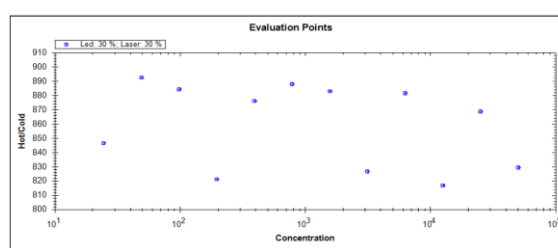
Aptamer (264) vs. Fc $K_D = 28 \mu\text{M} \pm 0.9 \mu\text{M}$ Aptamer (264) vs. IgG $K_D = \text{no binding}$ 

Figure 47: Determination of binding constants by microscale thermophoresis. Left: Binding of the aptamer 264 to the Fc-fragment. The binding constant is at least 28 μM . Right: Binding of the aptamer 264 to a human IgG antibody. For this experiment no binding is detectable at all.

It must be concluded that the aptamer target system consisting of the aptamer 264 and the Fc-fragment of human IgG antibodies reveals to be unsuitable for demonstrating a proof of principle for the intended assay. To show that the problems are mainly caused by the aptamer itself and its poor affinity another aptamer target pair was chosen for further experiments.

4.2.1.3 Indirect immobilisation of VEGF aptamers on the cell surface

The aptamers V7t1 and Del5-1 against the human vascular endothelial growth factor (VEGF) show high specificity and affinities in the nanomolar range according to literature (124,123). The sequences of both aptamers can be found in the appendix 6.2.5. The binding constants were determined through MST measurements by Maren Lönne in an ongoing dissertation and yielded K_D values of 75 nM for Del5-1 and 23.2

nM for V7t1. For immobilisation via biotin and streptavidin the aptamers were used with biotinylation at their 3'-end.

The two aptamers were immobilised by the same procedure used above for the aptamer 264 without DNA helix spacer. The modified cells were subsequently incubated with FITC labelled VEGF in a concentration range from 100-1200 nM. The aptamer 264 was used as a negative control because it should not show any affinity to VEGF. The cells were analysed by flow cytometry after incubation. The experimental data in **Figure 48** show that aptamer Del5-1 stays functional after immobilisation and is able to bind fluorescently labelled VEGF. The fluorescence signals of the aptamer V7t1 are lower but still above the negative controls.

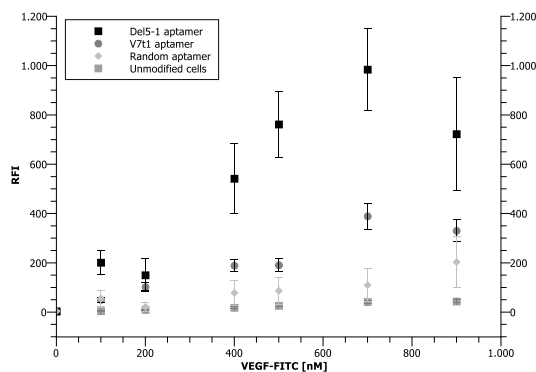


Figure 48: VEGF binding to aptamers immobilised via biotin-streptavidin on cells. Both investigated aptamers show binding of the fluorescence labelled VEGF after immobilisation via biotin-streptavidin on the cell surface.

Although the immobilisation of functional aptamer using a biotin-streptavidin bridge could be shown successfully for the VEGF aptamer Del5-1, problems with the other aptamers might result from the immobilisation approach. The modification of the cells using biotin and streptavidin is also very complicated, tedious and time consuming. The reasonable conclusion of this is the evaluation of other immobilisation approaches. Later sections therefore investigate the potential of immobilising aptamers directly on the cell surface (4.2.2).

4.2.1.4 Indirect immobilisation of aptamers on the yeast *Pichia pastoris*

After showing the immobilisation of aptamers on the surface of CHO cells it was tried to show that the modification with biotin, streptavidin and an aptamer can also be applied to other cell types and organisms. For this purpose another biotechnological

important organism, the yeast *Pichia pastoris*, was chosen as subject. *Pichia pastoris* is used in various processes for the production of recombinant proteins or vaccination compounds like virus like particles (126). Because these processes would also benefit from a high secretor screening, *Pichia pastoris* is an interesting model for this study.

The *Pichia pastoris* host strain GS115 was obtained as kryo culture from Maria Zahid (co-worker, Institut für Technische Chemie) and cultivated as described in the appendix 6.1.9. To test if the immobilisation via biotin-streptavidin is possible on the surface of *P. pastoris*, the cells were incubated with NHS-FITC of increasing concentrations and analysed by flow cytometry. NHS is the active chemical that is used in combination with biotin for the biotinylation of the cell surface in the first step of the immobilisation assay. It binds to available amino groups that should also be found on *P. pastoris* cells. After binding, the immobilised FITC should than be detectable by flow cytometry. As **Figure 49** shows NHS-FITC is able to bind to the cell surface. Increasing concentrations lead to higher fluorescence values. For all further experiments the highest concentration of 1000 μM was chosen. A microscopic image in **Figure 49** also shows the successful labelling of the cells.

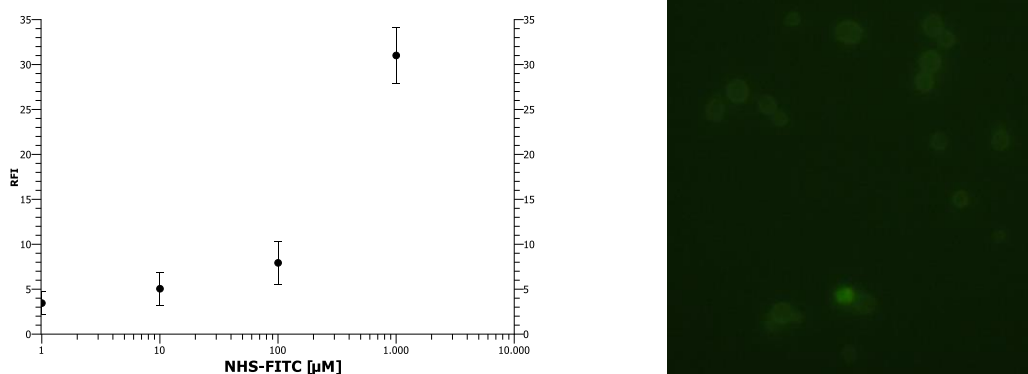


Figure 49: Labelling the yeast *P. pastoris* with NHS-FITC. The cell surface of the cells is also accessible for the reactive compound.

As a next step the cells were modified with NHS-biotin and incubated with streptavidin-FITC to test if streptavidin can be bound by the biotinylated cell surface on *P. pastoris* cells. **Figure 50** shows the flow cytometry analysis of the modified cells. It proves that streptavidin is bound and yields increasing fluorescence intensities with higher concentrations.

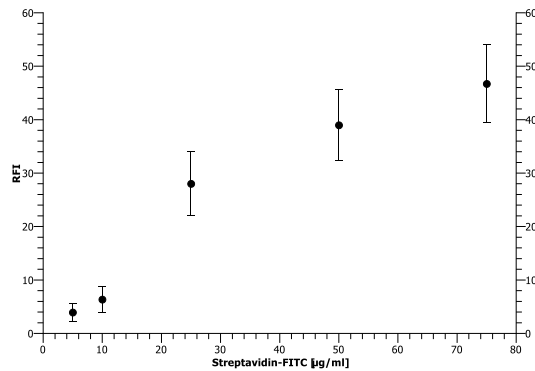


Figure 50: Analysis of *P. pastoris* after biotinylation and incubation with streptavidin-FITC. The protein binds to the biotinylated cell surface.

The results indicate that *P. pastoris* also fulfills the requirements for immobilising aptamers by the biotin-streptavidin approach. To investigate if the modifications with biotin, streptavidin and the aptamer have any influence on the cultivation of the yeast, a comparative cultivation was performed with an aptamer modified and an unmodified *P. pastoris* culture. The biotinylated aptamer 264 was used as a model for this study and immobilised as described in the appendix 6.1.17. The cultivation was done in BMGY media (buffered glycerol-complex medium), which consists of 1 % (w/v) yeast extract, 2 % (w/v) peptone, 100 mM potassium phosphate, 1.34 % (w/v) YNB (yeast nitrogen base), 4×10^{-5} % (w/v) biotin, 0.004 % histidine (w/v) and 1 % glycerol with a pH of 6.0. The cultures were inoculated by adding 3 ml of modified *P. pastoris* with an OD_{600} of 1 to 27 ml of medium in 250 ml shake flasks. The temperature and agitation were kept constant at 30°C and 250 rpm.

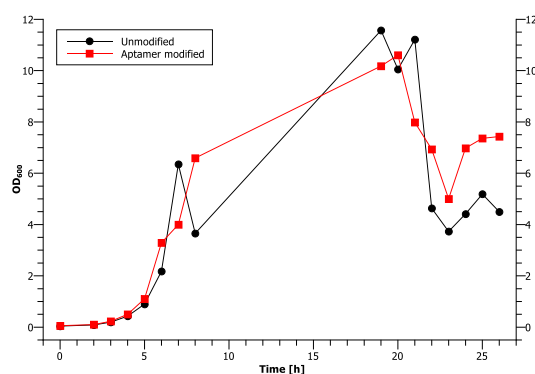


Figure 51: Comparative cultivation of modified and unmodified *P. pastoris* cells.

Figure 51 depicts the cell density monitored by measuring the OD_{600} . The two cultures show no difference in their growth behavior. The modification and development of an

assay based on immobilized aptamers should therefore also be applicable for *P. pastoris* intended for further cultivation.

4.2.2 Direct immobilisation of aptamers

Direct immobilisation of aptamers on the cell surface would be beneficial because of time and cost savings. In addition the process would work without introducing proteinogenic substances like streptavidin, which can be complicated in GMP regulated processes like cell line development. Furthermore the procedure would be straightforward compared to the multiple steps needed for the modification with biotin and streptavidin as described in 4.2.1. Due to the ease of modifying aptamers, they can be used with an activatable group at one of their ends, which can then be used for coupling to other functional groups.

4.2.2.1 Direct immobilisation – proof of principle using beads as immobilisation substrates

Prior to investigating the direct immobilisation of aptamers on the cell surface, experiments with aptamers directly bound on beads were carried out. Aptamer modified beads have recently been shown to work as protein detection platforms in flow cytometry (127). Here the experiments were thought as initial step to study the aptamer target binding for later cell based studies.

Beads with immobilised lysozyme aptamer

The DNA aptamer targeting lysozyme was chosen as model system because of the good and cheap availability of its target. The aptamer originates from an affinity capillary electrophoresis-based SELEX and has been used in a chromatographic application (128). The binding constant was described to be in the nanomolar range by different techniques (122). The aptamer sequence (Lys-Apt) can be found in appendix 6.2.5.

The immobilisation on beads was performed according to the standard protocol presented in appendix 6.1.14. Shortly, amino modified aptamers were incubated with EDC-activated carboxy-modified beads, resulting in a covalent binding of the aptamers to the bead surface. The amount of bound aptamer was determinant as described in

6.1.14, resulting in 505 pmol/mg beads. Beads modified with a random oligonucleotide (R47) sequence were prepared as negative control for the binding experiments. The sequence can be found in the aptamer list 6.2.5. The amount of immobilised aptamer for the negative control was determined to be 823 pmol/mg beads. The amount is higher than for the Lys-Apt beads which may be a result of the different length of the aptamers, the lysozyme aptamer is 80 nt long while the R47 is only 47 nt long.

To detect the lysozyme bound by the aptamer modified beads via flow cytometry, the protein had to be labelled with a fluorescent dye. Lysozyme was labelled with the green fluorescing dye FITC according to a standard procedure (6.1.11). The dye to protein (D/P) ratio was calculated based on absorbance measurements of the protein and the dye. For lysozyme the D/P ratio was 0.7.

First experiments were done with a concentration range of 0-10 μM for the FITC labelled lysozyme. Beads with the lysozyme aptamer and beads with the negative control were incubated with the target solution and kept in the dark as described in the methods appendix 6.1.18. After incubation the beads were directly subjected to flow cytometry analysis.

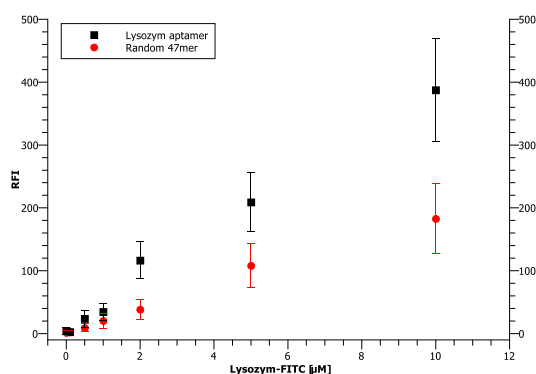


Figure 52: Binding of lysozyme to beads modified with lysozyme aptamer and a negative control consisting of beads with a random oligonucleotide.

The measured fluorescence values are higher for the beads carrying the lysozyme aptamer but there is also a considerable amount of unspecific binding to the negative control (**Figure 52**). This unspecific binding is believed to be caused by electrostatic interactions taking part between the negatively charged phosphate backbone of the aptamers and the positively charged protein lysozyme. Lysozyme has an isoelectric point (pI) of 11, which leads to a positive charge in the used binding puffer of pH 7.5. Interactions based on charge are crucial for aptamer binding as can be seen in **Figure 53**. The picture shows the example of the thrombin RNA aptamer binding to the positively

charged region (blue) of thrombin. But ionic interactions can also result in unspecific binding to non-target proteins with clusters of positive charge on their surface.

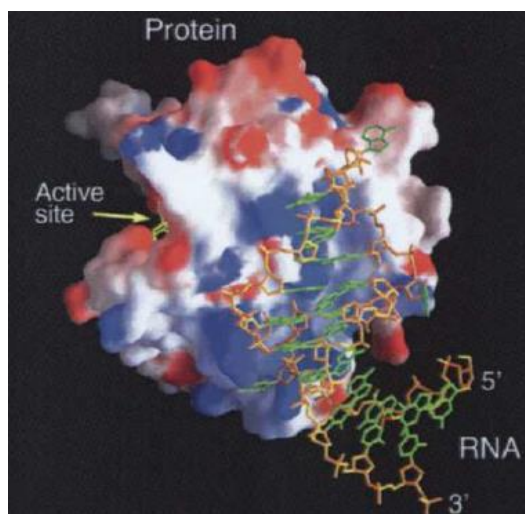


Figure 53: Thrombin RNA aptamer binding to the positively charged region of thrombin. The single stranded oligonucleotide can be seen as a negatively charged polymer due to the phosphate backbone (129).

Investigation of the influence of the pI on protein binding to aptamer-modified beads

To systematically investigate the influence of the pI on unspecific binding, the experiments were repeated with the non target protein BSA, which has a pI of 4.7, resulting in a negatively charged protein molecule in the used buffer. BSA was labelled with FITC as described (6.1.11) to render it susceptible to flow cytometry detection. The D/P ratio calculated for BSA-FITC was 4.2. Both aptamer and control beads were then incubated with BSA-FITC solutions in a concentration range of 0-10 μM as described above. After incubation with fluorescently labelled proteins the beads were directly measured by flow cytometry.

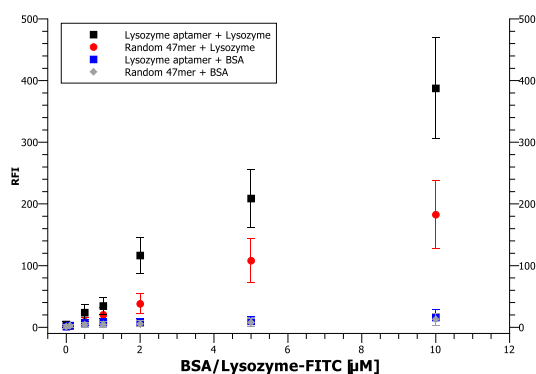


Figure 54: Comparison of lysozyme and BSA binding to beads modified with the lysozyme aptamer and a negative control consisting of a random oligonucleotide sequence.

Neither the lysozyme aptamer beads nor the negative control show binding of BSA (**Figure 54**). This appears to be logical, as the BSA and the aptamer beads both are negatively charged resulting in repulsion of beads and protein. To further investigate the effect of a proteins isoelectric point on unspecific binding to aptamer beads another protein, cytochrome C, was taken into account. Cytochrome C is a protein with an isoelectric point of 10.5 which is similar to lysozymes pI of 11. Hence it is also positively charged in the used buffer pH 7.4. The molecular weight of both proteins is also very similar, with 12.4 kDa for cytochrome C and 14.3 kDa for lysozyme. Cytochrome C is therefore a good model to test unspecific binding of lysozyme caused by charge of the molecule to the aptamer modified beads. **Figure 55** shows the comparison of unspecific binding of cytochrome C and BSA to beads modified with the lysozyme aptamer and a random oligonucleotide. The binding of the positive charged cytochrome C is higher than that of the negatively charged BSA. There is no difference between cytochrome C binding to the lysozyme aptamer beads and the random oligonucleotide beads. The measured fluorescence values are smaller than the ones from lysozyme binding to the aptamer beads presented in **Figure 54**.

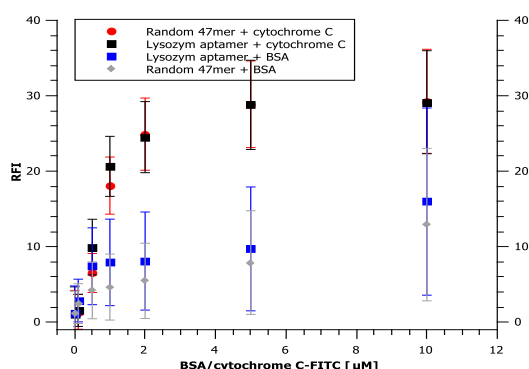


Figure 55: Comparison of unspecific binding for the two negative controls BSA and cytochrome C. Cytochrome C is positively charged in the used buffer, resulting in higher unspecific binding to the negatively charged aptamer beads.

The results of the binding studies with the lysozyme aptamer, the random oligonucleotide (R47) and the three proteins lysozyme, cytochrome C and BSA are summarized in **Table 4**.

Table 4: Summary of the binding studies with the lysozyme aptamer and all negative controls. Descriptions: Weak binding: “-“; binding “+“; stronger binding “+++“.

	BSA	Cytochrome C	Lysozyme
Lysozyme Aptamer	-	+	+++
Random oligo (R47)	-	+	+
Isoelectric point (pI)	4.7	10.5	11

In a further experiment it was tested if the unspecific binding of lysozyme to the negative control beads could be reduced by washing the beads after incubation. Additionally the concentration range used for incubation was expanded to 35 μM lysozyme. The beads were incubated with the fluorescently labelled lysozyme as described above and afterwards washed once with 400 μl binding buffer for 15 min. The samples were then measured by flow cytometry. The results are represented in **Figure 56**. It can be seen that the difference between the fluorescence values of the lysozyme aptamer beads and the negative control is bigger than in the previous experiment without the additional washing step (**Figure 52**). There is also a saturation of the fluorescence values for samples with target concentrations higher than 15 μM . This saturation was not observed before, probably because the specific binding was overlaid by the unspecific binding which is now reduced after the washing step.

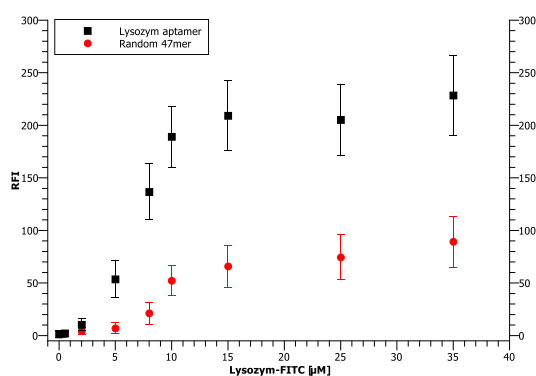


Figure 56: Incubation of aptamer-modified beads and a negative control (R47) with lysozyme concentrations up to 35 μM . The samples were treated with an additional washing step.

It can be concluded that the immobilisation of functional aptamers could be shown for the lysozyme aptamer and its target, although substantial unspecific binding could be observed. This unspecific binding is believed to be mainly caused by the target proteins high isoelectric point which results in a positive charged molecule that interacts with the

negative charged aptamer beads. Using an aptamer with a target protein exhibiting a near neutral or acidic pI might lead to less problems with unspecific binding.

Beads with immobilised aptamers targeting VEGF

After showing the successful immobilisation of functional lysozyme aptamers on beads, the procedure was reproduced with aptamers selected against VEGF. The aptamers V7t1 and Del5-1 were chosen for this purpose. The aptamers have a higher affinity and a more complex target than the lysozyme aptamer.

The immobilisation of the aptamers was done according to the standard protocol (6.1.14), 3'-amino-modified aptamers were used for the experiments. The amount of immobilised aptamer was subsequently determined and resulted in 1130 pmol/mg beads for Del5-1 and 1212 pmol/mg beads for V7t1.

Incubation of the aptamer beads with the fluorescently labelled target was done using the standard protocol described in (6.1.18) and afterwards the beads were washed once in binding buffer. Beads modified with a random oligonucleotide (R47) were again taken as negative control. The analysis of the beads by flow cytometry revealed stronger binding of the VEGF to the aptamer modified beads (**Figure 57**). The best results were obtained from the beads modified with the V7t1 aptamer, which shows more binding than the Del5-1 aptamer. The random oligonucleotide also shows increasing fluorescence with higher VEGF concentrations, but much lower than for the aptamer beads. The VEGF aptamers hence also stay functional after immobilisation on beads.

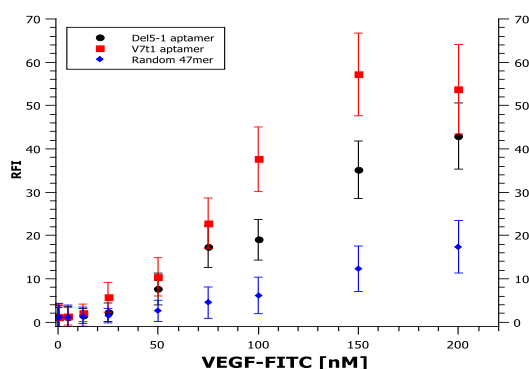


Figure 57: Incubation of VEGF aptamer modified beads and a negative control with VEGF-FITC.

The higher binding affinities of the VEGF aptamers compared to the negative control can also be seen clearly when comparing the histograms of the flow cytometry data.

Figure 58 shows the overlays of the histograms for V7t1 (red, left), Del5-1 (red, right)

and the random oligonucleotide beads for a VEGF concentration of 200 nM. The aptamer histograms are shifted to the right, caused by a higher fluorescence of the measure beads.

To include a negative control on the side of the target protein, the protein myoglobin was chosen and fluorescently labelled. Myoglobin from horse heart has a similar pI (7.2) as the predicted pI (7.6) of the aptamer target VEGF resulting from a calculation using an online tool (130).

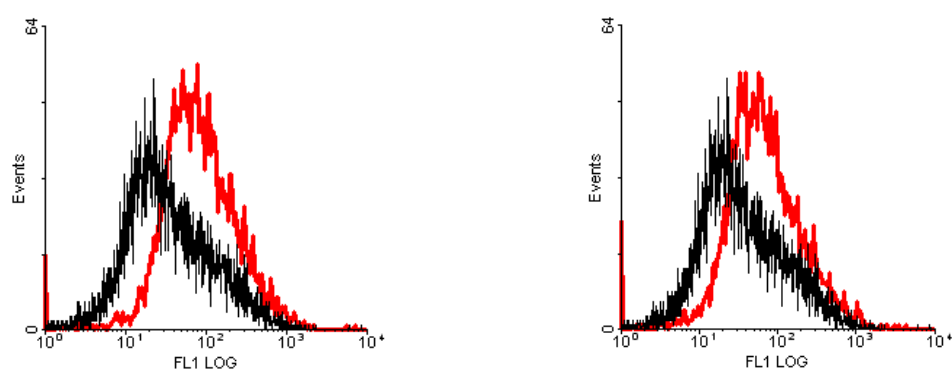


Figure 58: Histogram overlays for the aptamer-modified beads compared to the negative control. Left: V7t1 (red) and R47 (black). Right: Del5-1 (red) and R47 (black). VEGF concentration used for incubation was 200 nM.

The V7t1 and Del5-1 aptamer beads were incubated with the same concentrations of the fluorescently labelled myoglobin and afterwards analysed by flow cytometry. The results are depicted in **Figure 59** and obviously show no binding of the negative control myoglobin to the aptamer beads.

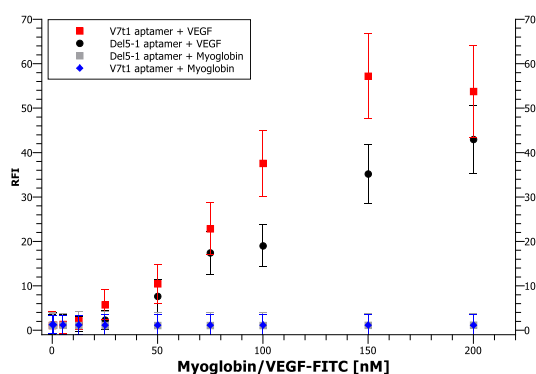


Figure 59: Comparison of VEGF and myoglobin binding to beads modified with the VEGF aptamers V7t1 and Del5-1. The negative control myoglobin is not bound by the beads.

The immobilisation of the VEGF aptamers on beads was successful, the aptamers proved to stay functional and able to bind their target with high affinity and specificity.

4.2.2.2 Direct immobilisation of aptamers on liposomes

A direct approach using activated amino groups has been used for immobilising aptamers for other applications like biosensors or microarrays. A straightforward procedure with activated amino groups was presented by Walter *et al.* for coupling amino modified aptamers onto microarray slides (22). The method uses cyanuric chloride to activate the aptamers terminal amino group. The aptamer is then able to bind to other amino groups. The coupling reaction is illustrated in **Figure 60**.

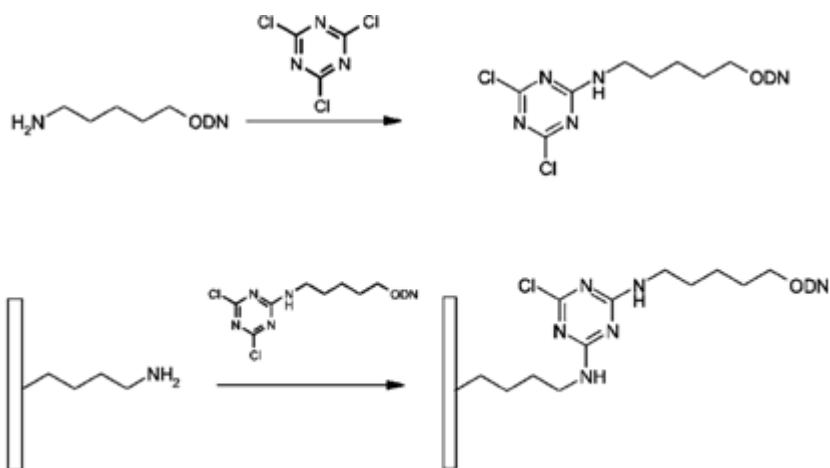


Figure 60: Activation of amino functionalised aptamers via cyanuric chloride and subsequent immobilisation on amino exhibiting surfaces (22).

This strategy should also work for cells, as they present amino groups on the cell surface that are potential targets. **Figure 61** shows a schematic of the intended immobilisation of the aptamer on the cell surface.

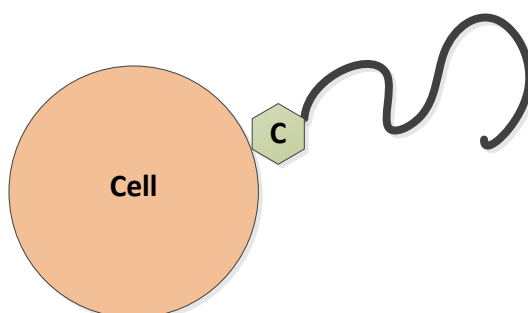


Figure 61: Schematic of the direct immobilisation of amino activated aptamers on the cell surface. C: cyanuric chloride.

Firstly Liposomes were used as cell models to test the direct immobilisation approach using cyanuric chloride in a model system with lower complexity than the cell surface. The liposomes or giant unilammellar vesicles (GUVs) were prepared by a lipid film

rehydration method described in 6.1.19. Two different types of lipids were used to form the GUVs, a standard lipid, 1,2-dioleoyl-*sn*-glycero-3-phosphocholine (DOPC) and a lipid with an amino group at the polar head, 1,2-distearoyl-*sn*-glycero-3-phosphoethanolamine-N-[amino(polyethylene glycol)-2000 (DSPE-PEG 2000 amine). For GUV formation the lipids were used with a ratio of 50:1 (DOPC:DSPE-PEG 2000 Amine) to prevent steric interference between neighbouring aptamers after immobilisation. The molecular structures of the two lipids are illustrated in **Figure 62**.

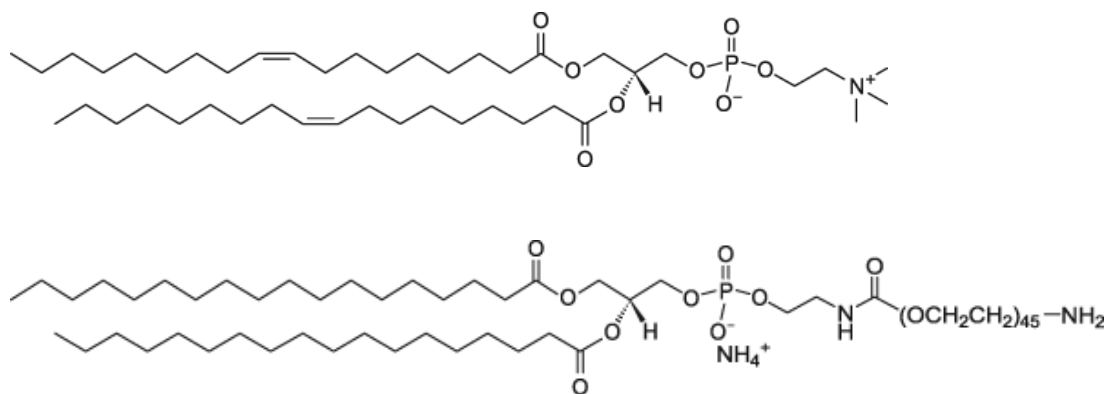


Figure 62: Structures of the lipid molecules used for vesicle formation. Top: DOPC. Bottom: DSPE-PEG (2000) amine.

The produced GUVs were harvested and analysed by light microscopy to inspect their shape and determine their size. Afterwards, a sample containing GUVs was analysed by flow cytometry to assure the particles can be detected by the instrument.

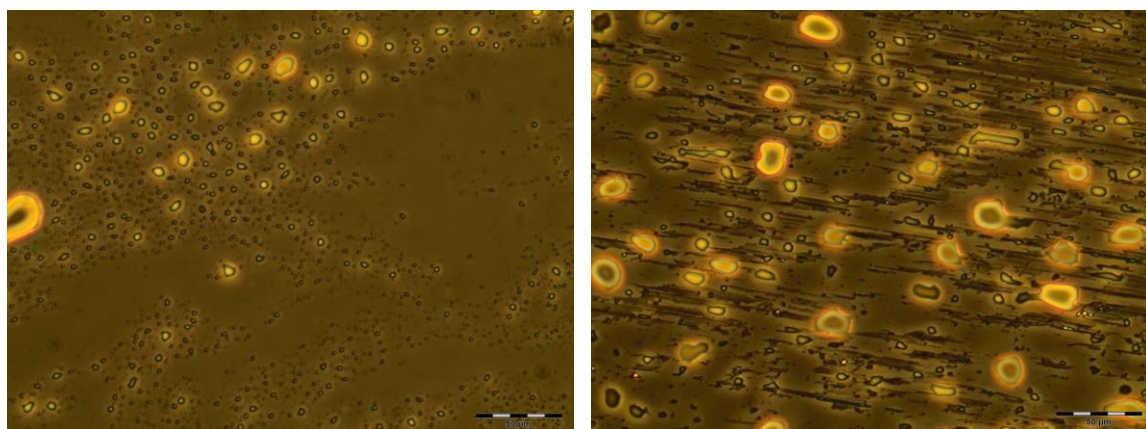


Figure 63: Images of GUVs prepared by film rehydration. The vesicles show a heterogenous size distribution. Vesicles with diameters between 10-20 μm equaling those of mammalian cells can be found in both pictures.

The results show that the GUVs are formed in various sizes of up to 25 μm , which lies in the same range as most mammalian cells (10-20 μm) (**Figure 63**). The analysis by flow cytometry shows that GUVs are indeed detectable by the instrument (**Figure 64**).

The detectability is a prerequisite for studying the following immobilisation of aptamers.

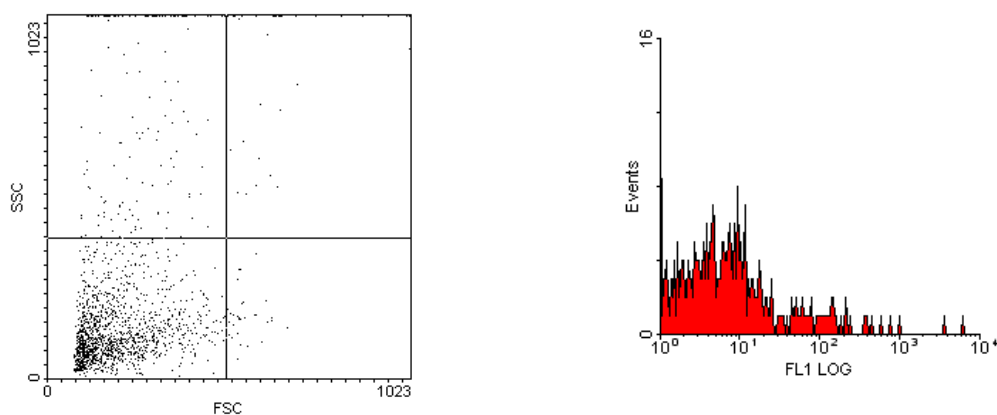


Figure 64: Flow cytometry analysis of GUVs. The vesicles can be detected using the same protocol and settings as for CHO cells. Left: FSC/SSC dotplot. Right: Autofluorescence detected by the FL1 detector is low and similar to CHO cells.

The GUVs containing the amino-modified lipid were subsequently incubated with 10 μ M cyanuric chloride-activated lysozyme aptamers that were amino-modified at their 5'-terminus and labelled with FITC at the 3'-terminus. The GUVs were incubated for 15 min and then washed once with PBS before subjecting them to analysis by flow cytometry. The incubated GUVs showed a higher fluorescence than the unmodified ones, indicating a immobilisation of the aptamers on the GUVs (**Figure 65**). The large error bars are presumably caused by the difficult accessibility of the individual vesicles by the activated aptamers. The GUVs tend to cluster resulting in shielded vesicles that are only partly modified. This results in a high variation of the fluorescence.

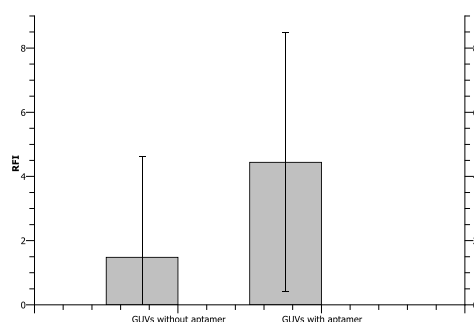


Figure 65: Fluorescence of the vesicles without aptamer and the ones that were incubated with cyanuric chloride activated and fluorescence labelled aptamer.

Although the results from the liposome formation were promising, it was decided to skip the consequent optimisation approaches and move on to direct immobilisation of aptamers on real cells.

4.2.2.3 Direct immobilisation of aptamers on cells

After successfully immobilising aptamers on beads and liposomes, the method was transferred to cells. CHO K1 cells were taken as model cells because of their industrial relevance for production of proteins and their ease of cultivation. For initial experiments the aptamer 264 against the Fc-fragment of IgGs was chosen. The experiments should demonstrate if the direct immobilisation works better than the indirect approach shown in section 4.2.1 and results in any detectable binding of the target.

Firstly 5'-amino-modified 264 aptamer with a FITC label at the 3'-terminus was used for immobilisation to check if the aptamers can be bound covalently to the cell surface.

CHO K1 cells were incubated with increasing concentrations of the aptamer. Two variants of the fluorescently labelled aptamer were compared, one with a normal amino modification (264AF) and one with an additional hexaethylenglycol spacer between the amino group and the aptamer sequence (264ASF). If the accessibility of the normal amino function would be somehow compromised by the aptamers fold, the use of a spacer could result in higher immobilisation efficiency.

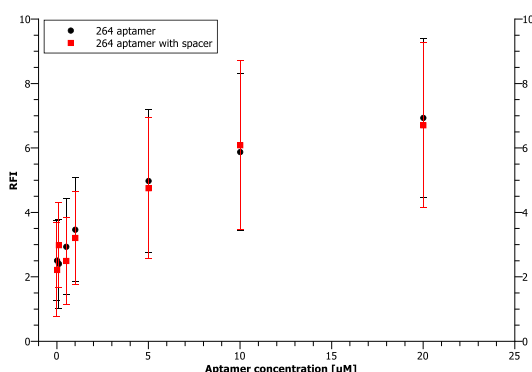


Figure 66: Comparison of the immobilisation of the cyanuric chloride activated aptamer 264 with an additional spacer and without. There is no measurable difference between both aptamers.

Figure 66 shows that the direct immobilisation approach works but there is no difference between the immobilisation efficiency of the aptamer with or without the spacer. The amount of immobilised aptamer increases with higher concentration of the aptamer used for incubating the cells. The fluorescence values appear to get saturated at concentrations above 10 µM.

After demonstrating the successful immobilisation of aptamers by directly coupling them to the cell surface, it was investigated if the aptamer is able to bind its target. Therefore cells were modified with different aptamer concentrations and incubated with

a high concentration of FITC labeled Fc-fragment (20 μM). Afterwards the cells were analysed by flow cytometry to detect the fluorescence from the cell-bound Fc-fragment.

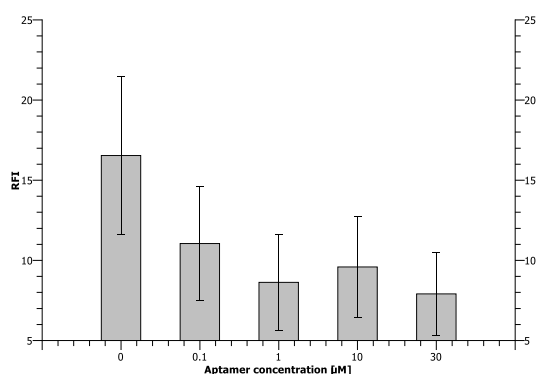


Figure 67: Binding of fluorescence labelled Fc fragment to cells modified with cyanuric chloride activated aptamers. Cells were incubated with various concentrations of the activated aptamer and afterwards incubated with 20 μM Fc-fragment.

Figure 67 shows that no significant binding of the Fc-fragment to the modified cells can be detected. These results and the failed attempt using the indirect immobilisation approach show that the problem is probably related to the aptamer 264. The thermophoresis experiments support this assumption as they reveal a low affinity of the aptamer towards the Fc-fragment (4.2.1.2). To prove that the strategy of immobilising functional aptamers on living cells is in principle possible, the model system was changed to another aptamer-target system.

For further experiments the aptamer against lysozyme (Lys-Apt) was chosen, because it proved to stay functional on beads (4.2.2.1) and its target molecule, in contrast to the Fc-fragment, is easily accessible in high amounts.

The cells were modified with the cyanuric chloride-activated lysozyme aptamer (5'-amino group) by incubating the cells with 10 μM of the activated aptamer as described in appendix 6.1.16. To check for unspecific binding of the positively charged lysozyme to the aptamer, the protein cytochrome C, which has a similar pI, was used as a negative control. The cytochrome C was also labelled with the fluorescent dye FITC. Unmodified CHO K1 cells were employed as additional negative controls and incubated with FITC-labelled lysozyme and cytochrome C. The cells were all analysed by flow cytometry to detect the fluorescence of the cell bound proteins.

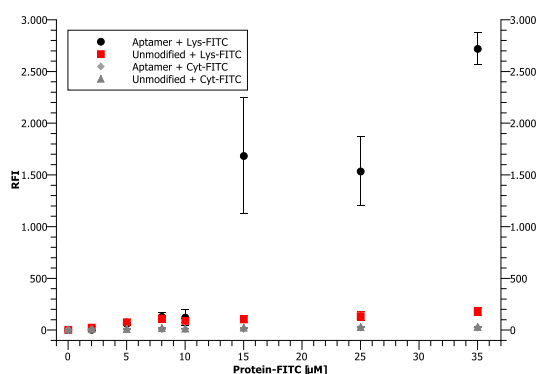


Figure 68: Incubation of lysozyme aptamer-modified and unmodified cells with lysozyme and the negative control cytochrome C. High concentrations of lysozyme are bound by aptamer-modified cells but not the negative controls.

There are high fluorescence values for the Lys-Apt modified cells for lysozyme concentrations above 15 μM compared to the negative controls (**Figure 68**).

To demonstrate the feasibility of the approach for further aptamer-target pairs, immobilisation experiments were performed using two aptamers against VEGF. The aptamers V7t1 and Del5-1 also proved to stay functional after immobilisation on beads after direct coupling (4.2.2.1). The aptamer V7t1 was also capable of binding its target after immobilisation via biotin on streptavidin coated beads (4.2.1.1).

After standard activation of the 3'-amino groups by cyanuric chloride 10 μM of the aptamers were used for incubating 10^6 CHO K1 cells. The cells with immobilised aptamer were then incubated with FITC labelled VEGF and myoglobin in a concentration range of 100-1200 nM. Myoglobin was used as a negative control because it has a pI similar to VEGF.

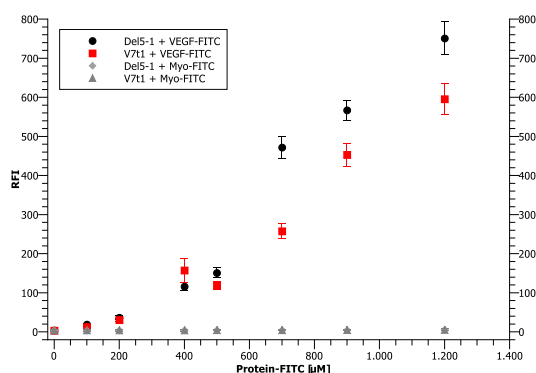


Figure 69: Flow cytometry results of aptamer-modified CHO cells incubated with VEGF-FITC and the negative control myoglobin-FITC.

Figure 69 shows that the aptamer-modified cells bind the aptamer target VEGF but not the negative control myoglobin. The results demonstrate that it is possible to immobilise functional aptamers on the cell surface by direct coupling after cyanuric chloride activation. In order to develop assays based on this finding it is a prerequisite to investigate the effects of the cell surface modification on the cells viability and growth. This topic is described in the following section.

4.2.2.4 Cultivation of modified cells – effects on cell viability and growth

The immobilisation of cyanuric chloride-activated aptamers on the cell surface works by covalent binding to molecules present on the exterior cell membrane. The modification might interfere with the function of these molecules which could potentially be harmful to the cell. With regard to the development of assays for living cells it is therefore necessary to investigate the effects of the immobilisation procedure on the cells viability and growth.

The immobilisation via biotin-streptavidin (91) is known to have no negative effects and cells have successfully been cultured after modification.

To investigate the effect of the direct immobilisation approach with cyanuric chloride-activated aptamers, a comparative cultivation of modified and unmodified CHO cells was monitored over a period of 120 hours. The cells were incubated with fluorescently labelled aptamers activated by the standard cyanuric chloride method (6.1.16). The cultivation was done in 125 ml shake flasks, which were filled with 21 ml starting culture of a cell density of 400.000 cells/ml. The shake flasks were wrapped in aluminium foil to prevent the cultures from light. Samples were taken three times per day to analyse cell density and viability by CEDEX and levels of glucose and lactate with a YSI analyser. In addition the fluorescence of the cells was analysed by flow cytometry once a day.

Figure 70 shows the growth and viability of the two cell populations during cultivation. There is nearly no difference between the cultivations. The modified cells reach even a higher cell density than the unmodified cells.

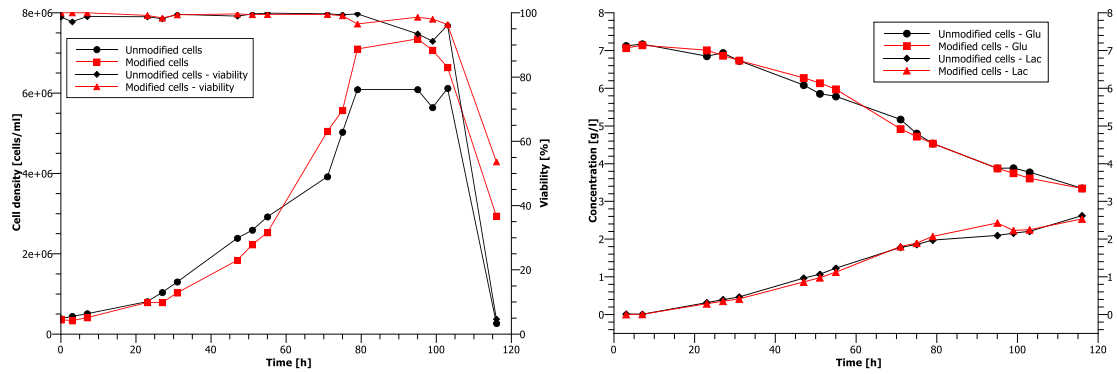


Figure 70: Comparative cultivation of aptamer-modified and unmodified cells. Left: Cell density and viability. Right: Glucose and lactate values during cultivation. No negative effect of the modification on cell viability and growth could be observed.

The metabolic behaviour of the two populations is also very similar as can be seen by the course of the glucose and lactate graphs in **Figure 71**. The analysis of the cell fluorescence by flow cytometry shows a higher value for the modified cells with the fluorescently labelled aptamer, but only for the sample taken immediately after inoculation (**Figure 71**). The samples of the following days all show the same fluorescence intensity as the unmodified cells, which exhibit common autofluorescence. The decay of the signal is not surprising as the cells continue to divide and hence dilute the amount of immobilised aptamers per cell. In addition it is possible that the fluorescence dye is bleaching out over time, although it was tried to prevent this by mantling the flasks with foil.

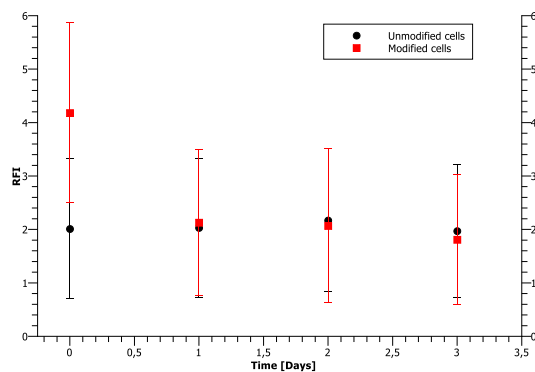


Figure 71: Analysis of cell fluorescence during the cultivation. As expected the fluorescence declines with time. Already after day one the fluorescence of the modified cells falls to the value caused by autofluorescence of the unmodified cells.

In summary no negative effects of the direct immobilisation procedure could be observed. The approach thus seems to be applicable for modification of living cells that can subsequently be cultured or further manipulated.

4.2.2.5 Investigation on a cell based aptamer-sandwich assay for VEGF detection

All experiments presented so far focused on the proof of principle that bead or cell immobilised aptamers are able to bind their target and that this binding can be detected by flow cytometry. Fluorescently labelled target proteins were used for this purpose. For the potential application of cell immobilized aptamers in a cell screening assay, another detection approach has to be developed. With regard to screening cells for the ability to produce a certain protein in high amounts, the protein itself will not be fluorescent like the artificially labelled proteins used for the experiments shown above. In order to detect these proteins which are captured by the aptamers on the cell surface, a sandwich assay containing another detection agent is conceivable. The following section presents the experiments performed with bead and cell immobilised aptamers to show a proof of principle of such an aptamer based sandwich assay. The principle composition of the assay is presented in **Figure 72**. The immobilised aptamer binds the target protein which is then bound by a second fluorescently labelled “detection aptamer”.

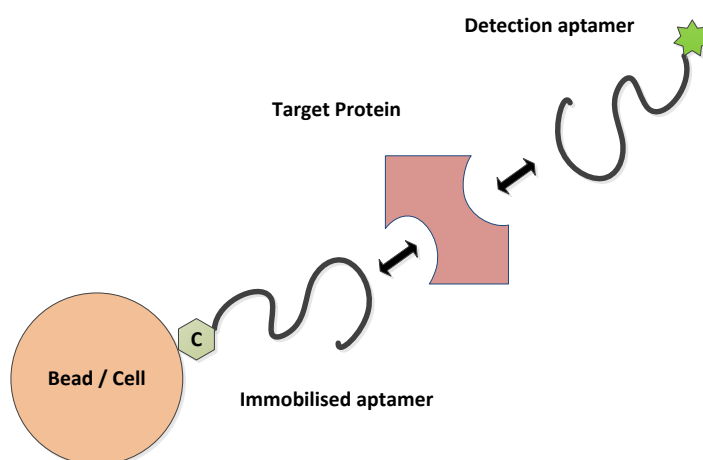


Figure 72: Schematic drawing of the aptamer-based sandwich assay. Immobilised aptamers bind the target which is then detected by a second labelled aptamer.

Initial experiments were again carried out using aptamers immobilised on beads. The VEGF aptamer V7t1 was bound to polystyrol beads, because it appeared superior to the other tested VEGF aptamer Del5-1. “Bioplex 200 COOH Beads 24” from Biorad were used for the experiments and modified according to the manufacturer (6.1.20). In summary, 3'-amino-modified aptamers were coupled to the carboxyl-groups on the beads surface via EDC coupling chemistry. 5000 of the aptamer modified beads were then incubated with 100 μ l (200 nM) of the unlabelled target protein VEGF and the

negative control myoglobin for 30 min in a rotator. Afterwards the beads were pelleted by centrifugation (4 min, 14000 g) and the supernatant discarded. The beads were finally resuspended in 50 μ l of the labelled detection aptamer and analysed with a Biorad Bioplex 200 system, which works by the same principle as a flow cytometer but is tailored to bead analysis. The detection aptamers were labelled with the fluorescent protein R-phycoerythrin (R-PE) as recommended by the manufacturer (6.1.11) and alternatively with the fluorescent dye Cy3 which should also be compatible with the instruments laser and detector settings. Cy3 was included as alternative label because it is much smaller (0.8 kDa) than the fluorescent protein R-PE (240 kDa) which might avoid steric hindrance of the aptamer during target binding. Both VEGF aptamers V7t1 and Del5-1 were tested as detection aptamers in the sandwich assay.

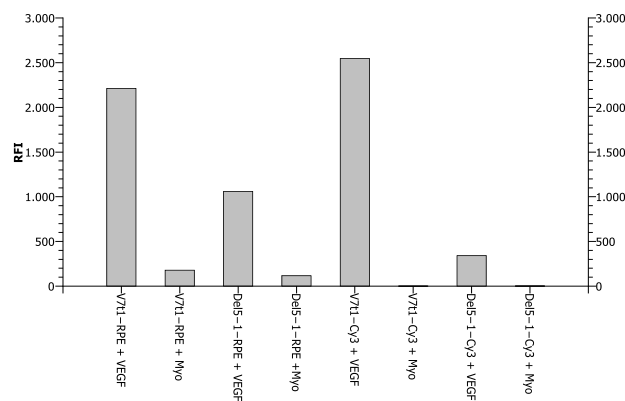


Figure 73: Aptamer-based sandwich assay on beads. The labels indicate the used detection aptamer and protein. Data presents median values without error bars.

Figure 73 gives an overview of the tested aptamer combinations that were used to detect the bound target protein VEGF. The results also include myoglobin as a negative control that should not be bound by the bead immobilised aptamer or by the second detection aptamer. The data meets the expectations quite well. All sandwich assays with the target protein VEGF give higher fluorescence signals than the samples containing the negative control myoglobin. The aptamer V7t1 again exhibits a stronger target binding than Del5-1. For the R-PE labelled aptamers there appears to be low unspecific binding to the myoglobin incubated beads whereas the corresponding samples with Cy3 label show signals close to zero.

To further assure the obtained result, the test was repeated and expanded with a negative control on the aptamer site of the assay. The aptamers 264 and 266 which do not bind VEGF were chosen for this purpose and used as 3'-amino modified versions. All

detection aptamers were used with a Cy3 label this time, which proved to work successfully in the previous analysis. The preparation of the beads was done as described in the appendix 6.1.20. Finally the samples were analysed on a Biorad MagPix instrument to measure the fluorescence intensities of the respective beads. **Figure 74** shows the obtained mean values of all samples. The labels explicitly describe the used components of the sandwich assay in the following order: The bead immobilised aptamer is named first, than the protein and at last the detection aptamer.

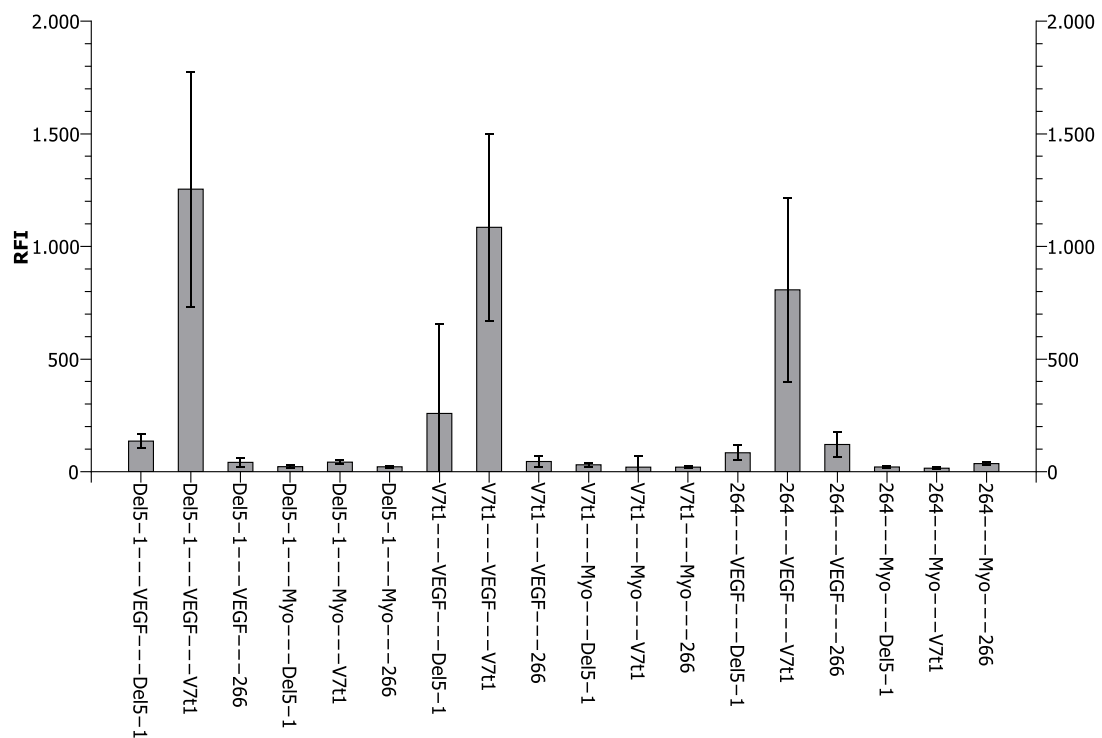


Figure 74: Systematic investigation on specificity of the bead-based aptamer sandwich assay. All detection aptamers are labelled with the fluorescence dye Cy3. Data presents mean values.

It can be seen that the sandwich assay preparations which contain the VEGF aptamer V7t1 work best and show the highest fluorescence values. The assay also works with two identical aptamers because VEGF is a homodimer and presents two identical binding sites. Those including the aptamer Del5-1 as detection aptamer are however yielding lower signals than those with V7t1. The samples which contain one or more negative control elements as parts of the sandwich assay show considerably lower fluorescence values except for the sample 264-VEGF-V7t1. This preparation yields a fairly high fluorescence although the immobilised 264 should not bind the VEGF. A possible explanation for this finding is a general unspecific binding of VEGF to the oligonucleotide exposing bead surface and its subsequent detection by the highly affine

V7t1 aptamer. Although the systematic investigation of specificity and affinity of the aptamer sandwich assay is not flawless, the results are quite promising. The development of a sandwich based assay for protein detection on particles in a flow cytometer seems feasible. By optimising sample preparation and washing procedures it could be tested if the unspecific binding can be reduced or eliminated.

The next step was the transfer of the sandwich assay from beads to the surface of real cells. CHO cells were chosen again as model system for this approach. Immobilisation of aptamers was achieved by the cyanuric chloride activation protocol described above 6.1.16. The 3'-amino-modified aptamer V7t1 was used for immobilisation on the cells and modified cells were subsequently incubated with a concentration series of unlabelled VEGF for 30 min. After incubation, the cells were centrifuged and supernatant was discarded. The cell pellet was resuspended in Cy3-labelled V7t1 aptamer and incubated for further 30 min. After centrifugation the pellet was again resuspended in aptamer binding buffer and analysed by flow cytometry to detect the bound aptamers. **Figure 75** shows the results of the aptamer-modified cells compared to a negative control with no immobilised aptamers on the cell surface. The data reveals no difference in signal intensity for the cell-based sandwich approach and the negative control. The fluorescence intensities are low and based on the data no binding is observable. This might be caused by problems with the sandwich assay and the detection aptamer which has to bind the target in the complex environment of the cell surface.

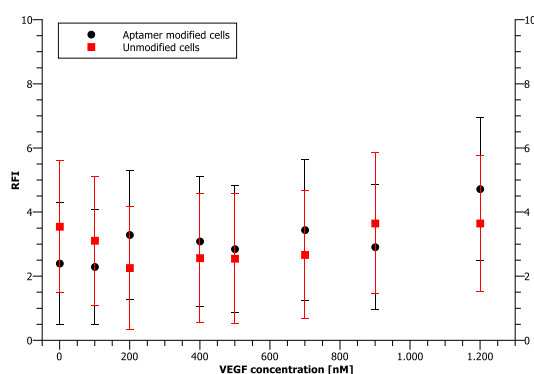


Figure 75: Analysis of modified cells used for a aptamer sandwich assay. The modified cells were incubated with increasing VEGF concentrations and subsequently incubated with a detection aptamer. No binding can be detected.

It can be concluded that the aptamer sandwich assay depicted in **Figure 72** works with limitations on aptamer modified beads. The successful transfer of the assay to cells

could not be achieved but the approach presents a good starting point for further experiments on the development of the assay.

5 Conclusions and outlook

The aim of this work was the investigation of aptamer applications for flow cytometry assays. These investigations should be performed by the development and analysis of adequate model systems. Two projects were carried out to explore the feasibility of aptamer-based assays. The first aimed at using aptamers as specific recognition reagents for labelling cell surface molecules in flow cytometry analysis. This task is typically performed by antibodies which have been used for decades as stains in flow cytometry. Aptamers could complement antibodies in various assays or even substitute them by offering higher storage stability at reduced costs. The second project was intended to investigate the possibility of an aptamer-based screening assay that employs flow cytometry and cell sorting to select cells with a high protein secretion. This application is of particular importance for the production of biopharmaceuticals which gain more and more importance and are needed to treat increasing numbers of patients in the ageing societies.

Part 1: Aptamers as stains for cell surface proteins in flow cytometry

A model system comprised of the aptamer TD05 was used to study the application of aptamers as cell surface stains for flow cytometry. The functionality and specificity of fluorescently labelled TD05 was verified in a protein microarray binding assay with the target protein IgM and other non-target proteins (4.1.1). The aptamer only showed binding to the IgM but not to the negative controls present in the experiment. Further negative controls were introduced to assure that the binding to IgM is specific and does not result from the oligonucleotide nature of the aptamer molecule. A random oligonucleotide sequence and a pool of $\sim 10^{12}$ different sequences were used for this purpose and compared to the aptamer in the above mentioned microarray assay. Both negative controls showed no binding to the target molecule, proving the specificity of the aptamer-target binding for TD05. The investigation was then transferred to the flow cytometry format. Firstly by analysing beads modified with the target molecule IgM, which were incubated with the fluorescently labelled aptamer and subsequently analysed. By comparing the binding of TD05 to IgM beads with binding to beads modified with the non-target protein BSA, it could be shown that the aptamer-target binding can be detected by flow cytometry. To verify the binding of TD05 to IgM molecules on the surface of the Ramos target cells, microscopy analysis of stained cells

were performed. The aptamer was able to stain Ramos cells, whereas CHO cells were not stained after incubation with TD05. Cultured Ramos cells were subsequently incubated with TD05 and analysed by flow cytometry (4.1.4). The results show strong binding to the target cells. CHO cells and more closely related CCRF-CEM cells were used as negative controls to exclude the possibility of unspecific binding to common cell surface structures. None of the negative controls was bound by the aptamer. The random sequence and oligonucleotide pool were also used to further assure the specific binding of TD05 to Ramos cells. The observed binding for the controls was very low and the marginal staining is believed to result from unspecific binding to cell surface molecules. In order to confirm the proteinogenic nature of the cell surface target another experiment was conceived in which Ramos cells were treated with a proteinase to partially digest the proteins on the cell surface. When compared to untreated cells, the proteinase treated cells showed fewer binding of the aptamer thereby supporting the hypothesis of IgM as the target molecule.

The aptamer TD05 was also used to fabricate a new kind of detection agent by coupling the aptamer to fluorescent nanoparticles called quantum dots (4.1.5). The conjugates were afterwards characterised in binding studies by using protein microarrays as described above for TD05 labelled with a standard organic dye. The conjugates proved to be able to recognise IgM and showed no binding to the protein negative controls. The conjugates were subsequently used to label Ramos cells and analyse the staining by flow cytometry. The conjugates failed to show specific binding to the target cells. The unspecific binding to the control cells is believed to result from non-specific cellular uptake of the aptamer-QD conjugates. The use of aptamer functionalised QDs still presents a promising alternative to established antibody-based staining in flow cytometry. Especially with regard to multicolour applications, QDs offer advantages because of their good excitability and their narrow emission spectra. Further optimisation of the application protocols with regard to incubation times and washing steps is needed to find conditions enabling the specific staining of cells with this novel reagents.

Part 2: Immobilisation of aptamers on the cell surface and their characterisation by flow cytometry

In the second part of this thesis, the investigations focused on the immobilisation of functional aptamers on the cell surface with the ultimate goal of demonstrating a proof

of principle for a flow cytometry screening of secretory cells used in biopharmaceutical production. Starting from scratch the immobilisation of aptamers was first done on bead microspheres, which served as basic models for cells. Different aptamers were tested for their ability to still recognize their target after immobilisation. The immobilisation was performed by two different approaches. Immobilisation of biotinylated aptamers on streptavidin beads did not yield functional aptamers in all experiments. For direct immobilisation on beads the results were more promising. Whether or not an aptamer stays functional after immobilisation depends on its fold and the functionality has to be tested and confirmed for each aptamer individually, before further applications can be developed.

The indirect immobilisation of aptamers on the cell surface via a streptavidin bridge was shown step by step for the aptamer 264 which was selected against the Fc-fragment of human IgGs (4.2.1.2). Although the immobilisation was successful, the aptamer was not functional on the surface and it could not be shown to bind its target. Various approaches were investigated to solve this problem but later performed binding studies by MST revealed a very low affinity of the aptamer-target interaction in solution. After immobilisation the affinity will probably even be lower due to sterical impairment. The low affinity of the target is problematic because higher Fc-fragment concentrations also lead to increased unspecific binding to the cell surface. The failure of this aptamer-target system was a huge drawback for the project because it could have been used to screen antibody producing cells with the cell surface capture assay. However, by using a different aptamer-target system, it could be shown that an aptamer against VEGF was still able to bind its target after immobilisation on the cell by the indirect approach (4.2.1.3). Flow cytometry measurements showed increased binding of the fluorescently labelled protein which was incubated with the cells at different concentrations.

Furthermore it was demonstrated that the immobilisation of aptamers by the indirect approach via a streptavidin bridge is also feasible for other cells than CHO. The biotechnologically important yeast *P. Pastoris* was successfully modified with the aptamer matrix and a comparative cultivation showed no adverse effects on the growth of the cells.

To circumvent the tedious multi step method of modification required for the indirect immobilisation, a new method of immobilisation was developed. Amino-modified aptamers, which were activated via cyanuric chloride, were used for direct

immobilisation of aptamers on the cell surface (4.2.2.3). The approach is based on the binding of the activated amino group to other amino groups on the cell surface and proved to work well for a model system of amino-exposing liposomes and CHO cells. Aptamers targeting VEGF also stayed functional after immobilisation on cells and were able to bind their target proteins, which could be shown by flow cytometry.

In order to be used in later cell sorting applications, it is an absolute prerequisite that the used immobilisation procedure has no negative effect on the cells viability and growth. This work demonstrated the successful cultivation of cells directly modified with cyanuric chloride activated aptamers (4.2.2.4). The results indicate that cells can be further cultured and expanded for further screening after this modification.

Finally, a possible detection method for a later application in screening for high secreting cells was investigated. While all previous investigations were performed with fluorescently labelled target proteins, the next step involved the evaluation of an aptamer based sandwich detection assay (4.2.2.5). In a final application the amount of secreted protein captured by the immobilised aptamers has to be determined by either using a fluorophore-quencher system or a second detection aptamer. It could be shown that a sandwich detection assay works quite well for bead immobilised aptamers, although some issues with unspecific binding to the used beads could be found. However, when transferred to the cell surface the detection by a second aptamer failed to work. This might be because of the more complex environment found on the cell surface which leads to sterical hindrance of the assay components. The unspecific binding, which was observed in the bead-based investigations is a problem often encountered in the development of aptamer applications and presents a major hurdle for the use of aptamers in analytical assays. Unspecific binding of aptamers can in general occur to positively charged surfaces due to the aptamers negatively charged phosphate groups and to other oligonucleotide structures by base pairing and partial hybridisation. For further development of the assay it would be useful to develop a target release system consisting of a secreting cell with a product that can be bound reliably by a well characterised aptamer. This release system could then be studied in detail for the development of a functioning detection system and a proof of principle for the isolation of cells with a high secretory performance.

6 Appendices

6.1 Methods

6.1.1 Preparation and analysis of reverse phase protein microarrays for analysis of fluorescently labelled aptamers and aptamer-quantum dot conjugates

The protein microarrays were fabricated by spotting protein solutions on aldehyd functionalized glass chips (VSS-25, Vantage Silylated Aldehyde Slides, CEL, USA) A contact free spotter was used for this purpose GeSiM (Modell: NanoPlotter 2.1). Eight droplets with a volume of approximately 0.2 nl were deposited per spot. The spotting process was performed at room temperature and a humidity of 70 %. PBS was used as spotting buffer. The chips were incubated for further 30 min under this conditions and then dried for 30 min at room temperature at atmospheric humidity.

The following samples were spotted:

	Proteinsolution	Spotted concentration [mg/ml]			
Negative controls	BSA	1	-	-	-
	FCS	1	-	-	-
	(PFEI)	1	-	-	-
Target protein	IgM	1	0,5	0,1	0,01

The schematic pattern of a spotted microarray block is shown in **Figure 76**. The four concentrations of IgM are spotted on the left, followed by a gap of three columns and the negative control proteins. For the analysis of the aptamer quantum dots only BSA and FCS were used as negative controls.

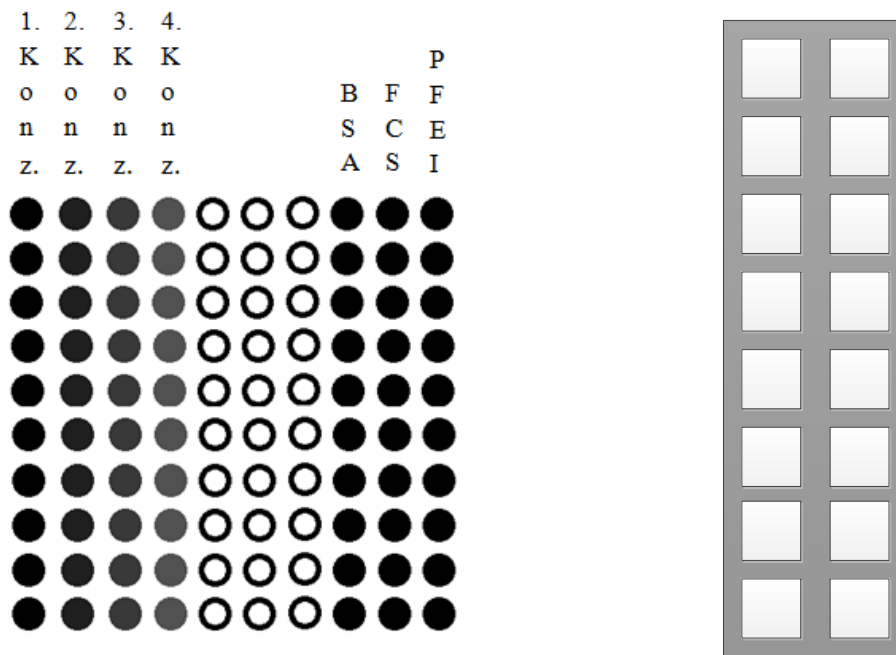


Figure 76: Schematic pattern of a plotted microarray block (left). A fully spotted chip consisted of 16 of these blocks (right). 1. Konz.: 1 mg/ml; 2. Konz.: 0.5 mg/ml; 3. Konz.: 0.1 mg/ml; 4. Konz.: 0.01 mg/ml.

The microarrays were blocked with a solution of BSA in PBS (1% w/v) for 30 minutes and afterwards washed with PBS for 5 min and two times with H₂O for 1 min. Next the rubber support was applied to create isolated chambers for each block on the chip. 50 µl of the aptamer or aptamer-QD conjugate in TD05 binding buffer were applied into each chamber. The microarray was incubated overnight at RT and then each chamber washed three times for 10 min with 100 µl binding buffer. After taking of the rubber support the chips were washed again three times for 10 min in binding buffer. The chips were finally dried by centrifugation or compressed air and scanned by using a dedicated fluorescence scanner.

The used scanner was a GenePix®4000B (Axon Instruments, USA). The chips were scanned with the preinstalled settings for the dye. The aptamer-QD655 chips were scanned with the settings for Cy5 which are suitable for excitation and detection of QDs with 655 nm emission maximum. The laser power was 100 % and different gains were used as indicated for the results.

The obtained images were analysed with the software GenePixPro 6.0 (Molecular Devices, USA). The presented relative signal intensity is calculated by subtracting the measured background mean (BM) from the signal mean (SM) of the respective spot. Error bars show the standard error of the value calculated on the basis of all replicates.

6.1.2 Microscopic analysis of aptamer-stained Ramos cells

The samples for the microscopic analysis of aptamer-stained Ramos cells were prepared as follows:

- 1 ml cells per sample were taken from culture and washed once with 1 ml PBS. The washing was done by centrifuging the cells in Eppendorf tubes for 5 min at 200 g and resuspending them in PBS
- Afterwards the cells were washed 1 x with TD05 binding buffer and 1x with binding buffer containing 2 % FCS
- Cells were centrifuged again and resuspended in 100 µl aptamer in binding buffer with 2% FCS
- The samples were incubated for 45 min
- Afterwards the samples were washed 1 x with binding buffer with 2 % FCS and 1 x with binding buffer
- The cell pellets were stored on ice until analysis (max 1 h)
- For analysis the cells were resuspended in 50 µl binding buffer and applied onto a microscopic slide
- The fluorescence was analysed with an Olympus IX 50 fluorescence microscope using the NG filter (Exc. 530-550; Em. BA 590) which filters for Cy3 fluorescence

6.1.3 Protein coupling to tosyl-activated beads

The proteins IgM and BSA were coupled to tosyl-activated beads (Dynabeads-280-Tosyl, Invitrogen, USA) according to the suppliers protocol. Washing fractions were collected from the process to calculate the amount of coupled protein. The subsequent analysis of the solution at 280 nm using a Nano Drop ND-1000 spectrophotometer revealed a disturbance of the protein measurement which made it impossible to calculate the protein amount on the beads. The disturbance might be caused by substances leaching out of the beads.

For the flow cytometry analysis, 1 µl of the modified bead solution were incubated with 100 µl of aptamer in binding buffer for 60 min at RT in the dark. Afterwards the beads were separated from the supernatant using a magnetic stand, resuspended in 300 µl binding buffer and analysed by flow cytometry.

6.1.4 Staining of cells with fluorescently labelled aptamers for flow cytometry analysis

The sample preparation was as follows (washing is done by resuspending the cell pellet in buffer and then centrifugating it for 5 min, 200 g):

- Cells were washed 1 x with PBS
- Cells were washed 1 x with TD05 binding buffer
- Cells were split into Eppendorf tubes at 1 ml with $\sim 10^6$ cells/ml
- Cells were pelleted in the Eppendorf tubes by centrifugation as described above
- Cell pellets were resuspended in 100 μ l of the aptamer-FITC solution in binding buffer with respective concentration.
- Incubation for 60 min on an eppendorf tube shaker in the dark at RT
- Centrifugation as above, discarding the supernatant
- The pellets were kept on ice in the dark until analysis
- For analysis the pellets were resuspended in 300 μ l binding buffer and subjected to flow cytometry

All flow cytometry data was analysed using the software WINMDI 2.8 (J. Trotter, Scrips Institute, USA) to obtain mean fluorescence intensities and additional data for the cells.

6.1.5 Proteinase K treatment of Ramos cells

Ramos cells were taken from culture, diluted to a concentration of $5 \cdot 10^6$ cells/ml with PBS and 3 ml of the suspension centrifuged for 5 min at 200 g. The supernatant was discarded and the cell pellet resuspended in 3 ml proteinase K (0.1 mg/ml) in PBS. The cells were incubated for 11 min at 37 °C in an eppendorf tube shaker at 450 rpm. Afterwards the reaction was quenched/stopped with 200 μ l FCS (1 mg/ml) and the tubes kept on ice for a few minutes. The cells were then washed with 6 ml binding buffer and centrifuged for 5 min at 200 g at RT. After discarding the supernatant the pellet was resuspended in 16 ml binding buffer. The cells were then subjected to the standard aptamer labelling protocol (6.1.4).

6.1.6 Fabrication of aptamer-QD conjugates

The fabrication and characterisation of the aptamer-QD conjugates was done in cooperation with Annette Müller during the experimental work of her Bachelor thesis in Q1/2012. The conjugates were prepared with a 8 μM stock solution of carboxyl modified QD655 (Invitrogen, USA). 6.25 μl of the stock solution were mixed with 50 μl 10 mM SBB (pH 7.4) and 12 μl aptamer solution (5'-amino modified 150 μM). 1.425 μl 1-Ethyl-3-(3-dimethylamino-propyl)carbodiimide hydrochloride (EDC) (10 mg/ml,) prepared fresh in ddH₂O were added to the solution. The reaction was incubated for 3 h at RT while shaking on an eppendorf tube shaker at 400 rpm. Afterwards the conjugates were washed eight times by adding 200 μl 50 mM SBB (pH 8.3) and centrifugating for 2.5 min and 4000 g at 25 °C in a 50 kDA MWCO spin column. After the last washing step the supernatant was transferred into a new tube. 30 μl 10 mM SBB (pH 7.4) were added.

6.1.7 Staining of cells with aptamers and aptamer-QD conjugates for flow cytometry

Cells were taken from culture and diluted with PBS to yield a cell concentration of $1 \cdot 10^6$ cells/ml. Samples of 1 ml were transferred to reaction tubes. Cells were then washed by centrifugation (200 g for 5 min) 1x with PBS, 1x with aptamer binding buffer and finally resuspended in 100 μl of the respective concentration of labelled aptamer. The samples were incubated for 60 min at RT on an Eppendorf tube shaker at 450 rpm. After incubation, the cells were pelleted in a centrifuge (200 g for 5 min), the supernatant was discarded and the pellets kept on ice until analysis (max 1 h). For analysis the pellets were resuspended in 300 μl aptamer binding buffer and measured in a flow cytometer. After gating the living cells via FSC/SSC the fluorescence was analysed in the respective detector (FITC: FL1; Cy3: FL2; QD655: FL3).

6.1.8 Micro BCA assay

The micro BCA assay was obtained from Thermo Fisher Scientific and used according to the manufacturer. The assay was used to determine the concentration of VEGF after purification and after labelling with FITC.

6.1.9 Cell cultivations

Ramos and CCRF-CEM cells were obtained from Deutsche Sammlung von Mikroorganismen und Zellkulturen (DSMZ, Braunschweig, Germany). All information on these cell lines was obtained from the DSMZ website (www.dsmz.de, accessed on 01.07.2011)

Ramos cells (DSMZ ACC No. 603)

Species: human (*Homo sapiens*)

Cell type: Burkitt lymphoma

Origin: established from the ascitic fluid of a 3-year-old boy with American-type Burkitt lymphoma in 1972; cells were described to be EBV-negative but EBV infectible, to carry the (8;14) translocation and TP53 mutations

Morphology: round cells growing singly or in clumps in suspension

Medium: 80% RPMI 1640 + 20% h.i. FBS

Subculture: split culture 1:2 to 1:3 twice a week; seed out at ca. 0.8×10^6 cells/ml; maintain at ca. $0.5-1.5 \times 10^6$ cells/ml

CCRF-CEM cells (DSMZ ACC No. 240)

Species: human (*Homo sapiens*)

Cell type: T cell leukemia

Origin: established from the peripheral blood of a 3-year-old Caucasian girl with acute lymphoblastic leukemia (ALL) at relapse (terminal) in 1964 (first continuous human T-ALL cell line)

Morphology: round cells growing singly in suspension and as adherent epitheloid cells forming a monolayer

Medium: 90% RPMI 1640 + 10% h.i. FBS

Subculture: split saturated culture every 2-4 days; cells form monolayers until confluence and will then go into suspension; after transfer of suspension cells to a new flask, a new monolayer will develop; it may be necessary to use trypsin/EDTA or vigorous pipetting to detach the adherent cells; seed out after thawing at $0.5-1.0 \times 10^6$ cells/ml

CHO K1 cells

Species: Chinese hamster (*Cricetulus griseus*)

Cell type: ovary

Medium: Miltenyi CHO MACS with 8 mM glutamine

Subculture: split culture every 3-4 days;

Pichia Pastoris GS 115

The *Pichia pastoris* host strain GS115 has a mutation in the histidinol dehydrogenase gene (*his4*) that prevents them from synthesising histidine. Cultures were prepared fresh from frozen stocks provided by Maria Zahid (126).

The cultivation is described in 4.2.1.4 and was done in BMGY media (buffered glycerol-complex medium), which consists of 1 % (w/v) yeast extract, 2 % (w/v) peptone, 100 mM potassium phosphate, 1.34 % (w/v) YNB (yeast nitrogen base), 4×10^{-5} % (w/v) biotin, 0.004 % histidine (w/v) and 1 % glycerol with a pH of 6.0.

6.1.10 Production of VEGF using a recombinant *E.coli* strain

The human vascular endothelial growth factor (VEGF₁₆₅) was produced by culturing a recombinant *E.coli* strain and purifying the protein from inclusion bodies formed by the bacterium. The strain *E. coli* BL21DE3, transformed with the pET16b-VEGF165-Xa-His vector, was obtained from Maren Lönne (co-worker, Institut für Technische Chemie) and used for this purpose. A map of the vector is shown in **Figure 77**. The protein sequence coded by the vector is as follows:

```
MGHHHHHHHHSSGHMHIEGRAPMAEGGGQNHHEVVKFM DVYQRSYCHPIET  
LVDIFQEYPDEIEYIFKPCVPLMRCGGCCNDEGLECVPT EESNITMQIMRIKPHQ  
GQHIGEMSFLQH NKCECRPKKDRARQENPCGPCSERRKHLFVQDPQTCKCCK  
NTDSRCKARQLELNERTCRCDKPRR
```

The sequence starts with a 20 amino acid long section carrying the His-tag followed by the 165 AS long sequence of the VEGF obtained from the Protein Data Bank (Acc. No. NP_001165097).

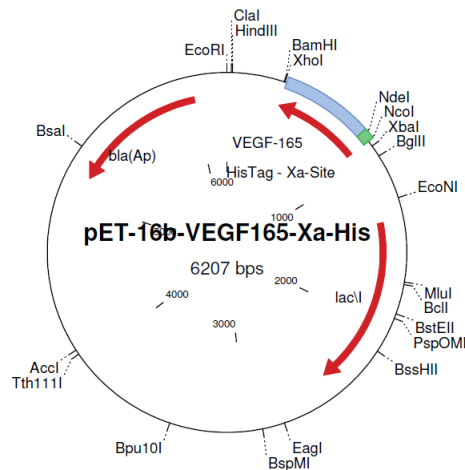


Figure 77: Map of the vector pET16b-VEGF165-Xa-His, which was used to produce recombinant VEGF with an *E.coli* culture. Image obtained from Maren Lönne, co-worker, Institut für Technische Chemie.

The cultivation was performed at 37°C and 150 rpm in LB-Medium containing carbenicillin (150 µg/ml). The induction was performed using a 200 mM IPTG stock solution after the culture reached OD₆₀₀ of 0.5 resulting in a final IPTG concentration of 1 mM. The cells were cultivated for further 4 hours and harvested by centrifugation at 6000g. The cell pellet was stored at -20°C until the downstream process.

The cell disruption and cleaning of the inclusion bodies was performed according to Siemeister *et al.* (131) the solubilisation of VEGF from the inclusion bodies was performed according to Pizarro *et al.* (132). The subsequent purification of VEGF was done according to a method developed by Maren Lönne in her ongoing dissertation at the Institute of Technical Chemistry. The process consists of an ion-exchange chromatography followed by dialysis and a heparin affinity chromatography.

Ion exchange chromatography

After solubilisation of the inclusion bodies at pH 9.8 the partially negatively charged VEGF was bound to a Sartobind Q75 membran adsorber and separated from differently charged proteins by washing with 25 mM CHES, 1mM Urea, 100 mM L-Arg pH 9. After elution using 25 mM HEPES, 1 mM Urea, 1 M NaCl, pH 7.1, the VEGF containing fractions are collected and later dialysed using dialysis tubes with 6-8 kDa cut off (Spectrum laboratories Inc., USA). The respective chromatogram of the ion exchange chromatography is shown in **Figure 78**. The dialysis is performed against PBS pH 8 (at least 100x volume of the sample) for at least 4 hours at 4°C.

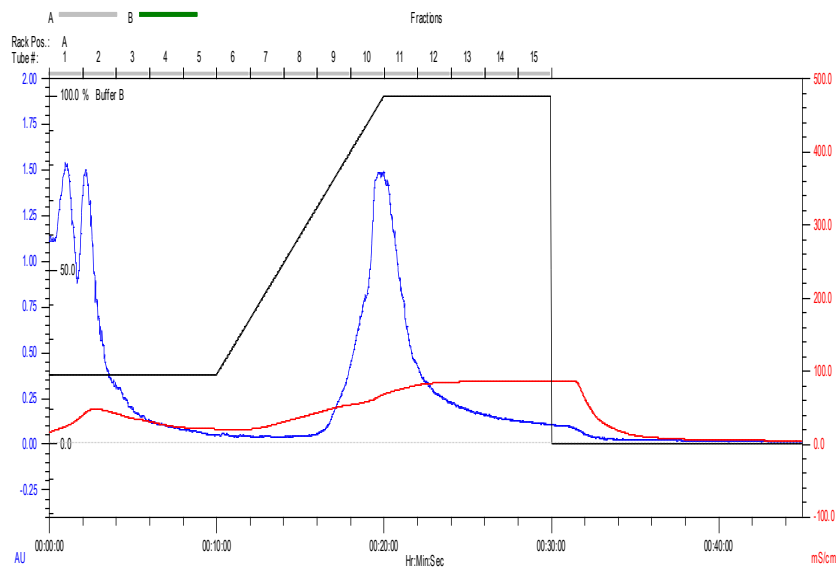


Figure 78: Chromatogram of the IEX chromatography for purifying VEGF. The VEGF is eluted using a salt gradient. The VEGF containing fractions 10 and 11 are taken for further downstream steps.

Heparin affinity chromatography

Afterwards the sample is subjected to a heparin affinity chromatography using a HiTrap Heparin column 1 ml (GE Life Science). After sample loading the column is rinsed with 15 ml PBS pH 8. The VEGF is eluted by using PBS with 2 M NaCl pH 8. The respective chromatogram is shown in **Figure 79**. The VEGF containing fractions are stored at $-20\text{ }^{\circ}\text{C}$ until further use. The VEGF concentration was measured by BCA assay.

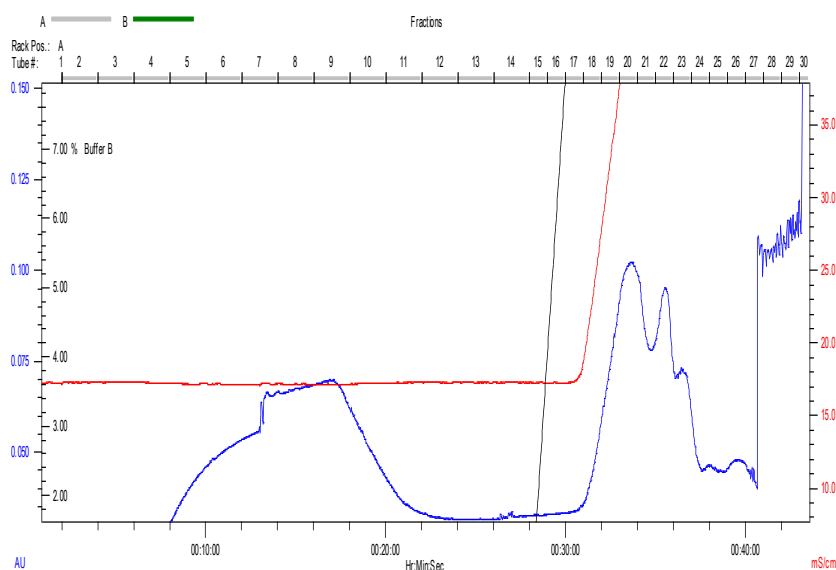


Figure 79: Chromatogram of the heparin affinity separation for purifying VEGF. The VEGF is eluted using a salt gradient. The containing fractions 19-24 are collected. Detection wavelength 280 nm.

6.1.11 Labeling of aptamers with R-phycoerythrin (R-PE)

For the experiments with the Biorad Bioplex 200, aptamers were labeled with the fluorescent protein R-PE using a R-PE rapid conjugation kit (LYNX, USA). The conjugation was performed according to the suppliers instructions. In summary, a third of the volume contained in the ready to use R-PE kit was used to label 695 pmol of aptamer. The reaction mixture was incubated for three hours at RT. After incubation 2 μ l of quencher was added and the solution was left for 30 min before further use.

6.1.12 Labeling of proteins with fluorescein isothiocyanate (FITC)

The proteins lysozyme (Lys), bovine serum albumin (BSA), cytochrome C (Cyt-C) and myoglobin (Myo) were obtained from Sigma Aldrich, Germany. The human VEGF165, was produced in-house using a recombinant *E. coli* strain and purified according to section 6.1.10. The proteins were labelled with FITC (Sigma Aldrich, Germany) according to the manufacturer. The dye to protein ratio (D/P) was assessed by measuring the protein (280 nm) and fluorophore (495 nm) absorbance on a NanoDropTM-1000 spectrophotometer.

6.1.13 Immobilisation of aptamers on streptavidin-modified beads

Dynabeads M-280 streptavidin from Invitrogen, USA, were used for the experiments. The modification with biotin-labelled aptamers was performed according to the product information sheet (<http://www.lifetechnologies.com/order/catalog/product/11205D>; accessed on 20.01.2014):

The used binding and washing (B&W) buffer is prepared double concentrated (2x):

10 mM Tris-HCl pH 7.5

1 mM EDTA

2 M NaCl

Modification procedure:

1. Beads are diluted to 1 μ g/ μ l by adding 1 μ l of the stock solution to 99 μ l B&W (2x).
2. Add 100 μ l DNA solution (in dd H₂O).

3. The solution was incubated for 15 min in a rotator.
4. The beads were separated from the solution using a magnetic stand.
5. The beads were washed 3x with 200 μ l 1x B&W buffer for 10 min in a rotator.
6. Finally the beads are resuspended in PBS and stored at -4°C until further use.

6.1.14 Immobilisation of aptamers on carboxyl-modified magnetic beads

Terminal amino-modified aptamers were coupled to carboxyl-modified magnetic beads (BioMag® Maxi Carboxyl, Bangs Laboratories Inc., Fishers, IN, USA) utilising EDC coupling chemistry. All coupling and washing steps were performed in Eppendorf tubes under rotation of 20 rpm in a rotator. Magnetic separations were performed manually utilising a magnetic stand.

Per experiment, 100 μ l of the magnetic particle suspension (20 mg/ml) were washed with 100 μ l 25 mM MES pH 6 for 10 min twice. Afterwards, 100 μ l of 25 μ M aptamer solution in MES was added and incubated for 30 min at room temperature. EDC solution (10 mg/mL) was prepared in ice-cold MES immediately before use and 30 μ l of this solution were added to the magnetic beads. The coupling was performed at 4°C overnight. To remove unbound aptamer, the aptamer-modified magnetic beads were washed with 100 μ l of 50 mM Tris pH 7.4 for 10 min four-times. Finally, the magnetic beads were washed with binding buffer for 20 min twice, transferred to fresh binding buffer and stored at 4°C . The amount of immobilized aptamer was calculated via subtraction of the amount of the aptamer remaining in solution after immobilisation (including the aptamer found in the washing fractions) from the amount of aptamer in the original solution. Aptamer concentrations were determined with a NanoDrop™ 1000 spectrophotometer utilising the respective buffer as a blank. The concentrations were calculated based on the Lambert–Beer equation utilising the corresponding extinction coefficient.

6.1.15 Activation of aptamers via cyanuric chloride

Amino-modified aptamers were activated for coupling to other amino groups by using cyanuric chloride (22). 100 μ l of the aptamer (200 μ M in H_2O) were mixed with 80 μ l of freshly prepared SBB buffer 0.1 M, pH 8.3. Cyanuric chloride was freshly solved in acetonitril (HPLC grade) at a concentration of 20 mg/ml. 10 μ L of the cyanuric chloride

solution were added to the 180 μl aptamer solution, mixed and incubated for 1 h at room temperature. Afterwards, the non reacted cyanuric chloride was removed by excessive buffer exchange with SBB 0.1 M, pH 8.3 utilising Vivaspin 6 columns with a 3 kDa cut off. The final concentration of the activated aptamer was measured with a NanoDropTM 1000 spectrophotometer.

6.1.16 Immobilisation of cyanuric chloride-activated aptamers on living cells

CHO K1 cells were obtained from a shake flask culture, washed once with Dulbecco's PBS and diluted to a concentration of 10^6 cells/ml. After centrifugation (200 g, 5 min) the cell pellet containing 1 million cells was resuspended in 100 μL of the activated aptamer (10 μM) in SBB 0.1 M, pH 8.3 and incubated for 15 min under rotation at room temperature. Subsequently the cells were centrifuged again and the pellet washed once with 500 μl of the respective aptamer binding buffer. The resulting pellet with the aptamer modified cells was then used for the flow cytometry assay.

6.1.17 Immobilisation of aptamers on living cells using a biotin-streptavidin bridge

Approximately 3×10^6 cells/ml (CHO) or cultures with OD_{600} 1 (*P. pastoris*) were used for the immobilisation procedure. The cells were taken from shake flask culture and washed once with PBS. The cells were then split into reaction tubes in 1 ml portions containing 3×10^6 cells/ml and centrifuged at 200 g for 5 min, as in all following wash steps. The cell pellets were resuspended in 1 ml NHS Biotin (1 mM) and incubated for 10 min in a rotator. The cells were subsequently washed once with PBS. Afterwards the cell pellets were resuspended in 1 ml streptavidin (50 $\mu\text{g}/\text{ml}$ in PBS) and incubated for 5 min in a rotator. After a washing step with PBS the pellets were resuspended in 200 μl of biotinylated aptamer (6 μM in binding buffer) and incubated for 15 min on a rotator. The cells were finally washed with the aptamer binding buffer and subsequently used for incubation with the target protein (CHO) or for further cultivations (*P. pastoris*).

The DNA helix spacer was constructed by hybridisation of the elongated 264 aptamer (264 He) and the oligonucleotide-modified biotin (He B). The two partners were mixed with a volume of 50 μl each in 264 binding buffer to result in the desired concentration

of the aptamer with assembled spacer. The mixture was heated for 3 minutes at 90 °C and then left to cool to room temperature for approximately 30 minutes.

6.1.18 Flow cytometry analysis of protein binding to modified beads and CHO K1 cells

The aptamer-modified beads or cells were incubated with 200 µl of the fluorescently labelled protein for 30 min in the dark at room temperature while rotating. Afterwards the beads or cells are separated from the supernatant using a magnetic separator or a centrifuge, respectively. Finally the beads or cells are resuspended in 400 µl aptamer binding buffer and analyzed with an Epics XL-MCL flow cytometer (Beckman-Coulter, Brea, CA) or an FACS Vantage SE flow cytometer/sorter (BD Bioscience, San Jose, CA). At least 10000 events were analyzed per run. The fluorescence intensities resulting from the labelled proteins are recorded per event and subsequently analyzed using the software WinMDI 2.8. The mean fluorescence intensities are used as values corresponding to the amount of protein bound to beads or cells. For analysis signals are only taken from living cells by gating the population based on forward and side scatter signals in the corresponding dotplot.

6.1.19 Preparation of liposomes / GUVs (giant unilamellar vesicles) by lipid film rehydration

The GUVs were prepared according to a film rehydration protocol by Avanti Polar Lipids (133), USA based on Needham *et al.* (134).

1. Prepare a lipid stock solution (1 mg/ml) in chloroform:methanol (2:1 v/v) and mix the two used lipids (DOPC and DSPE-2000 amine) in a ratio of 50:1.
2. Place a 50 µl drop of lipid solution using a 50-µl glass syringe onto one side of a roughened Teflon disk. Quickly spread the lipid solution over the entire Teflon surface using the syringe needle. With the “lipid” side up, place the disk into a 100-ml beaker.
3. Remove the volatile organic solvents from the lipid by placing the beaker in vacuo for 2 hours. Light sensitive mixtures (as used in this thesis) that contain

polyunsaturated lipids should be protected from light using aluminum foil. Purge the vacuum with nitrogen gas.

4. Cover the beaker loosely with Parafilm and prehydrate the lipid film with a warm (45-50 °C) water-saturated nitrogen jet for 15 minutes. This was done by heating the gas stream in glass pipe system embedded in a waterbath and directing it through a wash flask. Pictures of the equipment set up for this purpose are shown in **Figure 80**.
5. Preheat the buffer (PBS) to be encapsulated at a room temperature. Using a disposable plastic syringe fitted with a 0.2 μm syringe filter, gently add the rehydration buffer onto the pre-hydrated lipid film. Add enough buffer to completely immerse the entire Teflon disk. Seal the beaker with Parafilm to prevent water evaporation and incubate overnight at room temperature. Typically, vesicles will form after the system is left to swell overnight.
6. During the incubation period, the lipid film will swell and strip away from the Teflon surface to form small “clouds” of vesicles. At this time, vesicles are ready for harvest and can be collected by gentle aspiration using a Pasteur pipette.

The pictures below show the equipment, which was set up for the prehydration step by a warm and water-saturated nitrogen jet:



Figure 80: A glass flask and a water bath were used to heat up nitrogen and enrich it with water. The jet was then directed to the beaker with the Teflon disk to prehydrate the lipids.

After harvesting, the vesicles were transferred to an Eppendorf reaction tube and concentrated by centrifugation (5 min, 200 g), discarding of the supernatant and resuspension of the vesicles in a smaller volume (e.g. 50 μ l) of PBS. The vesicles were then used for further experiments.

6.1.20 Modification of beads for analysis via Biorad Bioplex 200 and MagPix

The Beads used for the experiments with the Biorad Bioplex 200 and MagPix instruments were prepared according to the following procedure (manufacturers instructions, latex beads used for the Bioplex experiments were separated by centrifugation instead of magnetic separation) (135):

1. Bring a fresh aliquot of -20°C EDC powder to room temperature.
2. Resuspend the amine-substituted oligonucleotide to 1 mM in dH₂O.
3. Resuspend the stock vial of beads by vortexing at speed 7, followed by sonication for 15 sec.
4. Transfer desired volume of the stock beads (based on the scale) to an appropriately sized tube (1.5 ml).
5. Place the tube into a magnetic separator and allow separation to occur for 30-60 sec. This step is only performed for magnetic beads. The latex beads are separated by centrifugation at 5000 g for 5 min.
6. With the tube still positioned in the magnetic separator, carefully remove the supernatant without disturbing the beads.
7. Remove the tube from the magnetic separator and resuspend the beads in 50 μ l of 0.1 M MES, pH 4.5, by vortex and sonication for approximately 20 sec.
8. Prepare a 1:10 dilution of the 1 mM capture oligo to the resuspended beads and mix by vortexing.
9. Add 2 μ l (0.2 nmole) of the 1:10 diluted aptamer to the resuspended beads and mix by vortexing.
10. Prepare a fresh solution of 10 mg/ml EDC to the beads and mix by vortexing.
11. Incubate for 30 min at room temperature in the dark.
12. Add 1.0 ml of 0.02% Tween-20 to the coupled beads.
13. Use a fresh aliquot of EDC powder to prepare a second fresh solution of 10 mg/ml EDC in dH₂O.

14. Add 2.5 μ l of fresh 10 mg/ml EDC to the beads and mix by vortexing.
15. Incubate for 30 min at room temperature in the dark.
16. Add 1.0 ml of 0.02% Tween-20 to the coupled beads.
17. Place the tube into a magnetic separator and allow separation to occur for 30-60 sec.
18. With the tube still positioned in the magnetic separator, carefully remove the supernatant without disturbing the beads.
19. Remove the tube from the magnetic separator and resuspend the coupled beads in 1.0 ml of 0.1% SDS by vortex.
20. Place the tube into a magnetic separator and allow separation to occur for 30-60 sec.
21. With the tube still positioned in the magnetic separator, carefully remove the supernatant without disturbing the bead pellet.
22. Remove the tube from the magnetic separator and resuspend the coupled beads in 100 μ l of aptamer selection buffer, by vortex and sonication for approximately 20 sec.
23. Enumerate the coupled beads by hemacytometer:
 - a. Dilute the resuspended coupled beads 1:100 in dH₂O.
 - b. Mix thoroughly by vortex.
 - c. Transfer 10 μ l to the hemacytometer.
 - d. Count the beads within the 4 large corners of the hemacytometer grid.
 - e. Beads/ μ l = (sum of beads in 4 large corners) x 2.5 x 100
 - f. Note: maximum is 50000 beads/ μ l
 - g. Store coupled beads refrigerated at 2-8°C in the dark

For the aptamer sandwich assay, which was analysed with the Biorad MagPix device, the aptamer-modified beads were prepared as described above. The sample preparation was as follows:

- 5000 aptamer-modified beads were resuspended in 100 μ l VEGF binding buffer (TBSE)
- The beads were separated using a magnetic stand and resuspended in 100 μ l VEGF with a concentration of 1000 nM
- The beads were incubated for 30 min at room temperature in a rotator

- After separating the beads using a magnetic stand, the beads were resuspended in 100 μl of the Cy3-labelled detection aptamer with a concentration of 300 nM
- After further incubation for 30 min at room temperature in a rotator, 125 μl of binding buffer were added and the samples were analysed with the device

6.1.21 Measurement of binding affinity by microscale thermophoresis

Microscale thermophoresis is a method for determining binding constants based on an effect which is called “thermophoresis” and terms the movement of molecules along a temperature gradient. The movement depends on changes in size, charge and solvation shell of the molecules. Thermophoresis can be detected by fluorescence from either the molecule itself (e.g. through tryptophan residues) or fluorescence labels such as FITC, that are attached to the molecule. By using titration experiments it is possible to monitor the change of movement that is accompanied with increased binding of the interaction partners. Affinity constants can be calculated from the resulting data. **Figure 81** shows the principle of thermophoresis as presented by the company NanoTemper, Munich, Germany.

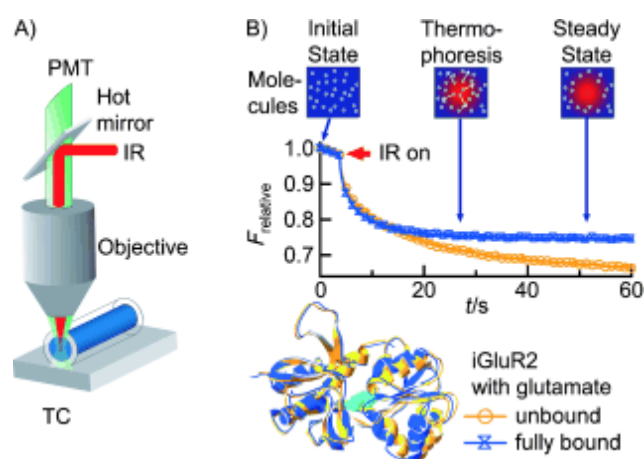


Figure 81: The principal setup and resulting data from a thermophoresis experiment (left). The solution in the capillary is heated with an IR-laser which is directed onto the capillary by a mirror. The IR-laser is focused on a local spot of the capillary. The fluorescence inside the capillary is detected by a photodiode and normalized. The fluorescence value is then plotted against the analysis time (right). After switching on the IR-laser, the temperature in the focused area increases, leading to thermophoresis of the molecules. This movement is then detected by a decrease of the normalized fluorescence. Binding of molecules to each other results in the formation of complexes that migrate slower, which can be detected by MST analysis. The obtained data can then be used to calculate binding constants for the interaction. Schematic obtained from Seidel *et al.* (136).

The measurements performed with this technique were done to determine the binding constant of the anti-IgG aptamer 264. The results are shown in 4.2.1.2. The experiments were conducted with a constant concentration of 100 nM of the FITC labeled 264 aptamer and a concentration series of the Fc-fragment. The highest concentration of IgG was 5 μ M, from which 15 1:1 dilutions were prepared for the analysis. Tween-20 was used with a final concentration of 0.05 % in the analysis buffer to prevent adherence at the capillary walls of the device. The measurements with the aptamer 264 and the polyclonal human IgG were performed using the device for label free analysis. In this case the IgG concentration was kept constant at 500 nM and a concentration series of the aptamer 264 was prepared. The highest concentration used was 50 μ M from which 1:1 dilutions were prepared. The samples were also prepared with a final concentration of 0.05 % Tween-20.

6.2 Materials

6.2.1 Chemicals

Table 5: Overview of used chemicals.

Substance	Supplier, country
Acetonitril (HPLC-Grade)	VWR International, LLC, Germany
Cyanuric chloride	Fluka (Sigma-Aldrich), USA
Dimethylsulfoxid (DMSO)	Carl Roth GmbH & Co.KG
EDC	Sigma-Aldrich, USA
EDTA-Disodium salt	Fluka (Sigma-Aldrich), USA
Ethanol	VWR International, LLC, Deutschland
FITC-conjugated ChromPure Human IgG, Fc Fragment	Jackson ImmunoResearch Laboratories, Inc, USA
Glycerin	AppliChem GmbH, Germany
Glycin	Fluka (Sigma-Aldrich), USA
HCl, concentrated	Fluka (Sigma-Aldrich), USA
IPTG	Sigma-Aldrich, USA
Magnesiumsulfat	Fluka (Sigma-Aldrich), USA
Mangansulfat	Fluka (Sigma-Aldrich), USA
Methanol (HPLC-Grade)	Carl Roth GmbH & Co.KG
NHS-FITC	Sigma-Aldrich, USA
Peptone	Biotechnica internacional S.A. DE C.V., Mexiko
Potassiumchloride	Fluka (Sigma-Aldrich), USA
Potassiumdihydrogenphosphate	Merck KGaA, Deutschland
Sodiumchloride	Merck KGaA, Germany

Sodiumhydroxide	Fluka (Sigma-Aldrich), USA
Sodiumphosphate	Fluka (Sigma-Aldrich), USA
Streptavidin-FITC	Sigma-Aldrich, USA
Yeast Nitrogen Base (YNB)	Fluka (Sigma-Aldrich), USA
Yeastextract	Carl Roth GmbH & Co.KG

6.2.2 Disposables

Centrifugal concentrators, Vivaspin 6 (3 kDa cut off), Sartorius Stedim Biotech, Germany

Centrifuge tubes, 15 ml and 50 ml, Sarstedt AG & Co., Nümbrecht, Germany

Erlenmeyer flasks, 125 ml, 250 ml, VWR International GmbH, Darmstadt

Reaction tubes, Sarstedt AG & Co., Nümbrecht, Germany

Sterile filters, Minisart 0,2 µm, Sartorius Stedim Biotech, Germany

Syringes, Omnifix, Braun, Germany

T-Flasks, 25 and 75 cm², Sarstedt Teruma Europe NV, Leuven

Halbmikroküvette, Sarstedt AG & Co., Nümbrecht

Pipett tips, Sarstedt AG & Co., Nümbrecht, Germany

6.2.3 Equipment

Equipment	Company
Spectrophotometer, Nano Drop ND-1000	NanoDrop Technologies, Inc., Wilmington, De, USA
Spectrofluorometer, Nano Drop ND-3300	NanoDrop Technologies, Inc., Wilmington, De, USA
Microarray scanner: GenePix@4000B	Axon Instruments, USA
Incubator, HeraCell 240	Heraeus Holding GmbH, Hanau, Germany
Cedex cell counter	Innovatis, Roche GmbH, Germany
Arium 611, Ultrapure Water System	Sartorius Stedim Biotech, Germany
Microarray spotter: NanoPlotter 2.1	GeSiM
Shaker	IKA Werke GmbH, Staufen
Centrifuge, Multifuge 3 s, Megafuge 1.0 RS	Heraeus Holding GmbH, Hanau
Balance, Analytik AC 210S	Sartorius Stedim Biotech, Germany

Centrifuge, Eppendorf 5415C	Eppendorf AG, Germany
Fluorescence microscope, Olympus IX 50	Olympus Corporation, Tokio, Japan
FPLC, BioLogic Duo-Flow Systems	Bio-Rad, München
Autoclave, Systec V-150	Systec GmbH, Wetzlar
Cell sorter, FACS Vantage SE	BD Biosciences, Heidelberg, Germany
Software Cell Quest Pro v 3.5	
Laser: Coherent Enterprise II, Argon Ion (488 nm)	
Filters: FL1: 515-545 nm; FL2: 564-606 nm; FL3: 665-685 nm	
Flow cytometer, Epics XL-MCL	Beckman Coulter, Krefeld, Germany
Software WinMDI 2.8	
Laser: Argon Ion (488 nm)	
Filters: FL1: 505-545 nm; FL2: 560-590 nm; FL3: 660-690 nm	
Electrophoresis system	Thermo Fisher Scientific, Bonn, Germany
Gel documentation, Gel IX Imager	Intas Science Imaging Instruments GmbH, Göttingen, Germany
Microplate Reader, Epoch	BioTek Instruments Inc., VT, USA
Shaker Rotator Bio-RS-24,	Peqlab, Erlangen, Germany
Magnetic stand - Dynamag-2	Life Technologies, Darmstadt, Germany
YSI 2700 Select Analyzer	YSI Inc. Life Sciences, Yellow Springs, USA

6.2.4 Buffer compositions

Phosphate buffered saline (PBS)

137 mM NaCl, 2.7 mM KCl, 10 mM Na₂HPO₄, KH₂PO₄, pH 7.4

TD05 Binding buffer

137 mM NaCl, 2.7 mM KCl, 10 mM Na₂HPO₄, KH₂PO₄, 5mM MgCl₂, pH 7.4

(137)

264 Binding buffer

20 mM Tris HCl, 150 mM NaCl, 4 mM KCl, 1 mM MgCl₂, 1 mM CaCl₂, pH 7.3

Lysozyme aptamer binding buffer

MgCl₂ buffer: 10 mM Tris-HCl, 5 mM MgCl₂, pH 7.5 (128)

VEGF aptamer binding buffer (TBSE)

10 mM Tris-HCl, 100 mM NaCl, 0,05 mM EDTA, 50 mM KCl, pH 7.0 (123)

6.2.5 Aptamers and oligonucleotides

Aptamers and oligonucleotides for negative controls were ordered from Biospring GmbH, Germany, or from IDT Inc., USA and stored according to manufacturers recommendations.

TD05 aptamer (137)

5' AAC ACC GGG AGG ATA GTT CGG TGG CTG TTC AGG GTC TCC TCC CGG TG 3'

Random oligonucleotide - 47 bases (R47) - generated using the online tool "Random DNA Generator" provided by the Maduro lab at the University of California in Riverside (<http://www.faculty.ucr.edu/~mmaduro/random.htm> - accessed on 06.06.2011)

5' AAA CCG CGT CTC TAC GAC CGG TGC TCG ATT TAA TTT CGC TGA CGT GA 3'

Pool of random 47mers (Pool)

Approximately 10¹⁴ different sequences according to manufacturer.

264 aptamer

5'TAC GAC TCA CTA TAG GGA TCC TTG CTT ACA TTA CGA CGT ACT GAA TTC CCT TTA GTG AGG GTT 3'

264 aptamer with elongation for helix spacer formation

5` T GTG GTC TAT GTC GTC GTT CG TAC GAC TCA CTA TAG GGA TCC TTG CTT ACA TTA CGA CGT ACT GAA TTC CCT TTA GTG AGG GTT 3`

Biotin oligo for helix spacer formation (98)

5'-CGA ACG ACG ACA TAG ACC ACA 3' Biotin

Lysozyme aptamer (122,128)

5'-AGC AGC ACA GAG GTC AGA TGG CAG CTA AGC AGG CGG CTC ACA
AAA CCA TTC GCA TGC GGC CCT ATG CGT GCT ACC GTG AA-3'

VEGF aptamers

V7t1 (124):

5' TGT GGG GGT GGA CGG GCC GGG TAG A 3'

Del5-1 (123):

5' ATA CCA GTC TAT TCA ATT GGG CCC GTC CGT TGG TGG GTG TGC TGG
CCA G 3'

7 References

1. Statistisches Bundesamt (2012) Sterbestatistik und Lebenserwartung in Deutschland. <https://www.destatis.de/DE/ZahlenFakten/GesellschaftStaat/Bevoelkerung/Sterbefaelle/AktuellPeriodensterbetafel.html>.
2. Meyer, M., Scheper, T. and Walter, J.-G. (2013) Aptamers: versatile probes for flow cytometry, *Appl Microbiol Biotechnol*, **97**, 7097-7109, <http://dx.doi.org/10.1007/s00253-013-5070-z>.
3. Roederer, M., Bigos, M., Nozaki, T., Stovel, R.T., Parks, D.R. and Herzenberg, L.A. (1995) Heterogeneous calcium flux in peripheral T cell subsets revealed by five-color flow cytometry using log-ratio circuitry, *Cytometry*, **21**, 187–196.
4. Chattopadhyay, P.K., Hogerkorp, C.-M. and Roederer, M. (2008) A chromatic explosion: the development and future of multiparameter flow cytometry, *Immunology*, **125**, 441–449.
5. Life Technologies Inc. USA <http://www.lifetechnologies.com/de/de/home/support/tutorials.html>. - accessed on 28.02.2014.
6. Davidson, B., Dong, H.P., Berner, A. and Risberg, B. (2012) The diagnostic and research applications of flow cytometry in cytopathology, *Diagn. Cytopathol.*, **40**, 525–535.
7. Müller, S. and Bley, T. (2011) High Resolution Microbial Single Cell Analytics. Springer-Verlag Berlin Heidelberg, Berlin, Heidelberg.
8. Czechowska, K., Johnson, D.R. and van der Meer, J.R. (2008) Use of flow cytometric methods for single-cell analysis in environmental microbiology, *Curr. Opin. Microbiol.*, **11**, 205–212.
9. Preffer, F. and Dombkowski, D. (2009) Advances in complex multiparameter flow cytometry technology: Applications in stem cell research, *Cytometry B Clin Cytom*, **76**, 295–314.
10. Nurse, P. and Hayles, J. (2011) The cell in an era of systems biology, *Cell*, **144**, 850–854.
11. Moretti, P., Behr, L., Walter, J.G., Kasper, C., Stahl, F. and Scheper, T. (2010) Characterization and improvement of cell line performance via flow cytometry and cell sorting, *Eng. Life Sci.*, NA.
12. Johnson, K.W., Dooner, M. and Quesenberry, P.J. (2007) Fluorescence activated cell sorting: a window on the stem cell, *Curr Pharm Biotechnol*, **8**, 133–139.
13. Stoltenburg, R., Reinemann, C. and Strehlitz, B. (2007) SELEX--a (r)evolutionary method to generate high-affinity nucleic acid ligands, *Biomol. Eng.*, **24**, 381–403.
14. McKeague, M. and Derosa, M.C. (2012) Challenges and opportunities for small molecule aptamer development, *J Nucleic Acids*, **2012**, 748913.
15. Kulbachinskiy, A.V. (2007) Methods for selection of aptamers to protein targets, *Biochemistry Mosc.*, **72**, 1505–1518.

16. Nitsche, A., Kurth, A., Dunkhorst, A., Pänke, O., Sielaff, H., Junge, W., Muth, D., Scheller, F., Stöcklein, W. and Dahmen, C. *et al.* (2007) One-step selection of Vaccinia virus-binding DNA aptamers by MonoLEX, *BMC Biotechnol*, **7**, 48.
17. Tang, Z., Shangguan, D., Wang, K., Shi, H., Sefah, K., Mallikratchy, P., Chen, H.W., Li, Y. and Tan, W. (2007) Selection of Aptamers for Molecular Recognition and Characterization of Cancer Cells, *Anal. Chem*, **79**, 4900–4907.
18. Ellington, A.D. and Szostak, J.W. (1990) In vitro selection of RNA molecules that bind specific ligands, *Nature*, **346**, 818–822.
19. Tuerk, C. and Gold, L. (1990) Systematic evolution of ligands by exponential enrichment: RNA ligands to bacteriophage T4 DNA polymerase, *Science*, **249**, 505–510.
20. Lübbecke, M., Walter, J.-G., Stahl, F. and Scheper, T. (2012) Aptamers as detection molecules on reverse phase protein microarrays for the analysis of cell lysates, *Eng. Life Sci.*, **12**, 144–151.
21. Zhu, G., Lübbecke, M., Walter, J.-G., Stahl, F. and Scheper, T. (2011) Characterization of Optimal Aptamer-Microarray Binding Chemistry and Spacer Design, *Chem. Eng. Technol.*, **34**, 2022–2028.
22. Walter, J.-G., Kökpinar, O., Friehs, K., Stahl, F. and Scheper, T. (2008) Systematic investigation of optimal aptamer immobilization for protein-microarray applications, *Anal. Chem.*, **80**, 7372–7378.
23. Iliuk, A.B., Hu, L. and Tao, W.A. (2011) Aptamer in Bioanalytical Applications, *Anal. Chem*, **83**, 4440–4452.
24. Davis, K.A., Abrams, B., Lin, Y. and Jayasena, S.D. (1996) Use of a high affinity DNA ligand in flow cytometry, *Nucleic Acids Res*, **24**, 702–706.
25. Davis, K.A., Lin, Y., Abrams, B. and Jayasena, S.D. (1998) Staining of cell surface human CD4 with 2'-F-pyrimidine-containing RNA aptamers for flow cytometry, *Nucleic Acids Res*, **26**, 3915–3924.
26. Glaser, V. (2009) Oligo Market Benefits from RNAi Focus, *Genetic Engineering & Biotechnology News*, **29**.
27. Rob Carlson <http://www.synthesis.cc/>. - accessed on 28.02.2014.
28. Zhang, P., Zhao, N., Zeng, Z., Chang, C.-C. and Zu, Y. (2010) Combination of an Aptamer Probe to CD4 and Antibodies for Multicolored Cell Phenotyping, *American Journal of Clinical Pathology*, **134**, 586–593.
29. Baird, G.S. (2010) Where are all the aptamers?, *Am. J. Clin. Pathol.*, **134**, 529–531.
30. Martino, J.P. (1993) Technological forecasting for decision making. McGraw-Hill, New York, London.
31. Meyer, S., Maufort, J.P., Nie, J., Stewart, R., McIntosh, B.E., Conti, L.R., Ahmad, K.M., Soh, H.T. and Thomson, J.A. (2013) Development of an Efficient Targeted Cell-SELEX Procedure for DNA Aptamer Reagents, *PLoS ONE*, **8**, e71798.
32. Ye, M., Hu, J., Peng, M., Liu, J., Liu, J., Liu, H., Zhao, X. and Tan, W. (2012) Generating Aptamers by Cell-SELEX for Applications in Molecular Medicine, *Int J Mol Sci*, **13**, 3341–3353.

33. Schütze, T., Wilhelm, B., Greiner, N., Braun, H., Peter, F., Mörl, M., Erdmann, V.A., Lehrach, H., Konthur, Z. and Menger, M. *et al.* (2011) Probing the SELEX process with next-generation sequencing, *PLoS ONE*, **6**, e29604.
34. Shamah, S.M., Healy, J.M. and Cload, S.T. (2008) Complex target SELEX, *Acc. Chem. Res.*, **41**, 130–138.
35. Yang, M., Jiang, G., Li, W., Qiu, K., Zhang, M., Carter, C.M., Al-Quran, S.Z. and Li, Y. (2014) Developing aptamer probes for acute myelogenous leukemia detection and surface protein biomarker discovery, *J Hematol Oncol*, **7**, 5.
36. Morris, K.N., Jensen, K.B., Julin, C.M., Weil, M. and Gold, L. (1998) High affinity ligands from in vitro selection: complex targets, *Proc. Natl. Acad. Sci. U.S.A.*, **95**, 2902–2907.
37. Ulrich, H. and Wrenger, C. (2009) Disease-specific biomarker discovery by aptamers, *Cytometry*, **75**, 727–733.
38. van Simaey, D., López-Colón, D., Sefah, K., Sutphen, R., Jimenez, E. and Tan, W. (2010) Study of the molecular recognition of aptamers selected through ovarian cancer cell-SELEX, *PLoS ONE*, **5**, e13770.
39. Sefah, K., Tang, Z.W., Shangguan, D.H., Chen, H., Lopez-Colon, D., Li, Y., Parekh, P., Martin, J., Meng, L. and Phillips, J.A. *et al.* (2009) Molecular recognition of acute myeloid leukemia using aptamers, *Leukemia*, **23**, 235–244.
40. Mayer, G., Ahmed, M.-S.L., Dolf, A., Endl, E., Knolle, P.A. and Famulok, M. (2010) Fluorescence-activated cell sorting for aptamer SELEX with cell mixtures, *Nat Protoc*, **5**, 1993–2004.
41. Raddatz, M.L., Dolf, A., Endl, E., Knolle, P., Famulok, M. and Mayer, G. (2008) Enrichment of Cell-Targeting and Population-Specific Aptamers by Fluorescence-Activated Cell Sorting, *Angew. Chem. Int. Ed*, **47**, 5190–5193.
42. Avci-Adali, M., Metzger, M., Perle, N., Ziemer, G. and Wendel, H.P. (2010) Pitfalls of cell-systematic evolution of ligands by exponential enrichment (SELEX): existing dead cells during in vitro selection anticipate the enrichment of specific aptamers, *Oligonucleotides*, **20**, 317–323.
43. Sefah, K., Shangguan, D., Xiong, X., O'Donoghue, M.B. and Tan, W. (2010) Development of DNA aptamers using Cell-SELEX, *Nat Protoc*, **5**, 1169–1185.
44. Shangguan, D., Li, Y., Tang, Z., Cao, Z.C., Chen, H.W., Mallikaratchy, P., Sefah, K., Yang, C.J. and Tan, W. (2006) Aptamers evolved from live cells as effective molecular probes for cancer study, *Proceedings of the National Academy of Sciences*, **103**, 11838–11843.
45. Hamula, C.L.A., Zhang, H., Guan, L.L., Li, X.-F. and Le, X.C. (2008) Selection of Aptamers against Live Bacterial Cells, *Anal. Chem*, **80**, 7812–7819.
46. Parekh, P., Tang, Z., Turner, P.C., Moyer, R.W. and Tan, W. (2010) Aptamers Recognizing Glycosylated Hemagglutinin Expressed on the Surface of Vaccinia Virus-Infected Cells, *Anal. Chem*, **82**, 8642–8649.
47. World Health Organization (WHO) World Cancer Report 2014.
48. Hicke, B.J., Marion, C., Chang, Y.F., Gould, T., Lynott, C.K., Parma, D., Schmidt, P.G. and Warren, S. (2001) Tenascin-C aptamers are generated using tumor cells and purified protein, *J. Biol. Chem.*, **276**, 48644–48654.

49. Zhao, Z., Xu, L., Shi, X., Tan, W., Fang, X. and Shangguan, D. (2009) Recognition of subtype non-small cell lung cancer by DNA aptamers selected from living cells, *Analyst*, **134**, 1808.
50. Kunii, T., Ogura, S.-i., Mie, M. and Kobatake, E. (2011) Selection of DNA aptamers recognizing small cell lung cancer using living cell-SELEX, *Analyst*, **136**, 1310.
51. Chen, C.-H.B., Chernis, G.A., van Hoang, Q. and Landgraf, R. (2003) Inhibition of heregulin signaling by an aptamer that preferentially binds to the oligomeric form of human epidermal growth factor receptor-3, *Proc. Natl. Acad. Sci. U.S.A.*, **100**, 9226–9231.
52. Lupold, S.E., Hicke, B.J., Lin, Y. and Coffey, D.S. (2002) Identification and characterization of nuclease-stabilized RNA molecules that bind human prostate cancer cells via the prostate-specific membrane antigen, *Cancer Res.*, **62**, 4029–4033.
53. Shangguan, D., Meng, L., Cao, Z.C., Xiao, Z., Fang, X., Li, Y., Cardona, D., Witek, R.P., Liu, C. and Tan, W. (2008) Identification of Liver Cancer-Specific Aptamers Using Whole Live Cells, *Anal. Chem*, **80**, 721–728.
54. Ninomiya, K., Kaneda, K., Kawashima, S., Miyachi, Y., Ogino, C. and Shimizu, N. (2013) Cell-SELEX based selection and characterization of DNA aptamer recognizing human hepatocarcinoma, *Bioorg. Med. Chem. Lett.*, **23**, 1797–1802.
55. Jackman, D.M. and Johnson, B.E. (2005) Small-cell lung cancer, *Lancet*, **366**, 1385–1396.
56. Chen, H.W., Medley, C.D., Sefah, K., Shangguan, D., Tang, Z., Meng, L., Smith, J.E. and Tan, W. (2008) Molecular Recognition of Small-Cell Lung Cancer Cells Using Aptamers, *ChemMedChem*, **3**, 991–1001.
57. Funakoshi, T., Tachibana, I., Hoshida, Y., Kimura, H., Takeda, Y., Kijima, T., Nishino, K., Goto, H., Yoneda, T. and Kumagai, T. *et al.* (2003) Expression of tetraspanins in human lung cancer cells: frequent downregulation of CD9 and its contribution to cell motility in small cell lung cancer, *Oncogene*, **22**, 674–687.
58. Jiménez, E., Sefah, K., López-Colón, D., van Simaeys, D., Chen, H.W., Tockman, M.S. and Tan, W. (2012) Generation of lung adenocarcinoma DNA aptamers for cancer studies, *PLoS ONE*, **7**, e46222.
59. Shigdar, S., Lin, J., Yu, Y., Pastuovic, M., Wei, M. and Duan, W. (2011) RNA aptamer against a cancer stem cell marker epithelial cell adhesion molecule, *Cancer Science*, **102**, 991–998.
60. Song, Y., Zhu, Z., An, Y., Zhang, W., Zhang, H., Liu, D., Yu, C., Duan, W. and Yang, C.J. (2013) Selection of DNA aptamers against epithelial cell adhesion molecule for cancer cell imaging and circulating tumor cell capture, *Anal. Chem.*, **85**, 4141–4149.
61. Zhang, P., Zhao, N., Zeng, Z., Feng, Y., Tung, C.-H., Chang, C.-C. and Zu, Y. (2009) Using an RNA aptamer probe for flow cytometry detection of CD30-expressing lymphoma cells, *Lab Invest*, **89**, 1423–1432.
62. Li, N., Ebright, J.N., Stovall, G.M., Chen, X., Nguyen, H.H., Singh, A., Syrett, A. and Ellington, A.D. (2009) Technical and Biological Issues Relevant to Cell Typing with Aptamers, *J. Proteome Res*, **8**, 2438–2448.

63. Hamula, C.L., Zhang, H., Li, F., Wang, Z., Chris Le, X. and Li, X.-F. (2011) Selection and analytical applications of aptamers binding microbial pathogens, *TrAC Trends in Analytical Chemistry*, **30**, 1587–1597.
64. Dwivedi, H.P., Smiley, R.D. and Jaykus, L.-A. (2013) Selection of DNA aptamers for capture and detection of *Salmonella Typhimurium* using a whole-cell SELEX approach in conjunction with cell sorting, *Appl. Microbiol. Biotechnol.*, **97**, 3677–3686.
65. Cao, X., Li, S., Chen, L., Ding, H., Xu, H., Huang, Y., Li, J., Liu, N., Cao, W. and Zhu, Y. *et al.* (2009) Combining use of a panel of ssDNA aptamers in the detection of *Staphylococcus aureus*, *Nucleic Acids Research*, **37**, 4621–4628.
66. Duan, N., Wu, S., Chen, X., Huang, Y. and Wang, Z. (2012) Selection and Identification of a DNA Aptamer Targeted to *Vibrio parahaemolyticus*, *J. Agric. Food Chem*, **60**, 4034–4038.
67. Dwivedi, H.P., Smiley, R.D. and Jaykus, L.-A. (2010) Selection and characterization of DNA aptamers with binding selectivity to *Campylobacter jejuni* using whole-cell SELEX, *Appl Microbiol Biotechnol*, **87**, 2323–2334.
68. Tang, Z., Parekh, P., Turner, P., Moyer, R.W. and Tan, W. (2009) Generating Aptamers for Recognition of Virus-Infected Cells, *Clinical Chemistry*, **55**, 813–822.
69. World Health Organization (WHO) (2012) World Health Statistics 2012. Noncommunicable diseases: a major health challenge of the 21st century.
70. Michalet, X., Pinaud, F.F., Bentolila, L.A., Tsay, J.M., Doose, S., Li, J.J., Sundaresan, G., Wu, A.M., Gambhir, S.S. and Weiss, S. (2005) Quantum dots for live cells, in vivo imaging, and diagnostics, *Science*, **307**, 538–544.
71. Drummen, G.P. (2010) Quantum Dots—From Synthesis to Applications in Biomedicine and Life Sciences, *IJMS*, **11**, 154–163.
72. <http://www.nanocotechnologies.com/Resources/Images/c1740110-6b1b-4dac-bb24-3c25037fe7d8.gif> (20.03.2012). - accessed on 26.03.2012.
73. <http://www.cytodiagnosics.com/fluorescent-nanocrystals.php> (26.03.2012). - accessed on 26.03.2012.
74. Chattopadhyay, P.K., Price, D.A., Harper, T.F., Betts, M.R., Yu, J., Gostick, E., Perfetto, S.P., Goepfert, P., Koup, R.A. and Rosa, S.C. de *et al.* (2006) Quantum dot semiconductor nanocrystals for immunophenotyping by polychromatic flow cytometry, *Nat Med*, **12**, 972–977.
75. Ibáñez-Peral, R., Bergquist, P.L., Walter, M.R., Gibbs, M., Goldys, E.M. and Ferrari, B. (2008) Potential Use of Quantum Dots in Flow Cytometry, *IJMS*, **9**, 2622–2638.
76. Watson, A., Wu, X. and Bruchez, M. (2003) Lighting up cells with quantum dots, *BioTechniques*, **34**, 296-300, 302-3.
77. Kang, W.J., Chae, J.R., Cho, Y.L., Lee, J.D. and Kim, S. (2009) Multiplex Imaging of Single Tumor Cells Using Quantum-Dot-Conjugated Aptamers, *Small*, **5**, 2519–2522.
78. Li, Z., Huang, P., He, R., Lin, J., Yang, S., Zhang, X., Ren, Q. and Cui, D. (2010) Aptamer-conjugated dendrimer-modified quantum dots for cancer cell targeting and imaging, *Materials Letters*, **64**, 375–378.

79. Mazumder, S., Dey, R., Mitra, M.K., Mukherjee, S. and Das, G.C. (2009) Review: Biofunctionalized Quantum Dots in Biology and Medicine, *Journal of Nanomaterials*, **2009**, 1–17.
80. Bagalkot, V., Zhang, L., Levy-Nissenbaum, E., Jon, S., Kantoff, P.W., Langer, R. and Farokhzad, O.C. (2007) Quantum Dot–Aptamer Conjugates for Synchronous Cancer Imaging, Therapy, and Sensing of Drug Delivery Based on Bi-Fluorescence Resonance Energy Transfer, *Nano Lett*, **7**, 3065–3070.
81. Chu, T.C., Shieh, F., Lavery, L.A., Levy, M., Richards-Kortum, R., Korgel, B.A. and Ellington, A.D. (2006) Labeling tumor cells with fluorescent nanocrystal–aptamer bioconjugates, *Biosensors and Bioelectronics*, **21**, 1859–1866.
82. Zhang, J., Jia, X., Lv, X.-J., Deng, Y.-L. and Xie, H.-Y. (2010) Fluorescent quantum dot-labeled aptamer bioprobes specifically targeting mouse liver cancer cells, *Talanta*, **81**, 505–509.
83. Medley, C.D., Bamrungsap, S., Tan, W. and Smith, J.E. (2011) Aptamer-Conjugated Nanoparticles for Cancer Cell Detection, *Anal. Chem*, **83**, 727–734.
84. Duan, N., Wu, S., Yu, Y., Ma, X., Xia, Y., Chen, X., Huang, Y. and Wang, Z. (2013) A dual-color flow cytometry protocol for the simultaneous detection of *Vibrio parahaemolyticus* and *Salmonella typhimurium* using aptamer conjugated quantum dots as labels, *Anal. Chim. Acta*, **804**, 151–158.
85. Dwarakanath, S., Bruno, J.G., Shastry, A., Phillips, T., John, A., Kumar, A. and Stephenson, L.D. (2004) Quantum dot-antibody and aptamer conjugates shift fluorescence upon binding bacteria, *Biochemical and Biophysical Research Communications*, **325**, 739–743.
86. Wang, T.-y. (2005) Artificially Lipid-anchored Proteins Can Elicit Clustering-induced Intracellular Signaling Events in Jurkat T-Lymphocytes Independent of Lipid Raft Association, *Journal of Biological Chemistry*, **280**, 22839–22846.
87. Sarkar, D., Vemula, P.K., Zhao, W., Gupta, A., Karnik, R. and Karp, J.M. (2010) Engineered mesenchymal stem cells with self-assembled vesicles for systemic cell targeting, *Biomaterials*, **31**, 5266–5274.
88. Elliott, J.T. and Prestwich, G.D. (2000) Maleimide-Functionalized Lipids that Anchor Polypeptides to Lipid Bilayers and Membranes, *Bioconjugate Chem*, **11**, 832–841.
89. Peterson, B.R. (2005) Synthetic mimics of mammalian cell surface receptors: prosthetic molecules that augment living cells, *Org. Biomol. Chem*, **3**, 3607.
90. Kamitani, R., Niikura, K., Okajima, T., Matsuo, Y. and Ijiri, K. (2009) Design of Cell-Surface-Retained Polymers for Artificial Ligand Display, *ChemBioChem*, **10**, 230–233.
91. Sarkar, D., Vemula, P.K., Teo, G.S.L., Spelke, D., Karnik, R., Wee, L.Y. and Karp, J.M. (2008) Chemical Engineering of Mesenchymal Stem Cells to Induce a Cell Rolling Response, *Bioconjugate Chem*, **19**, 2105–2109.
92. Zhao, W., Teo, G.S.L., Kumar, N. and Karp, J.M. (2010) Chemistry and material science at the cell surface, *Mater Today (Kidlington)*, **13**, 14–21.
93. Egger, M., Heyn, S.P. and Gaub, H.E. (1992) Synthetic lipid-anchored receptors based on the binding site of a monoclonal antibody, *Biochim. Biophys. Acta*, **1104**, 45–54.

-
94. Ko, I.K., Kean, T.J. and Dennis, J.E. (2009) Targeting mesenchymal stem cells to activated endothelial cells, *Biomaterials*, **30**, 3702–3710.
95. Borisenko, G.G., Zaitseva, M.A., Chuvilin, A.N. and Pozmogova, G.E. (2009) DNA modification of live cell surface, *Nucleic Acids Res.*, **37**, e28.
96. Zhao, W., Loh, W., Droujinine, I.A., Teo, W., Kumar, N., Schafer, S., Cui, C.H., Zhang, L., Sarkar, D. and Karnik, R. *et al.* (2011) Mimicking the inflammatory cell adhesion cascade by nucleic acid aptamer programmed cell-cell interactions, *The FASEB Journal*, **25**, 3045–3056.
97. Tokunaga, T., Kuwahata, K. and Sando, S. (2013) Systematic Exploration of Lipophilic Tags That Allow Efficient Anchoring of Aptamers to Live Cell Surfaces, *Chem. Lett.*, **42**, 127–129.
98. Zhao, W., Schafer, S., Choi, J., Yamanaka, Y.J., Lombardi, M.L., Bose, S., Carlson, A.L., Phillips, J.A., Teo, W. and Droujinine, I.A. *et al.* (2011) Cell-surface sensors for real-time probing of cellular environments, *Nature Nanotech*, **6**, 524–531.
99. Tokunaga, T., Namiki, S., Yamada, K., Imaishi, T., Nonaka, H., Hirose, K. and Sando, S. (2012) Cell surface-anchored fluorescent aptamer sensor enables imaging of chemical transmitter dynamics, *J. Am. Chem. Soc.*, **134**, 9561–9564.
100. Mudhar, P. (2006) Biopharmaceuticals: Insight into today's market and a look to the future How is the biopharm market shaping up?, *Pharmaceutical Technology Europe*, **18**, 20–25.
101. Lai, T., Yang, Y. and Ng, S.K. (2013) Advances in Mammalian cell line development technologies for recombinant protein production, *Pharmaceuticals (Basel)*, **6**, 579–603.
102. Wurm, F.M. (2004) Production of recombinant protein therapeutics in cultivated mammalian cells, *Nat. Biotechnol.*, **22**, 1393–1398.
103. Backliwal, G., Hildinger, M., Chenuet, S., Wulhfard, S., Jesus, M. de and Wurm, F.M. (2008) Rational vector design and multi-pathway modulation of HEK 293E cells yield recombinant antibody titers exceeding 1 g/l by transient transfection under serum-free conditions, *Nucleic Acids Res.*, **36**, e96.
104. Browne, S.M. and Al-Rubeai, M. (2007) Selection methods for high-producing mammalian cell lines, *Trends in Biotechnology*, **25**, 425–432.
105. Porter, A.J., Racher, A.J., Preziosi, R. and Dickson, A.J. (2010) Strategies for selecting recombinant CHO cell lines for cGMP manufacturing: Improving the efficiency of cell line generation, *Biotechnol Progress*, **26**, 1455–1464.
106. Hossler, P. (2012) Protein glycosylation control in Mammalian cell culture: past precedents and contemporary prospects, *Adv. Biochem. Eng. Biotechnol.*, **127**, 187–219.
107. John R. Birch (2011) Protein Expression Technology Review. Improvements in Microbial and Mammalian Systems Design Drive Advances in the Field, *Genetic Engineering & Biotechnology News*, **17**.
108. Du, Z., Mujacic, M., Le, K., Caspary, G., Nunn, H., Heath, C. and Reddy, P. (2013) Analysis of heterogeneity and instability of stable mAb-expressing CHO cells, *Biotechnol Bioproc E*, **18**, 419–429.

109. Seth, G., Charaniya, S., Wlaschin, K.F. and Hu, W.-S. (2007) In pursuit of a super producer-alternative paths to high producing recombinant mammalian cells, *Curr. Opin. Biotechnol.*, **18**, 557–564.
110. Kumar, N. and Borth, N. (2012) Flow-cytometry and cell sorting: an efficient approach to investigate productivity and cell physiology in mammalian cell factories, *Methods*, **56**, 366–374.
111. Powell, K.T. and Weaver, J.C. (1990) Gel microdroplets and flow cytometry: rapid determination of antibody secretion by individual cells within a cell population, *Biotechnology (N.Y.)*, **8**, 333–337.
112. Kenney, J.S., Gray, F., Ancel, M.H. and Dunne, J.F. (1995) Production of monoclonal antibodies using a secretion capture report web, *Biotechnology (N.Y.)*, **13**, 787–790.
113. Gray, F., Kenney, J.S. and Dunne, J.F. (1995) Secretion capture and report web: use of affinity derivatized agarose microdroplets for the selection of hybridoma cells, *J. Immunol. Methods*, **182**, 155–163.
114. Marder, P., Maciak, R.S., Fouts, R.L., Baker, R.S. and Starling, J.J. (1990) Selective cloning of hybridoma cells for enhanced immunoglobulin production using flow cytometric cell sorting and automated laser nephelometry, *Cytometry*, **11**, 498–505.
115. Brezinsky, S., Chiang, G., Szilvasi, A., Mohan, S., Shapiro, R., MacLean, A., Sisk, W. and Thill, G. (2003) A simple method for enriching populations of transfected CHO cells for cells of higher specific productivity, *Journal of Immunological Methods*, **277**, 141–155.
116. Pichler, J., Hesse, F., Wieser, M., Kunert, R., Galosy, S.S., Mott, J.E. and Borth, N. (2009) A study on the temperature dependency and time course of the cold capture antibody secretion assay, *Journal of Biotechnology*, **141**, 80–83.
117. Manz, R., Assenmacher, M., Pflüger, E., Miltenyi, S. and Radbruch, A. (1995) Analysis and sorting of live cells according to secreted molecules, relocated to a cell-surface affinity matrix, *Proc. Natl. Acad. Sci. U.S.A.*, **92**, 1921–1925.
118. Holmes, P. and Al-Rubeai, M. (1999) Improved cell line development by a high throughput affinity capture surface display technique to select for high secretors, *J. Immunol. Methods*, **230**, 141–147.
119. Borth, N., Zeyda, M., Kunert, R. and Katinger, H. (2000) Efficient selection of high-producing subclones during gene amplification of recombinant Chinese hamster ovary cells by flow cytometry and cell sorting, *Biotechnol. Bioeng.*, **71**, 266–273.
120. Zuker, M. (2003) Mfold web server for nucleic acid folding and hybridization prediction, *Nucleic Acids Res.*, **31**, 3406–3415.
121. Kelf, T.A., Sreenivasan, V.K.A., Sun, J., Kim, E.J., Goldys, E.M. and Zvyagin, A.V. (2010) Non-specific cellular uptake of surface-functionalized quantum dots, *Nanotechnology*, **21**, 285105.
122. Tran, D.T., Janssen, K.P.F., Pollet, J., Lammertyn, E., Anné, J., van Schepdael, A. and Lammertyn, J. (2010) Selection and Characterization of DNA Aptamers for Egg White Lysozyme, *Molecules*, **15**, 1127–1140.

123. Hasegawa, H., Sode, K. and Ikebukuro, K. (2008) Selection of DNA aptamers against VEGF165 using a protein competitor and the aptamer blotting method, *Biotechnol. Lett.*, **30**, 829–834.
124. Nonaka, Y., Sode, K. and Ikebukuro, K. (2010) Screening and improvement of an anti-VEGF DNA aptamer, *Molecules*, **15**, 215–225.
125. Miriam Lübbecke (2011) Neue Analyse- und Detektionsmethoden in der Microarray-Technologie - Dissertation.
126. Maria Zahid Production in *Pichia pastoris* and characterization of genetically engineered hepatitis B surface antigen virus-like particles - Dissertation.
127. Han, D., Hong, J., Kim, H.C., Sung, J.H. and Lee, J.B. (2013) Aptamer-based microspheres for highly sensitive protein detection using fluorescently-labeled DNA nanostructures, *J Nanosci Nanotechnol*, **13**, 7259–7263.
128. Han, B., Zhao, C., Yin, J. and Wang, H. (2012) High performance aptamer affinity chromatography for single-step selective extraction and screening of basic protein lysozyme, *Journal of Chromatography B*, **903**, 112–117.
129. Long, S.B., Long, M.B., White, R.R. and Sullenger, B.A. (2008) Crystal structure of an RNA aptamer bound to thrombin, *RNA*, **14**, 2504–2512.
130. www.expasy.org/compute_pI. - accessed on 09.09.2013.
131. Siemeister, G., Schnurr, B., Mohrs, K., Schächtele, C., Marmé, D. and Martiny-Baron, G. (1996) Expression of biologically active isoforms of the tumor angiogenesis factor VEGF in *Escherichia coli*, *Biochem. Biophys. Res. Commun.*, **222**, 249–255.
132. Pizarro, S.A., Gunson, J., Field, M.J., Dinges, R., Khoo, S., Dalal, M., Lee, M., Kaleas, K.A., Moiseff, K. and Garnick, S. *et al.* (2010) High-yield expression of human vascular endothelial growth factor VEGF(165) in *Escherichia coli* and purification for therapeutic applications, *Protein Expr. Purif.*, **72**, 184–193.
133. https://www.avantilipids.com/index.php?option=com_content&view=article&id=1601&Itemid=382. - accessed on 09.09.2013.
134. Needham D. and McIntosh T.J., E.E. (1988) Thermomechanical and Transition Properties of Dimyristoylphosphatidylcholine/Cholesterol Bilayers, *Biochemistry*, 4668–4673.
135. <http://www.bio-rad.com/de-de/product/bio-plex-pro-magnetic-cooh-beads-related-reagents>. - accessed on 22.01.2014.
136. Seidel, S.A.I., Wienken, C.J., Geissler, S., Jerabek-Willemsen, M., Duhr, S., Reiter, A., Trauner, D., Braun, D. and Baaske, P. (2012) Label-free microscale thermophoresis discriminates sites and affinity of protein-ligand binding, *Angew. Chem. Int. Ed. Engl.*, **51**, 10656–10659.
137. Mallikaratchy, P., Tang, Z., Kwame, S., Meng, L., Shangguan, D. and Tan, W. (2007) Aptamer Directly Evolved from Live Cells Recognizes Membrane Bound Immunoglobulin Heavy Mu Chain in Burkitt's Lymphoma Cells, *Molecular & Cellular Proteomics*, **6**, 2230–2238.

Curriculum Vitae

Personal Data

Name	Michael Meyer
Date of birth	24.09.1985
Place of birth	Hildesheim
Nationality	German

04/2011 - 05/2014 Doctoral research assistant at the Institute of Technical Chemistry Leibniz University Hannover, Supervisor: Prof. Dr. T. Scheper
Doctoral thesis title: “Applications of aptamers in flow cytometry assays”

10/2008 - 03/2011 Master studies (M.Sc.) Life Science, Leibniz University Hannover, Final grade: (A) – excellent
Title of the master thesis: “Identification of off-target drug interactions using a novel bioanalytical tool” – research project performed at Imperial College London in the group of Prof. Dr. David R. Klug, Chemical Biology Center

10/2005 - 09/2008 Bachelor studies (B.Sc.) Life Science, Leibniz University Hannover, Final grade: (A) – excellent
Title of the bachelor thesis: “Bionanoarrays” – Supervisor: Prof. Dr. T. Scheper, Institute of Technical Chemistry

Research experience abroad

04/2010 – 12/2010 Imperial College London

- Research project and master thesis supervised by Prof. David R. Klug; Department of Chemistry - Chemical Biology Center

03/2009 – 04/2009 Technion, Israel Institute of Technology in Haifa

- Research project supervised by Prof. Yuval Shoham, Department of Biotechnology & Food Engineering

Publications

- 2013 Meyer M, Scheper T, Walter J (2013) Aptamers: versatile probes for flow cytometry. *Appl Microbiol Biotechnol* 97:7097-7109.
- 2014 M. Meyer, M. Loenne, J.-G. Walter, T. Scheper, „Investigation of immobilized Aptamer-Protein Binding by Flow Cytometry“, ACTA Manilana. Status: Submitted
- 2014 M. Meyer, J.-G. Walter, T. Scheper, „Direct coupling of aptamers on the cell surface“, Status: In preparation

Poster

- 2013 M. Meyer, J.-G. Walter, T. Scheper, „Aptamer-Quantum Dot Conjugates for Bioanalytical Applications“, Dechema Jahrestagung, Frankfurt a.M.
- 2013 M. Meyer, M. Loenne, J.-G. Walter, T. Scheper, „Application of immobilized aptamers in biotechnology“, Cost workshop 2013, Leipzig

“Hauptsache geil abliefern! Du musst abliefern, ich muss abliefern, am Ende fragt man doch nur, ob du geil abgeliefert hast!”

Bandleader Gurki aus Heinz Strunks Roman „Fleisch ist mein Gemüse“